Functional characterization of yeast kinetochore component, Nkp2

A Thesis submitted to the University of Hyderabad for the award of a Ph. D. degree in Department of Biochemistry, School of Life Sciences

By

Sirupangi Tirupataiah

(04LBPH10)

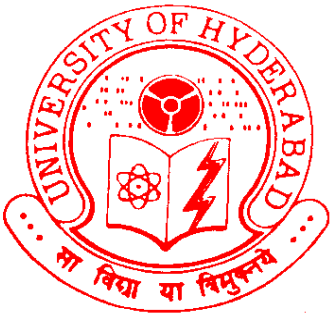

Department of Biochemistry
School of Life Sciences
University of Hyderabad
(P.O.) Central University, Gachibowli,
Hyderabad - 500 046
Andhra Pradesh (India)

March 2012

University of Hyderabad
School of Life Sciences
Department of Biochemistry

DECLARATION

I, Sirupangi Tirupataiah, hereby declare that this thesis entitled **"Functional characterization of yeast kinetochore component, Nkp2"** submitted by me under the guidance and supervision of Dr. Krishnaveni Mishra, is an original and independent research work. I also declare that it has not been submitted previously in part or in full to this University or any other University or Institution for the award of any degree or diploma.

Date:

Name: Sirupangi Tirupataiah

Signature of the student:

Regd. No. 04LBPH10

University of Hyderabad
School of Life Sciences
Department of Biochemistry

CERTIFICATE

This is to certify that this thesis entitled **"Functional characterization of yeast kinetochore component, Nkp2"** is a record of bonafide work done by Sirupangi Tirupataiah, a research scholar for Ph.D. programme in Department of Biochemistry, School of Life Sciences, University of Hyderabad under my guidance and supervision.

The thesis has not been submitted previously in part or in full to this or any other University or Institution for the award of any degree or diploma.

Signature of the Supervisor

Head of the Department

Dean of the School

University of Hyderabad
School of Life Sciences
Department of Biochemistry

ACKNOWLEDGEMENTS

It's a great privilege to express my deep sense of gratitude to my supervisor ***Dr. Krishnaveni Mishra*** *for giving me the opportunity to work in her laboratory. I also thank her for giving support and encouragement throughout the course of my work.*

I thank ***Prof.*** *O****.H. Setty,*** *Head, Department of Biochemistry, and former Head,* ***Prof. K.V.A. Ramaiah,*** *for making my research feasible with excellent infrastructure and lab facilities.*

I thank ***Prof. M. Ramanadham,*** *Dean, School of Life Sciences, and former Dean,* ***Prof. A. S. Raghavendra,*** *for providing the general facilities of the school.*

I would like to thank my Doctoral Committee members ***Prof. T. Suryanarayana*** *and* ***Prof. K. V.A. Ramaiah*** *for assessing my research work in between and for the useful discussions.*

I also express my sincere thanks to the entire faculty of School of Life Sciences who taught me science in my M.Sc. Biochemistry, which ultimately made me to choose research as my career.

I am also grateful to the non-teaching staff members of the Department of Biochemistry, School of Life Sciences for their kind assistance and cooperation.

I wish to extend my thanks to all my friends in School of Life Sciences who made my stay at University of Hyderabad a pleasant and memorable one.

I cannot finish without expressing my thanks to all my labmates: ***P.Nagesh, I. Srividya, E.Sreesankar, Abdul Hannan*** *and lab attendant* ***Aamir*** *for maintaining a cheerful atmosphere in the lab and extending help whenever needed in all these years of my stay in the lab.*

I thank ***DST, UGC, CSIR and DBT funding bodies*** *for providing necessary reagents during my work.*

And I am deeply grateful to the ***University Grant commission, India*** *for the financial support.*

Finally, and most importantly, many thanks go to my family for their support throughout this endeavor.

Sirupangi Tirupataiah

CONTENTS

List of Figures

List of Tables

List of Abbreviations

5-FOA	5-Fluoroorotic acid
ABF1	ARS-binding factor 1
ADE2	Adenine requiring
ADH4	Alcohol dehydrogenase isoenzyme type IV
ADP	Adenosine 5’ diphosphate
AME1	Associated with microtubules and essential
AMP	Ampicillin
ARS	Autonomous replicating sequence
BSA	Bovine serum albumin
CBF2	Centromere binding factor (also known as NDC10)
CBF3	Centromere binding factor 3
CDC13	Cell division cycle 13
CDE	Centromere DNA element
CEN	Centomere
ChIP	Chromatin immunoprecipitation
CHL4	Chromosome loss 4
CTF3	Chromosome transmission fidelity 3
CTF19	Chromosome transmission fidelity 19
CY3	Cyanine 3
DAPI	4',6-Diamidino-2-phenylindole
DMSO	Dimethyl sulfoxide
DNA	Deoxyribonucleic acid
DTT	Dithiothreitol
EDTA	Ethylenediaminetetraacetic acid
EMD	Emery-Dreifuss muscular dystrophy
EST2	Ever shorter telomeres
ESC1	Establishes silent chromatin1
FISH	Fluorescence in-situ hybridization
GFP	Green fluorescent protein
HCl	Hydrochloric acid
HIS	Histidine
HML	Hidden MAT left

HMR	Hidden MAT right
HRP	Horseradish peroxidise
IFN-β	Interferon beta
IML3	Increased minichromosome loss
KAN	Kanamycin
KOH	Potassium hydroxide
LB	Luria-Bertani broth
LEU	Leucine requiring
LiAC	Lithium Acetate
LMNA	Lamin A
LOH	Loss of heterozygosity
MAD1	Mitotic arrest deficient 1
MAD2	Mitotic arrest deficient 2
MAD3	Mitotic arrest deficient 3
MAT	Mating type (locus)
MCM16	Mini chromosome maintenance 16
MCM17	Mini chromosome maintenance 17
MCM21	Mini chromosome maintenance 21
MCM22	Mini chromosome maintenance 22
MET15	Methionine requiring
MHM	Multi heterozygous markers
MPS3	Monopolar spindle 3
MTW1	Mis twelve-like
mRNA	Messenger RNA
NaCl	Sodium chloride
NAD	Nicotinamide adenine dinucleotide
NHEJ	Non-homologous end joining
NKP1	Non essential kinetochore 1
NKP2	Non essential kinetochore 2
NPC	Nuclear pore complex
NSP1	Nucleoskeletal-like protein 1
NTS	Nontranscribed spacer
OD	Optical density
OKP1	Outer kinetochore protein
ORC	Origin recognition complex
PCR	Polymerase chain reaction
PEG	Polyethylene glycol
PML	Promyelocytic leukemia
Pol	Polymerase
PVDF	Polyvinylidene Fluoride
RAP1	Repressor activator protein 1

rDNA	Ribosomal DNA
RIF1	RAP1-interacting factor 1
RIF2	RAP1-interacting factor 2
RLF2	RAP1 localization factor (known as Cac1)
RNA	Ribonucleic acid
S	Svedberg
SAM2	S-Adenosyl Methionine requiring
SAP	Scaffold attachment factor, acinus, PIAS
SATB1	Special AT-rich sequence binding protein-1
SC	Synthetic complete
SD	Synthetic deficient
SDS	Sodium dodecyl sulphate
SDS-PAGE	Sodium dodecyl sulfate polyacrylamide gel electrophoresis
SFC	Splicing factor compartment
SGD	Saccharomyces genome database
SGO1	Shugoshin 1
SIR	Silent information regulator
snRNPs	Small nuclear ribonucleoproteins
SOB	Super optimal broth
SPB	Spindle pole body
SPC25	Spindle pole component 25
STAT	Signal transducer and activator of transcription
SUP11	Tyrosine tRNA Artificial chromosome
SUN	Sad1-UNC-84 domain protein
TAD3	tRNA-specific adenosine deaminase
TCA	Trichloroacetic acid
Tel	Telomere
TID3	Two hybrid interaction with DMC1 (known as NDC80)
TLC1	Telomerase component 1
TPE	Telomere position effect
Tris	Tris (hydroxymethyl)-aminomethane
tRNA	Transfer RNA
TRP1	Phosphoribosylanthranilate isomerase
URA3	Orotidine-5'-phosphate (OMP) decarboxylase
WT	Wildtype
YIF1	YIP1-interacting factor 1
Yku70/80	Yeast KU 70/80
YPD	Yeast extract peptone dextrose
YPK	Yeast extract peptone potassium acetate

Chapter - 1

General Introduction & Objectives

1.1 Nuclear architecture of a eukaryotic cell

The organization of chromosomal domains in the cell nucleus is a key contributor to genome function. Chromosomes are non-randomly positioned in the nucleus and occupy spatially distinct and well-defined sub-compartments of the nucleus referred to as the chromosomal territory (Cremer and Cremer, 2001; Parada and Misteli, 2002). In addition to chromosomal territories, specialized sub-compartments can be discerned in the nucleus. For instance, the nucleolus is the site for ribosomal DNA transcription and processing (Olson et al., 2000), or Splicing factor compartment that stores components required for processing of pre mRNA and provides them to the site of transcription in its vicinity (Misteli, 2000; Spector, 1990; Spector et al., 1991) and PML bodies (Dundr and Misteli, 2001). Using cytological techniques like fluorescence in-situ hybridization (FISH) and chromosomal painting along with live cell imaging microscopy and more advanced spinning-disc confocal imaging, chromosome organization has been studied. This organization has implications in genome stability and gene regulation (Meaburn and Misteli, 2007; Parada and Misteli, 2002; Parada et al., 2004).

Nuclear processes like transcription, RNA processing, DNA replication and repair occur in spatially constrained discrete regions within the nucleus. These "compartments" are membraneless sub-organelles characterized by a distinct set of resident proteins. The structural basis of this organization is not very well understood. Macromolecular self assembly and interaction with the nuclear skeleton or matrix have been proposed to play a role this compartmentalization (Misteli, 2001). Any disturbance in the architectural framework of nuclear compartments leads to diseased state of the cell. For example, mutations in *EMD* or *LMNA* genes encoding nuclear envelope structural proteins and causes a heritable degenerative disease called Emery–Dreyfuss muscular dystrophy (EDMD), that leads to muscle wasting and cardiomyopathy (Capell and Collins, 2006). The search for molecular mechanisms have shown that mutation in *EMD* or *LMNA* cause disturbance in the architecture of cell due to defect in nuclear architecture. The nuclear envelope links the nucleus to the rest of the cell, not only by harbouring nuclear pores that regulate the molecular transport, but also interconnecting

the nucleus to the cytoplasm through direct interaction with cytoskeleton elements, including cytoplasmic actin and microtubules. This shows that proper nuclear organization is essential for normal functioning of the cell, but however, the molecular mechanisms that act as driving forces for spatial distribution and maintenance of nuclear compartments are still largely unclear. For example, it remains unclear whether the symptoms of EDMD result directly from structural defect in the nuclei of muscle cells or a histone methylation patterns in lamin A mutants (Bank et al., 2011). Even though a lot of cell biological data has been accumulated based on tracking of chromosomes and the proteins associated with them, a systematic analysis of the structural and molecular basis of chromosome organization in the context of nuclear architecture has not been done.

1.2 Spatial organization of sub-nuclear compartments

Two conceptually distinct models were proposed to describe the positioning of chromosomal domains in separate sub-nuclear compartment of cell nucleus. First, genome organization may be determined by the distinct structural and physical properties of transcriptionally active and silenced regions of the genome. Gene rich and transcriptionally active regions are generally considered decondensed whereas silenced genome regions are generally in a more condensed state. It is possible that structurally similar regions might have occupied a distinct sub-nuclear compartment (Iborra and Cook, 2002). Self -organization model proposes that, the silenced regions of several chromosomes may associate with each other in three-dimensional space at the nuclear periphery and active regions are physically segregated from silenced regions and occupy the interior region of the nucleus (Cremer and Cremer, 2001).

The most prominent example for self-organization of sub-nuclear compartment is nucleolus. Clustering of transcriptionally inactive regions of several chromosomes occurs in the nucleolus where the tandem repeats of ribosomal genes from several chromosomes congregate. The nucleolus disintegrates during cell division when ribosomal DNA is repressed and reappears during late telophase when ribosomal DNA

transcription resumes (Dundr et al., 2000; Olson et al., 2000). Disappearance of nucleolus by inhibition of ribosomal RNA synthesis and de novo formation of micronucleoli by introduction of extra copies of rDNA provides an experimental evidence for self-organization of sub-nuclear compartments (Oakes et al., 1998; Oakes et al., 1993). The clustering effect might be due to the interaction of heterochromatin and euchromatin specific proteins.

Self-organisation of genomic domains is also observed by regulatory interactions between multiple chromosomes with shared transcription factors (Misteli, 2009). For example, in humans, activation of *IFN-β* gene located on chromosome 9 is proximal to its regulatory enhancer regions on chromosome 4 and 18 showing that functionally co-regulated regions on different chromosomes coalesce by transient interactions of regulatory and transcriptions factors (Apostolou and Thanos, 2008). Similarly, clustering of all *tRNA* genes located on distinct chromosomes in three-dimensional space near the nucleolus in *Saccharomyces cerevisiae* also suggests that regions in different chromosomes coalesce for efficient transcription and processing (Thompson et al., 2003). Taken together, these data support that self-organization is the most convincing model to bring about stable spatial genome organization because it accounts for several prominent features of chromosome and gene positioning patterns.

An alternative to a self-organization model suggests that spatial genome organization is based on the interaction of chromatin regions with specific architectural elements of the cell nucleus such as components of the nuclear matrix or other as yet unidentified protein(s). For example, SATB1 is a thymocyte specific architectural protein that appears to form a nuclear network and specific chromatin regions of thymocyte specific genes associated with it, in an activity dependent manner (Parada et al., 2004).

A further likely contributors to spatial genome organization are centromeres and telomeres. Centromeres are chromosomal elements that are found in all eukaryotes and contain repetitive sequences. In many organisms including yeast and mammals, centromeres are clustered together into multiple groups within the nucleus (Jin et al., 2000; Martou and De Boni, 2000). In other organisms, including *Drosophila* and plants,

centromeres are anchored to the nuclear periphery (Abranches et al., 1998; Hochstrasser et al., 1986). These observations suggest that centromeres might contribute to genome organization by bringing chromatin from several chromosomes together and maintaining heterochromatic foci. Because centromeric heterochromatin regions can act as silencers in trans, their silencing activity might also constrain the ability of chromatin regions from multiple chromosomes to dissociate from each other (Csink and Henikoff, 1998; Dernburg et al., 1996).

1.3 Heterochromatin and euchromatin compartments in eukaryotic nucleus

Several experimental models support that gene poor and transcriptionally inactive heterochromatin are preferentially associated or found at nuclear periphery and gene rich and highly transcribed regions at centre of the nucleus (Kozubek et al., 2002; Lukasova et al., 2002; Tanabe et al., 2002). This pattern of spatial organization of sub-nuclear compartments is an intriguing and attractive mechanism to bring about the chromosomal domains and genes is largely driven by the sum of all interactions acting on a given genomic region by regulatory elements associated with one chromosome or another tethering to the nuclear periphery and nucleating a target gene or clustering of active genes more interior of the nucleus. This pattern of spatial organization varies in different cell types and even in same cell type, re-organization of nuclear compartments takes place during cell division and in response to external stimuli (Cremer et al., 2006; Kim et al., 2004; Misteli, 2005; Walter et al., 2003). All these observations suggest that chromosomes or target genes occupy spatially distinct sub-compartments thereby reducing its degrees of spatial freedom and thus contributing toward the formation of a global localization pattern. However, this spatial organization cannot apply to all genes, and probably not even majority of genes. The same correlation has been made for single genes in numerous experimental evidences where inactive regions move from nuclear periphery to the centre of the cell nucleus.

Taken together, these data support that genome functions occur in the context of nuclear architecture. However, the mechanisms involved in the organization of sub-

nuclear compartments within the three dimensional space of the nucleus are not known much. Therefore, elucidation of the molecular mechanisms underlying in the non-random organization of eukaryotic nucleus may help to better understand its genome function.

1.4 Organization of transcriptional silent domains in *S. cerevisiae*

A striking example of the spatial organization of chromosomes is seen at the HM loci, telomere regions and rDNA locus that are refractory to transcription (silenced) in budding yeast, *Saccharomyces cerevisiae* (Fox and McConnell, 2005; Lustig, 1998; Rusche et al., 2003). Telomeres are specialized nucleoprotein structures with tandem repeats of $TG_{(1\text{-}3)n}$, which serve as protective "caps" on chromosome ends. In yeast, telomere and subtelomeric regions are highly compacted like the heterochromatin of higher eukaryotes and are inaccessible to RNA polymerase II (Gottschling et al., 1990). These highly ordered telomeres are clustered together into 3-8 foci at the nuclear periphery (Hediger et al., 2002; Loayza and de Lange, 2004). These clusters also contain the cryptic mating-type loci *HML* and *HMR* on either arms of chromosome III. *HML* and *HMR* contain the genes encoding for α mating type and *a* mating type respectively. These two copies of mating information are transcriptionally repressed and serve as donors for the active mating type locus, *MAT* (Brand et al., 1985; Rine and Herskowitz, 1987). Both telomeres, along with the sub-telomeric regions, and the HML/R loci are heterochromatinized (Rusche et al., 2003). *rDNA* locus contains about 100-200 copies of 9.1kb array of genes encoding 35S and 5S ribosomal RNA separated by nontranscribed spacer regions NTS1 and NTS2 on chromosome XII and maintain as silenced domain (Bryk et al., 1997; Smith and Boeke, 1997).

Immunoflourescence studies showed that all 64 telomeres of the 32 chromosomes in a diploid *Saccharomyces cerevisiae* are clustered together into 3-8 foci during interphase near the nuclear periphery (Gotta et al., 1996). Telomeres are co-localized with *HM* loci forming a sub-nuclear heterochromatin compartment at the nuclear periphery (Laroche et al., 2000). When subtelomere regions were observed in a population of living cells, they were consistently found to be at nuclear periphery

(Bystricky et al., 2005; Hediger et al., 2002; Schober et al., 2008; Therizols et al., 2010). Telomeres are known to be clustered at nuclear periphery by two redundant pathways. Telomere end binding heterodimer protein Yku70/80p anchors telomeres to the nuclear periphery through interaction with unidentified membrane proteins of nuclear envelope and/or the nuclear pore complex (Hediger et al., 2002). In the absence of any one of the heterodimeric subunits of Yku, some telomeres lose their association with nuclear periphery and delocalize more into the nuclear interior while others remain anchored to nuclear periphery by a Sir4-dependent mechanism (Laroche et al., 1998). The interaction between the C-terminal domain of Sir4 and the perinuclear protein, Esc1p, is sufficient which in turn is bound to telomeres and anchor them to the nuclear periphery (Andrulis et al., 2002; Hediger et al., 2002; Taddei et al., 2004). Mps3p, a SUN (Sad1-UNC-84) domain protein of inner nuclear membrane that is enriched at the SPB also interacts with Sir4p through its N-terminal acidic domain and tethers the telomeres to the nuclear periphery (Bupp et al., 2007).

1.4.1 Sub-nuclear organization favours gene silencing

The highly ordered organization of silent chromatin consisting of the telomeres and *HM* loci, at nuclear periphery maintains higher concentration of Sir (silent information regulator) proteins in its vicinity, which is essential for efficient repression of silent chromatin (Gotta et al., 1996). The tandem repetitive DNA at the telomeres provides sequence specific binding sites for Repressor and Activator protein (Rap1p) and pools this protein near telomeres (Gilson et al., 1993; Longtine et al., 1989). This Rap1p along with DNA repair/telomere binding protein Yku70p sequesters silent information regulators at the telomeres (Moretti et al., 1994; Tsukamoto et al., 1997).

More importantly, several lines of experimental evidences suggest that the subnuclear clustering of the two heterochromatin parts of the chromosome at the nuclear periphery favours gene silencing. Firstly, *yku70* mutations that disrupt the clustering of telomeres and Sir proteins, disrupt silencing (Laroche et al., 1998). Secondly, ectopic loci that are flanked by silencers are able to establish silencing when placed proximal to telomeres or silencer flanked ectopic regions are normally active in transcription, but

can be silenced on overexpression of Sir3 or Sir4 proteins or dispersion of Sir proteins throughout the nucleus by disrupting telomere organization (Maillet et al., 1996; Marcand et al., 1996). Thirdly, silencing can be established by artificially tethering ectopic loci to the nuclear periphery (Andrulis et al., 1998). This was elegantly demonstrated by artificially targeting proteins of the endoplasmic reticulum to a silencer defective *HMR* locus via Gal4 DNA binding domain leading to the establishment of silencing (Andrulis et al., 1998; Brand et al., 1987). These proteins promote repression by tethering the *HMR* locus to telomeric pools of Sirp, found at the nuclear periphery. Therefore, from the above experimental lines of evidence, it is clear that sub-nuclear organization of telomeres at the nuclear periphery is crucial for establishing and maintaining silencing. Recent experiments have further demonstrated at least three proteins are important for this peripheral localization of telomeres. Esc1, an inner nuclear membrane, Sir4p and Yku70/80p, the telomere end binding protein that has essential roles in DNA repair by non-homologous end joining, all are required for this peripheral anchoring (Gartenberg et al., 2004). However, the structural basis, like the underlying nuclear architecture component that these proteins anchor the telomeres to and the basis of clustering of specific telomeres into separate groups per se is not understood.

1.4.2 Silencing at *HM* loci, telomeres and rDNA loci

Heterochromatin is established in yeast in a multi-step pathway. Specific DNA sequences, termed as silencer elements *E* and *I*, flank the silenced region of the *HM* loci. These sequences recruit DNA binding proteins: Rap1, Abf1 and Orc1. These silencer bound proteins in turn, recruit the Silent Information Regulators (Sir1p, Sir2p, Sir3p, and Sir4p). Sir2p, an evolutionarily conserved NAD-dependent histone deacetylase, begins to deacetylate specific sites on histones H3 and H4 in the nucleosomes. These deacetylated nucleosomes serve as high affinity binding sites for Sir3p and Sir4p. The Sirp bound nucleosomes are refractory to transcription, and thus such regions are silenced or heterochromatinized. The mechanism of heterochromatin establishment at the telomeres is very similar; however, instead of 3 different silencer elements recruiting

three different proteins, the telomere repeat sequences themselves serve as multiple binding sites for Rap1. The C-terminal domain of Rap1 binds Sir4, an interaction antagonized by two other Rap1 binding proteins Rif1 and Rif2 (Mishra and Shore, 1999; Moretti et al., 1994; Rusche et al., 2002). This Rif- mediated antagonism is also

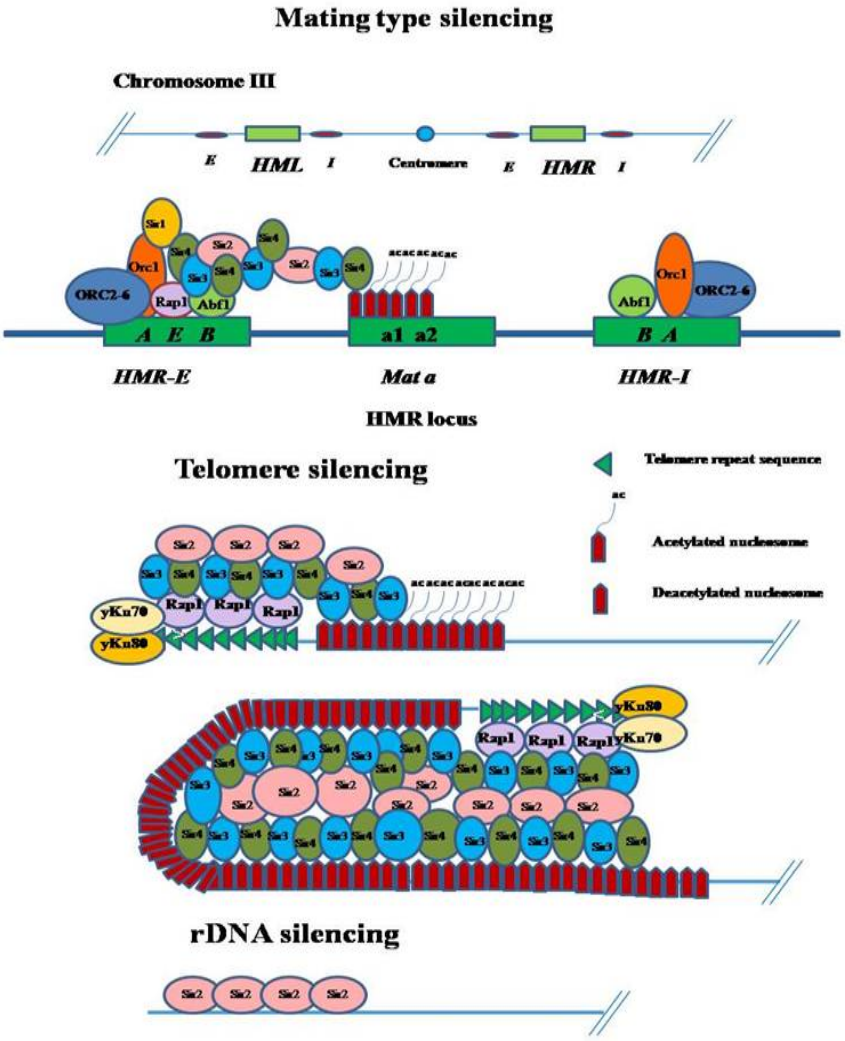

Figure 1: Schematic representation of gene silencing: Silent information regulator Sir4 recruits to the telomere binding protein Rap1 and thereby recruits other Sir proteins and hypoacetylated histones forming a compact structure that is inaccessible to *RNA* polymerase II. Mating locus recruits Sir1-4 and shows stable repression. At rDNA locus, Sir2 hypoacetylates nucleosomes and maintains silencing.

counteracted by the DNA end-binding heterodimer complex Yku70/Yku80 which anchors the telomeres to the nuclear envelope via Sir4 binding (Bertuch and Lundblad,

2003; Laroche et al., 1998; Mishra and Shore, 1999). These proteins recruit other Sir proteins to form a holo-Sir complex. Sir proteins spread from sites of nucleation and deacetylate the histones H3 and H4 and then bind more stably to the deacetylated nucleosome (Moazed et al., 2004). Silencing at *rDNA* locus is different from the *HM* loci and telomeres only Sir2, protein involves to establishing and maintaining silencing (Smith and Boeke, 1997).

Although Sir proteins are essential for repression of RNA polymerase II dependent transcription (Aparicio et al., 1991), the mechanism by which Sir proteins block transcription is still unclear. It has been proposed that Sir proteins mediate silencing by compacting chromatin into a more condensed state making it inaccessible to RNA polymerase II (Rusche et al., 2003). Experimental evidence for this model comes from studies that show that restriction enzymes and DNA methylases, which were ectopically expressed in the cell, bind less frequently to the HM loci and telomeres than active regions (Chen and Widom, 2005; Gottschling, 1992). However, Sir protein binding is not enough for gene silencing. For instance, Sir proteins have been shown to bind from *HML* to the telomere but reporter genes inserted into this intervening region are not silenced (Bi, 2002). The current understanding is that silencing requires an unknown but crucial step in establishment of gene silencing other than binding of Sirp to nucleosomes.

1.5 Chromosome organization and Genome stability

Accurate transmission of genetic material from mother to daughter cell requires proper segregation of chromosomes during cell division. The generation and survival of all organisms depends on numerous processes that need to be tightly coordinated to ensure the genome integrity and to promote genome propagation. A key event in the cell cycle is the efficient and error-free DNA replication and faithful segregation of every pair of duplicated chromosomes to daughter cells. A complete understanding of the regulation and control over cell division is critical to elucidate the mechanisms that govern self-renewal, proliferation and development of the organism. Defects in chromosome segregation lead to aneuploidy, where entire chromosomes are gained or

lost. Aneuploidy is a hallmark of most tumor cells and has been postulated to be major factor in the evolution of cancer; this could be due to mis-segregation during cell division. Cancer is generally considered an age-associated disease where somatic cells accumulate spontaneous miscarriages (DePinho, 2000).

One of the early steps in cancer progression is accumulation of higher mutation rate than normal. However, on the basis of rates of spontaneous misegregation observed in human cells, the steady accumulation of mutation does not account for the number of genetic changes that are present in most tumors (Bielas et al., 2006; Lengauer et al., 1998; Loeb et al., 2003). Several cancerous cells show genome instability, in the form of mutations and chromosome rearrangements. For example, common mutations found in colon cancer cells increase genome instability (Grady, 2004). Two types of elements have a key role in chromosome rearrangements; those that act as trans acting factors to prevent mutation and DNA rearrangements, among them are replication, repair and checkpoint proteins whereas cis acting chromosomal hotspots of instability such as fragile sites and highly transcribed DNA sequences. Although such events can be harmful for the cell and the organism, they also drive evolution at the molecular level and generate genetic variation. Genetic instability can also have a specialized role in the generation of variability in developmentally regulated processes, such as immunoglobin diversification (Maizels, 2005). Notably, there is a well established principle that cancer risk increases with age in mammals; similarly, increase in genome stability that is linked to ageing in budding yeast is also seen. This constitutes a rational explanation for the association of high cancer risk with age in mammals.

Genetic instability is further classified into different classes according to the type of events stimated. Micro and minisatellite instability (MIN) leads to repetitive-DNA expansion or contractions and can occur by mismatch repair (MMR) impairment or by homologous recombination (HR). Gross chromosomal rearrangements within two genetically linked DNA fragment by HR or end joining between non-homologous DNA fragments leads to translocation, duplication, inversion or deletion events. Genetic instability is also caused by failures in either mitotic chromosome transmission or the spindle checkpoint leading to abnormality in chromosome number.This phenomenon is referred to as chromosomal instability (Draviam et al., 2004).

1.6 Kinetochore architecture in budding yeast

For the past two decades, proteomics, microscopic studies and other biochemical approaches have allowed the isolation of the kinetochore sub-complexes. Several features of these kinetochores in yeast provide advantages for experimental analysis. Budding yeast is a good experimental model organism to address the role of kinetochore in chromosome segregation during mitosis and meiosis. In budding yeast, kinetochore assembles at the centromeric DNA in a sequence specific manner. The centromere is a ~125bp sequence, and is comprised of three elements (CDEI, II and III) which help in assembly of kinetochores. However, in humans and fission yeast, centromeric sequences are extended over several kilobases. Although these centromeres contain certain repeated sequences, the position of the centromeres is thought to be specified by epigenetic mechanisms rather than sequence specific binding events (Blower et al., 2002; Cheeseman et al., 2004). From enhanced microscopy and tomography experiments, another unique feature of budding yeast kinetochore has emerged: a single microtubule attaches to each kinetochore, whereas in other organisms multiple microtubules attached to a single kinetochore (Dorn et al., 2005).

Kinetochores act as molecular motors which connect centomeres to the microtubules. The kinetochore could be composed of more than 65 proteins; majority of them are organized into 14 subcomplexes according to their relative position in the centromeric DNA and microtubules. Kinetochores are categorized into three distinct regions: a) inner kinetochore protein complex, capable of binding to centromere DNA sequences and providing a DNA-protein platform upon which other kinetochore protein complexes assemble; b) central kinetochore protein complex bridges the inner kinetochore to the microtubule-binding outer kinetochore protein complex and c) outer kinetochore proteins connect the microtubules and other microtubule associated proteins (MAPs), to the kinetochore. Members of all these kinetochore proteins have vertebrate homologs, suggesting that the overall kinetochore structure has been conserved from yeast to mammals (Tytell and Sorger, 2006).

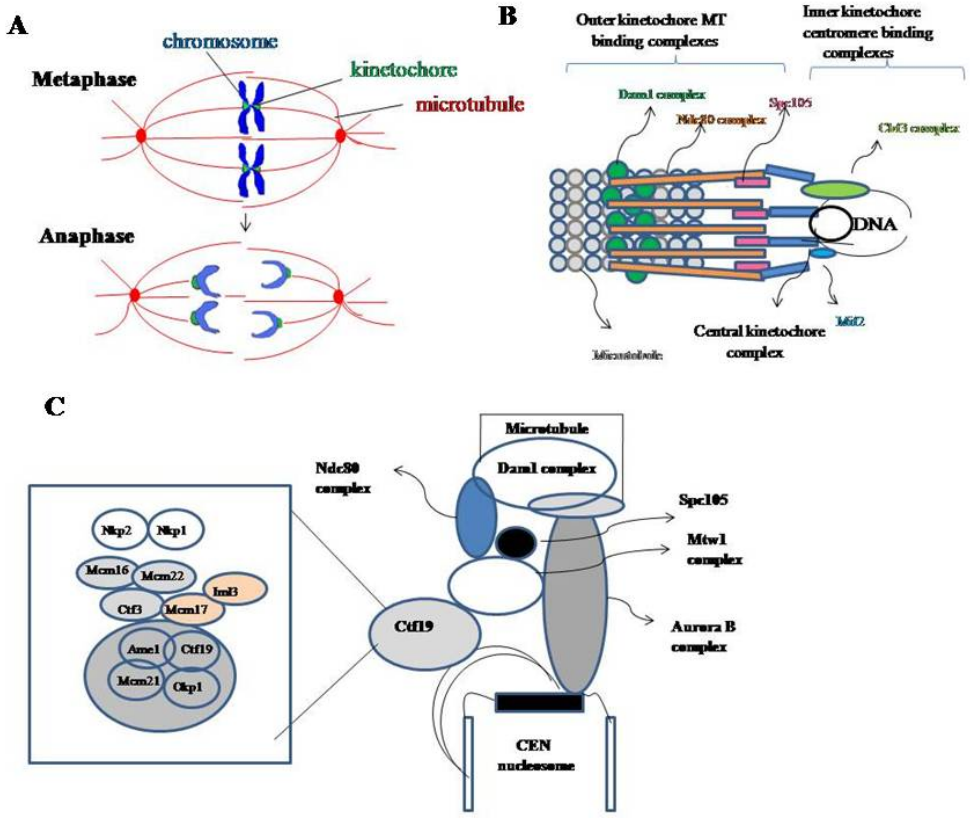

Figure 2: Chromosome segregation and kinetochore assembly: Accurate transmission of genetic material from mother cell to daughter requires proper assembly of kinetochores and stable interaction with microtubules. Panel B shows the structure of kinetochores that are assembled at centromere DNA region. Panel C shows the current predicted molecular organization of kinetochore complex.

1.7 Spindle assembly and checkpoint activation in defective kinetochores

Kinetochores are essential components for proper segregation of chromosomes during mitosis. The conserved mitotic checkpoint regulators monitor the formation of bipolar kinetochore-microtubule attachments and in the event of error, spindle checkpoint proteins arrest a cell in mitotic metaphase. The primary signal for activation of spindle checkpoint is the lack of attachment between the centromere and spindles, implicating kinetochores as the source of the signal. In fact, strains with deletions of kinetochore proteins Ndc10 and Spc25 are defective for the mitotic checkpoint,

indicating either that an intact kinetochore is required for checkpoint function or that these proteins signal to the mitotic checkpoint regulators (McCleland et al., 2003).

How kinetochores change through the cell cycle is not clear. In *Saccharomyces cerevisiae*, centromeres are clustered together and form a rosette-like structure and are positioned near the spindle pole body (which is embedded in the nuclear envelope) via microtubules throughout the cell cycle (Bystricky et al., 2004; Guacci et al., 1997; Jin et al., 2000) Centromeric clustering was recently confirmed by using more advanced technique of chromosome conformation capture (3C) coupled with massive sequencing performed on the yeast genome (Duan et al., 2010). The 3C technique relies on the capture by mild cross-linking of interaction chromatin segment can be elucidated by further intrachromosomal ligation, inverse PCR and so on (Dekker et al., 2002; Lieberman-Aiden et al., 2009; Simonis et al., 2006). This 3C technique confirmed centromere clustering in a rosette-like structure, with majority of interchromosomal contacts being concentrated near centomere DNA sequences (Duan et al., 2010; Rodley et al., 2009). Each centromere connects to the plus stand of microtubule through molecular motors called kinetochore (Joglekar et al., 2009). During interphase, the 16 assembled microtubules on kinetochores maintain the attachment between centromere and the spindle pole body SPB (Furuyama and Biggins, 2007). Although the microtubules grow and shrink continuously, the distance between centromere and SPB has been never closer than ~200nm during G1 phase. For a short period of time, centromeres are detached from the spindle pole body (SPB) in S-phase of the cell cycle. Centromere replication takes place in the late S-phase of cell cycle. The new SPB is formed *de novo* in the vicinity of the old SPB during early S-phase (Adams and Kilmartin, 2000; Lim et al., 1996; Pereira et al., 2001) and the new SPB might be too immature to generate microtubules when centromeres are to be recaptured. The old SPB usually organizes the microtubules for centromere recapture. It is hypothesized that, centromeres are forced to replicate in late S- phase of cell cycle, as by this time, the new SPB is matured and ready to recapture the centromere. All these controls and regulations suggest that the disruption of the kinetochore-microtubule architecture leads to a perturbation of the centromere clustering (Jin et al., 2000). One possible influence on chromosome organization in yeast thus appears to be the microtubule-dependent

anchorage of centromeres to the SPB that is embedded in the nuclear envelope throughout the cell cycle.

Through genome-wide protein interaction studies, it is known that Nkp2 colocalizes with the spindle pole body (Huh et al., 2003) and is a component of Ctf19. Other components of the Ctf19 complex, Iml3 and Mcm17, are involved in accurate segregation of sister chromatids and prevent non-disjunction of sister chromatids during meiosis II. These proteins are also involved in proper localization of Shugoshin protein (SgoI) to the heterochromatin free ~50kb pericentromeric domains thereby protecting it from separase-dependent cleavage. These pericentromeric regions are bound by the cohesins which helps in accurate chromosome segregation during cell division. Ctf19p is required for the increased binding of cohesins at the pericentromere regions, but whether this function is shared with other components of the Ctf19 complex is not known (Eckert et al., 2007; Ghosh et al., 2004; Marston et al., 2004).

One of the key questions in kinetochore biology is the molecular architecture of the kinetochore itself. Interactions between components have been identified through several approaches including synthetic lethal genetic analyses, immunoprecipitation experiments followed by proteomics, two hybrid analyses etc. However, as shown in Figure2, several interactions remain to be mapped. Also the importance of individual components in maintaining the fidelity of the chromosome segregation and their sub groups and sub functions are not clear.

In this work we report that *NKP2* encodes an important component of the kinetochore. Although our screen was designed to discover components involved in nuclear organization, the chromosome loss induced by *NKP2* dosage was scored as loss in silencing owing to is stochastic behaviour. As very little is known about the role of Nkp2 in the kinetochore, we pursued our investigations into the importance of Nkp2 function. We found that overexpression of kinetochore protein Nkp2, leads to loss of chromosomes at a low rate. However, loss of *nkp2* leads to increased genome instability via loss of chromosomes. We also carried out synthetic genetic interactions between multiple components of the kinetochore and *nkp2*Δ and find that some of those components cooperate with *NKP2* to promote chromosome transmission fidelity.

1.8 Objectives of the study

From the detailed overview presented above, it is evident that the spatial organization of genes and chromosomes plays an important role in nuclear functions. New imaging and biochemical techniques, studies of yeast nucleus have led to significant insight into chromosome arrangement and dynamics. Yeast telomeres provide a model system to investigate the molecular principles involved in chromosome –chromosome interactions and the assembly of chromosome based compartments. They also provide us with a tool to study the chromosome-nuclear envelope interactions. Keeping in view these observations, the present study has been undertaken with the objectives to investigate the molecular principles and understand many aspects of three dimensional chromosomal architecture, chromosome dynamics and functional compartmentalization. Given the implications for fundamental genome functions, a major objective to identify or better understand the principles that drive chromosomal organization.

To address this issue we performed

- Genetic screen for factors that disrupt nuclear envelope anchoring dependent silencing.
- Identification and characterization of components indentified in the screen.

Chapter - 2

Materials and Methods

2.1 Yeast methods

2.1.1 High efficiency yeast transformation

Yeast transformations with plasmids (including genomic library) or PCR products were done based on high efficiency LiAc protocol (Gietz and Woods, 2002). $5x10^6$ cells from the overnight incubated primary culture were added to the 25ml broth and incubated for 4-5 hrs at 30ºC with constant rotation. $1x10^8$ cells from the secondary culture were used for transformation. The cell pellet was washed in 1ml of 0.1 M LiAc and resuspended in 240µl of 50% Poly ethylene glycol (PEG). To this mixture, 36µl of 1M LiAc and 74 µl of transformation mix containing 40µl of salmon sperm DNA and 34µl of both plasmid/DNA fragment and sterile MilliQ water were added. Cells were vortexed briefly and incubated at 42ºC for 40 minutes. Then cells were spun at 13k for 15 sec and cell pellet was resuspended in 200µl of sterile water and plated on selective dropout media. If the selection was on G418 plates, the cell pellet was resuspended in 1ml of YPD broth and incubated at 30ºC for 10-12hrs to allow the expression of the gene and then plated on YPD media containing (200 µg/ml) G418 drug.

2.1.2 Extraction of genomic DNA from yeast cells

2.1.2.a. Zymolyase method

Cells grown overnight in 5ml of YPD or in selective broth were harvested by centrifuging at 3 k rpm for 5 min. The cell pellet was resuspended in 0.5 ml of 1M Sorbitol and 0.1M Na_2 EDTA (pH 7.5) and transferred into 1.5 ml microfuge tube. Cells were speroplasted by incubating the cell suspension with 20 µl of Zymolyase 100,000U (2.5 mg/ml) at 37ºC for 60 min. Cells were centrifuged for 1 min at 13 k rpm and the cell pellet was resuspended in 0.5 ml of 50mM Tris-Cl (pH 7.4) and 20mM Na_2 EDTA (pH 8.0). 50 µl of 10% SDS was added to the cell suspension, mixed well and then incubated at 65ºC for 30 min. 200 µl of 5M Potassium Acetate was then added to the cell suspension and placed in ice for 60 min. Cells were centrifuged for 5 min at 13 k rpm and supernatant was tranferred to a fresh microfuge tube. One volume (0.75 ml) of 100% isopropanol was added to the supernatant, mixed and allowed to sit at room temperatue for 5 min. Then centrifuged very briefly for 2 min at 13 k rpm and

supernatant was poured off. DNA pellet was air dried and resuspended in 0.3 ml of TE (pH 7.4) containing 20 µg/ml of Rnase A. DNA was incubatded at 37ºC for 30 min for degrading RNA. Then 30 µl of 3M Sodium Acetate (pH 7.0) was added to the DNA solution and mixed. To this, 0.2 ml of 100% isoproponal was added and mixed once again. DNA was recovered by centrifuging at 13 k rpm for 2 min. The supernatant was poured off, DNA pellet was air dried and resuspended in 30µl of TE (pH 8.0).

2.1.2.b. Rapid isolation of genomic DNA from yeast cells

Cells grown overnight in 5ml of YPD or in selective broth were harvested by centrifuging at 3 k rpm for 5 min. The cell pellet was washed in 0.5 ml of sterile distilled water and resuspended in 200 µl of breaking buffer. Glass beads (~ 200 µl volume) were added to the cell suspension and then 200 µl of phenol/chloroform/isoamylalchohol (25:24:1) was added and mixed. Cells were vortexed at high speed for 2 min. 200 µl of TE (pH 8.0) was added and once again vortexed briefly for 10 to 15 sec. Then the sample was centrifuged at 13 k rpm for 5 min at room temperature. The aqueous layer was transferred to a clean microfuge tube and 1 ml of 100% ethanol was added and mixed by inversion. DNA was recovered by centrifuging at 13 k rpm for 5 min. The supernatant was poured off, DNA pellet was air dried and resuspended in 30µl of TE (pH 8.0).

2.1.3 Extraction of whole cell protein from yeast cells by Trichloroacetic acid (TCA) method

Cells grown overnight in 5ml of YPD or in selective broth were harvested by centrifuging at 3 k rpm for 5 min. The cell pellet was resuspended in 200 µl of 20% TCA and glass beads were added up to the meniscus and then cells were lysed by vorteing for 1 min. Cell suspension was transferred into a new microfuge tube. Glass beads were washed twice with 200 µl of 5% TCA and the washes were added to the previous suspension. Cell pellet was collected by centrifuging at 3 k rpm for 10 min and resuspended in 200 µl of 1x Laemmli buffer. The laemmli buffer turns red because of the low pH of cell pellet. Therefore, 50 µl of 1M Tris base (no pH adjustment) was added to turn blue. The sample was boiled for 3 min and centrifuged again at 3 k rpm

for 10 min. Protein sample was transferred to a new microfuge tube and the pellet was discarded.

2.1.4 Spore enrichment

Diploid cells were grown on dextrose deficient YPK medium and incubated at 25ºC for 4-5 days. Tooth pick full of spores were resuspended in 500 µl of YPD broth. The cell suspension was vortex mixed and centrifuged at 13 k rpm for 10 sec. The cell pellet was resuspended in 1 ml of 100 µg/ml of zymolyase (100,000U) and incubated at 30ºC for 20 min. 500 µl of cell suspension was aliquot in separate microfuge tube and centrifuged at max speed for 30 sec. Cell pellet was washed in 1 ml of sterile water and resuspended in 100 µl of sterile water. Cells were then agitated for 2 min in upright position using vortex mixer at max speed. Aqueous cell suspension was discarded and the tube was rinsed with sterile water for several times. The spores were resuspended in 1 ml of 0.01% Nonidet P-4. Appropriate volume of cell suspension was plated on YPD medium and incubated at 30^0C for one day (refer Guthrie and Fink, 1991).

2.1.5 Silencing assay

Silencing assays were done to test the loss in silencing in yeast. For this, the yeast cells were initially grown in nutrient rich broth or selective broth dropped out for specific amino acids (for retaining plasmids) at 30ºC with appropriate rotation for overnight and then the culture was subjected to 10 fold serial dilution for 5 times. 5 µl of each dilution was spotted on complete medium to check the total number of cells grown and on selective medium for measuring the loss in silencing of reporter gene. For example, loss in silencing of *TRP1* reporter gene is tested by spotting on tryptophan dropout medium. In case, the reporter gene is *URA3*, then serially diluted cultures were spotted on the medium containing 1mg/ml of 5-FOA (5-Fluoro orotic acid). Expression of the *URA3* gene (Orotidine-5'-phosphate decarboxylase) leads to the conversion of 5-FOA into 5-fluorouracil, a toxic compound. This indicates that strains expressing *URA3* cannot grow in this medium and those repressing *URA3* can grow. Therefore, 5-FOA serves as a good indicator of the expression status of the *URA3* reporter gene. After spotting, plates are incubated at 30ºC for 2-3 days and analyzed loss in silencing by observing growth of cells.

2.1.6 Construction of mutants and tags in yeast

Strains with gene deletion and tagging were done as described in (Longtine et al., 1998). For gene knockout, DNA fragment was PCR amplified so as to contain selectable marker flanked by around 30 bp of DNA of the region of the gene of interest. This fragment was transformed into yeast by high efficiency LiAc protocol (Gietz and Woods, 2002). The flanking regions recombine with the genomic region of the gene of interest by homologous recombination and insert the selectable marker in place of the gene. Therefore, the gene is replaced by selectable marker. For gene tagging, the forward primer was designed by taking sequence just upstream of the stop codon and in frame so that it does not disrupt the reading frame of the tag and selectable marker which are going to be inserted in the downstream of the gene. These insertions were confirmed by screening PCR which gives diagnostic 500bp fragment. The sequences of the primers used for gene deletion, tagging and screening PCR are given in Table 3.

The strains that showed positive in screening PCR were further confirmed by genomic southern analysis. Genomic DNA from these strains was subjected to restriction digestion with appropriate enzymes that gives different fragments at gene locus of interest in wild type and deletion/tagged strains. The digested genomic DNA was transferred to nylon membrane and subjected to southern hybridization with radio labelled probe. The blot was then exposed to X-ray film to obtain the autoradiogram.

2.1.7 Tetrad dissection of yeast spores

Diploid cells were grown on dextrose deficient YPK medium and incubated at 25ºC for 4-5 days. Tooth pick full of spores were resuspended in 500 µl of YPD broth. The cell suspension was vortex mixed and centrifuged at 13 k rpm for 10 sec. The cell pellet was resuspended in different concentration of 100 µg/ml of zymolyase (100,000U) and incubated at 30ºC for few seconds to 2 minutes. Check under light microscope for tetrad which are intact and place 20µl of the suspension vertically from the middle of the YPD agar plate so that the suspension spread from one corner to other. Dissect the tetrad spores on YPD by using Olympus tetrad dissection microscope and plates were incubated for 2 days at 30ºC and patch four individual colonies on YPD to test auxotrophic markers segregates as 2:2 ratio.

2.1.8 Quantitative mating assay in yeast diploid cells

Quantitative mating assay was performed on diploid wild type and deletion mutants. Initially cells were grown on YPD or selective media at 30ºC for overnight. The mating tester either Mat a and Mat α strains (1 X 10^8 cells) were grown in YPD and mixed with 2 X10^6 diploid cells and collected on a nylon filter. Filters were transferred (cell side up) to YPD plates and incubated for 4 hrs at 30ºC to allow cells to mate. Diploid cells that have lost the MAT a locus become competent to mate with the mating tester MAT a and vice versa. Cells from the filter were then resuspended in buffer saline and plated at several dilution onto the SD plates and incubated at 30ºC until colonies were large enough to count. We also tested the mating locus mutant cells that have lost the either MAT a or MAT α by spot assay for this we incubated the diploid cells mix with the appropriate number of mating tester and incubated in liquid media for overnight and 10 fold serial dilutions were made and 5 µl of diluted samples spotted on synthetic deficient plates and YPD plates to test the lost of MAT locus.

We also performed quantitative mating assay on multiple heterozygous marker (MHM) wild type and deletion mutants to test the LOH events at MAT locus. To this we followed the similar protocol as described previously, but the exact number of MHM strains would be quantified by selecting the MHM strain in synthetic deficient supplemented with Histidine and Lysine, which permissive for growth of deletion mutants but not mating tester PT-1 cells.

2.1.9 Artificial chromosome (*SUP11*) loss assay

Artificial chromosome *SUP11* (Ade+) was introduced into the kinetochore mutants initially which are Ade- by crossed them with wild type strain carrying the artificial chromosome *SUP11* and tetrad dissection was performed to isolate mutants with *SUP11* from the spores. Wild type and mutant with *SUP11* initially selected them on Adenine drop out media for overnight at 30ºC to retain the *SUP11*. Several dilutions were made and plated them on YPD agar plates with minimal Adenine concentration (6µg/ml) and incubated at 30ºC until colonies become large enough (3- 4 days) to scored *SUP11* lost with half sectored red and white colonies.

2.1.10 Half-sector (LOH) assay in MHM strains

Half sector assay was performed on each diploid multiple heterozygous marker (MHM) strain to calculate the rate of loss of heterozygosity (LOH). Initially, wild type and MHM deletion mutant strains were grown on selective media plates to maintain the heterozygosity. Two colonies from each deletion mutants and wild type isolates were picked and resuspended in PBS and several dilutions were made, plated about 150 cells on large plates contained lead nitrate media and incubated at 30ºC for 3-7 days. The rate of LOH event per cell division was determined by obtaining the frequency of half-sectored colonies, either red/white or black/white among total colonies excluding fully those colonies that were completely coloured. The rate of LOH events calculates as

The rate of LOH= Half-sectored colonies / [All colonies- (2 X fully coloured colonies)]

2.2 Recombinant DNA methodology

2.2.1 Preparation of ultra competent DH5 α cells

Ultra competent cells of *DH5α* strain of *E.coli* were prepared by Inoue method described in (Sambrook and Russell, 2001). A single bacterial colony was inoculated in 25 ml of SOB/LB broth and incubated at 37ºC with constant rotation around 150-200 rpm for 6-8 hrs. This primary culture was then inoculated (4ml, 3ml, 2ml, 1ml) into four 250 ml conical flasks containing 100 ml of SOB broth and incubated at 18-22ºC with moderate shaking for overnight. Incubation was stopped when the OD reached 0.55 at 600nm and cells were harvested by centrifuging at 2500g for 10 min at 4ºC. Supernatant was poured off and centrifuge tube was stored open on a stack of paper towel for 2 min to drain away the broth completely. Cell pellet was resuspended in 32 µl of inoue transformation buffer for 100 ml of initial culture. Cells were harvested again by centrifuging at 2500g for 10 min at 4ºC. Supernatant was discarded and centrifuge tube was stored open on a stack of paper towel for 2 min to drain away the solution completely. The cells were then suspended in 2 ml of ice cold inoue transformation buffer and 0.15 µl of DMSO was added and mixed by swirling and stored in ice for 10 min. Bacterial suspension was aliquot into microfuge tubes and immediately snap froze

by immersing the tightly closed tubes in liquid nitrogen. Then the tubes were stored at -70ºC until needed.

2.2.2 Bacterial transformation

Ultra competent *E.coli* (*DH5α* strain) cells were thawed and aliquot into a sterile microfuge tube. 2.5µl of plasmid DNA of concentration around 10µg was added to 50µl of competent cells or 10 µl of ligation mixture was added to 100µl of competent cells. The tubes were stored in ice for 30 min and then transferred to 42ºC for exactly 90 sec. Then they were rapidly transferred to ice and kept for 1-2 min. 1ml of LB broth was added to each tube and incubated at 37ºC for 45 min. The samples were centrifuged at 5000 rpm for 1 min and the cell pellet was resuspended in 200µl of LB broth and plated on LB medium containing 100µg/ml of ampicillin or 50 µg/ml of Kanamycin. The plates were allowed to dry and incubated at 37ºC for overnight.

2.2.3 Alkaline lysis minipreparation for plasmid extraction from bacterial transformants

Plasmid DNA was isolated from bacterial transformants by alkaline lysis miniprep method described in (Sambrook and Russell, 2001). Single bacterial colony was inoculated in 5 ml of LB broth containing 100µg/ml of ampicilin and incubated at 37ºC and 160 rpm for overnight. 1.5ml of bacterial culture was transferred in a microfuge tube and centrifuged at 13 k rpm for 1 min. The cells were resuspended in 200µl of solution I and then solution II was added and mixed by gently inverting the tube for 5 times till the solution is turned clear and viscous. Ice cold 200µl of solution III was added and mixed immediately by inverting several times and left on ice for 5 min and the solution turns into a white precipitate. Then the sample was centrifuged for 8 min at 13 k rpm at 4ºC. Supernatant was gently pipette and transferred to another clear microfuge tube. To this solution 420µl of 100% isopropanol (0.7 volume) was added and mixed by inverting. DNA was precipitated by centrifuging at 13 k rpm for 10 min and the pellet was washed with 500µl of 70% ethanol and once again centrifuged at 13 k rpm for 2 min. Supernatant was discarded, DNA pellet was air dried and resuspended in 30-50 µl of TE pH8.0 containing 30 µg/ml of RNaseA.

2.2.4 Construction of plasmids

EST2 clone in multi copy plasmid **(**CKM206) was constructed by digesting 2a genomic library plasmid by *BamHI* and *SalI* enzymes and DNA fragment of size 3.8 kb containing full length *EST2* gene along with its promoter region was ligated into *BamHI* and *Sal1* digested multi copy vector, Yeplac181 (CKM6) listed in Table 2. Full length *NKP2* gene along with its promoter was amplified by PCR digested with *EcoRI* & HindIII and cloned into *EcoRI* and HindIII digested Yeplac 181multi copy vector (CKM204). Sequences of the primers used for cloning *NKP2* were given in Table.3.The other plasmids used in this work are listed in Table.2. Plasmids used as templates in PCR to generate yeast knockouts and tags are described in (Longtine et al., 1998).

2.3 Methods in yeast cell biology

2.3.1 Western blot

KRY549 (*NKP2*-13xmyc) and *ctf19* subcomplex mutants with NKP2-13xmyc strains was grown in liquid media for overnight at 30ºC. Whole cell protein from the tagged strains was extracted using standard TCA protocol described in (Lewis et al., 2007). Equal amounts of protein were loaded in two separate 10% polyacrylamide gels. After electrophoresis, proteins were transferred to two PVDF membranes and blocked with 5% non fat dry milk in TBST (150 mM NaCl, 10mM Tris-HCl pH8.0 and 0.1% Tween 20) buffer for one hour at RT. Then the membranes were incubated with anti myc antibody, (1:30,000 in 1% BSA in TBST buffer) for Nkp2-myc. The membranes were washed thrice in TBST buffer for 10 min each and incubated with secondary anti-rabbit-HRP antibody (1:10,000 in 1% BSA in TBST buffer) for Nkp2-myc for 1 hour at RT. Membranes were washed thrice with TBST for 10 min each and BioRad detection reagents and BioRad versadoc instrument were used for detecting the protein of interest as directed by manufacturers instructions. Same blots was stripped with stripping solution and probed with anti-Sir2 antibody (1:2,000 in 1% BSA in TBST buffer) for Sir2 for 2 hours at Room Temperature and incubated with secondary anti-rabbit-HRP antibody (1:10,000 in 1% BSA in TBST buffer) for Sir2 for 1 hour at RT to check the loading consistency.

2.3.2 Immunofluorescence

Immunofluorescence was done as described in (Gotta et al., 1996). Briefly, diploid yeast strains KRY109 (Sir4-13xmyc) was transformed with either empty vector CKM6 or *EST2, NKP2* multi copy plasmids listed in Table 2 and the transformants were grown in SC-Leu broth and KRY549(.NKP2-13xmyc:his) and other Ctf19 subcomplex mutants with NKP2-13xmyc strains listed in Table 1 were grown in liquid YPD Overnight grown 5ml cultures were fixed with 0.5 ml of formaldehyde and incubated at 30ºC in a shaker for 20 min. Cells were then washed thrice with sterile water and resuspended in 200 µl of 0.1M EDTA-KOH and 10mM DTT and incubated at 30ºC for 10 min. Cell suspension was centrifuged at 3 k rpm for 5 min. The cells were spheroplasted by resuspending in 200 µl of YPD broth containing 1.2M sorbitol and one-tenth volume of zymolyase (2.5mg/ml) and incubated at 30ºC for 30 min. Spheroplasts were washed thrice with 500 µl of YPD sorbitol and resuspended in 100 µl of YPD sorbitol. Spheroplasts were spotted on multi-well slides coated with polylysine. They were further permeabilized with methanol and acetone by incubating for 5 min and 1 min respectively at -20ºC. Spheroplasts were blocked with 1% bovine serum albumin and incubated with appropriate primary antibody dilutions (mouse NSP1 antibody 1:500, rabbit myc antibody 1:12,000, rabbit SIR2 antibody 1:2000) for overnight at 4^{o}C. Cells were then thoroughly washed thrice with PBST buffer for 5 min each and incubated with recommended dilutions of fluorescently labelled secondary antibody (alexa fluor tagged secondary anti mouse antibody 1:500, Cy3 tagged secondary anti rabbit antibody 1:500) in dark at room temperature for 45 min. Cells were thoroughly washed thrice with PBST buffer for 5 min each. After washes, slides were mounted in mounting medium containing DAPI and then viewed and photographed in a Leica confocal microscope. Images were processed using the same software.

Tables

Table 1: List of the yeast strains used in this study

All strains used in this study were isogenic to W303

Name	Genotype	Source/Reference
KRY1	W303-1A/W303-1B MAT a/MAT α	(Thomas and Rothstein, *1*989)
KRY2	W303-1A (*leu2-3,112 his3-11,15 ura3-1 ade2-1 trp1-1 can1-100 rad5-535*) MAT a	(Thomas and Rothstein, 1989)
KRY3	W303-1B (*leu2-3,112 his3-11,15 ura3-1 ade2-1 trp1-1 can1-100 rad5-535*) MAT α	(Thomas and Rothstein, 1989)
KRY9	*yku70*::*Kanmx6 hmrAeb*:: *3xUASg TRP1* + *gal4::Leu2* (Leu+)	(David Shore)
KRY12	*adh4::URA3*-TelVII L MAT α	(Gotschling et al., 1990)
KRY28	*hmrΔaeB :: 1XUASgURA3* MAT a	(Sternglanz)
KRY30	*his1*- MAT a (mating tester)	
KRY31	*his1*- MAT α (mating tester)	
KRY33	SIR4-13xmyc:*KanMx6* MAT α	(David Shore)
KRY38	W303-1B *ADE2*+ MAT α	(Susan Wente)
KRY48	*hmr ΔAeb*::3x UASg *TRP1* MAT α (YSB35b)	(Chien et al., 1993)
KRY62	*hmr AΔeΔb*::3x UASg *TRP1* MAT α *adh4::URA3*-TelVII L MAT α	This study
KRY109	*SIR4*-13xmyc:*KanMx6* (Diploid)	This study
KRY276	*nkp2::TRP1* MAT a	This study
KRY277	*nkp2*::*his5*+ MAT α	This study
KRY311	*nkp2*::*TRP1 hmrΔ*aeB:: *1XUASg URA3* MAT α	This study
KRY313	*nkp2::TRP1 adh4::URA3*-TelVII L MAT α	This study
KRY314	*nkp2*::*his5*+ *adh4::URA3*-TelVII L MAT α	This study
KRY315	*nkp2::TRP1/ nkp2*::*his5*+ MAT a/MAT α	This study
KRY501	W303 ade2 can1 leu2 his3/cyc1 *LacI::URA3*	

	LacO::TRP1(CENIV)/LACO::TRP1	
	spo13::hisG/Spo13(diploid)	(AW Murray1996)
KRY509	W303 ade2 can1 leu2 his3/cyc1 *LacI::URA3*	
	LacO::TRP1(CENIV) MAT a	This study
KRY510	W303 ade2 can1 leu2 his3/cyc1 *LacI::URA3*	
	LacO::TRP1(CENIV) MAT α	This study
KRY520	*ade2::hisG his3Δ leu2Δ lysΔ met15:: TRP1 trp1Δ63*	
	ura3Δ sam2::ADE2 NatMx on Chr IVL MAT α	(Gottschling 2008)
KRY521	*ade2::hisG his3 Δ 200 leu2 Δ lys2 Δ MET15*	
	*trp1 Δ 63 ura3 Δ sam2::*URA3 *HPhMx on*	
	Chr IVL MAT a	(Gottschling 2008)
KRY525	*sam2::ADE2*/*sam2*::*URA3 met15*::*TRP1/MET15*	
	NatMx4 on Chr IVL/*HpMx4* on Chr IVL (diploid)	This study
KRY526	KRY525 except *csm3::KanMx4/csm3::KanMx4* (diploid)	This study
KRY528	KRY525 except *ctf19::KanMx4/ctf19::KanMx4* (diploid)	This study
KRY532	KRY525 except *nkp2::KanMx6/nkp2::KanMx6* (diploid)	This study
KRY549	*NKP2*-13xMyc:*his5*+ *ADE2* MAT α	This study
KRY950	KRY2 *SUP11*	This study
KRY951	KRY950 *SUP11*except *ctf3::KanMx4* MAT a	(Marston 2009)
KRY952	KRY950 SUP11except *nkp1::KanMx4* MAT a	(Marston 2009)
KRY953	KRY950 *SUP11*except *nkp2::his5*+	This study
KRY954	KRY950 *SUP11*except *mcm16:: KanMx4*	This study
KRY955	KRY950 *SUP11*except *mcm17:: KanMx4*	This study
KRY956	KRY950 *SUP11*except *mcm21:: KanMx4*	This study
KRY957	KRY950 *SUP11*except *mcm22:: KanMx4*	This study
KRY958	KRY950 *SUP11*except *iml3:: KanMx4*	This study
KRY959	KRY950 *SUP11*except *ctf19:: KanMx4*	This study
KRY960	KRY950 *SUP11*except *nkp2::his5*+ *ctf3::KanMx4*	This study
KRY961	KRY950 *SUP11*except *nkp2::his5*+ *nkp1::KanMx4*	This study

KRY962	KRY950 *SUP11*except *nkp2::his5+ mcm16::KanMx4+*	This study
KRY963	KRY950 *SUP11*except *nkp2::his5+ mcm17:: KanMx4*	This study
KRY964	KRY950 *SUP11*except *nkp2::his5+ mcm21:: KanMx4*	This study
KRY965	KRY950 *SUP11*except *nkp2::his5+ mcm22:: KanMx4*	This study
KRY966	KRY950 *SUP11*except *nkp2::his5+ iml3:: KanMx4*	This study
KRY967	KRY950 *SUP11*except *nkp2::his5+ ctf19:: KanMx4*	This study
KRY1000	*NKP2*-13xMyc:*his5+ nkp2::his5+MPS3-HA-HIS3*	This study
KRY1001	KRY1000 *except mcm22::KanMx4* MAT α	This study
KRY1002	KRY1000 *except iml3::KanMx4* MAT a	This study
KRY1006	KRY1000 *except mcm21::KanMx4* MAT a	This study
KRY1009	KRY1000 *except ctf3::KanMx4* MAT α	This study
KRY1013	KRY1000 *except nkp1::KanMx4* MAT α	This study
KRY1015	KRY1000 *except mcm17::KanMx4* MAT a	This study
KRY1017	KRY1000 *except ctf19::KanMx4* MAT a	This study

Table 2: List of the plasmids used in this study

Name of the plasmid	Old Name	Brief Description
CKM6	YEplac181	2μ plasmid containing *LEU2* marker
CKM17		*p RAP1*-G_{BD} in pRS313
CKM18		*p RAP1*-G_{BD} – Rap1 in pRS313
CKM32		*CEN* plasmid containing *HIS3* marker
CKM51		G_{BD} -Yif1 in pMA424
CKM57	E94	*p RAP1*-G_{BD} – Sir4 in pRS313
CKM67	E335	pFA6a-kanMx6 (gene deletion)
CKM68	E336	pFA6a-TRP1 (gene deletion)
CKM69	E337	pFFA6a-His3Mx6 (gene deletion)
CKM74	E342	pFA6a-13XMyc –His3Mx6 (C-terminus tagging)
CKM90	E358	pFA6a-13Myc-kanMx6 (C-terminus tagging)
CKM202	2a Library plasmid	Consisting of Chr XII fragment (764622-768636) i.e., *NKP2* & *EST2*
CKM204	YEplac181+ *NKP2*	PCR product of *NKP2* digested with *HindIII* and *EcoRI inserted* into CKM6
CKM205	YEplac181+ *EST2*	*BamHI & SalI* cuts *EST2* from *2a* library plasmid

Table 3: List of primers and their sequences used for PCR in this study

Name of the primer	Primer sequence (5' to 3')	Purpose
F1 *NKP2*	GACAATTGTGCTCCCAATCTTGCTTTGAAATTACCATTATA GAACTCcggatccccgggttaattaa	*NKP2* gene deletion
F2 *NKP2*	GCCATTCCTGGCCTATTACAAATTATACAATCTTATATTAA TTAcggatccccgggttaattaa	*NKP2* deletion/C-terminal tagging
R1 *NKP2*	GGAATATCCTGTGGGGCAGGTTGACCGGGATGTCTGCT GCTAGTTTTCCgaattcgagctcgtttaaac	NKP2 gene C-tagging
Scr *NKP2*	GAAGATGGCAGAAACTCG	Screening PCR
5N1 *NKP2*	CGAAGCTTCAATGGATCGGCGAGGAATATC	Cloning full length *NKP2* gene with promoter
3N1 *NKP2*	AGGAATTCGGAAGGAGAAATCTAGAGG	Cloning full length *NKP2* gene
Yep13 F	GCTACTTGGAGCCACTATC	DNA Sequencing
Yep13 R	CCAGCAACCGCACCTGT	DNA Sequencing

Chapter - 3

Genetic screen for factors that disrupt Gbd-Yif1 mediated silencing

3.1 Introduction

As summarized in section 1.4, yeast heterochromatin is clustered at the nuclear periphery. These clusters contain the cryptic mating-type loci *HML* and *HMR* and telomeres. Both telomeres and the *HMR* and *HML* are also associated with silencer proteins (Sir1-4) (Gotta et al., 1996). Yeast telomeres contain tandem repeats of $TG_{(1-3)n}$ that serve as binding sites for Rap1p. The multiple Rap1 sites at the telomeres recruit Sir proteins directly. Sir proteins are essential for RNA polymerase II dependent gene silencing (Aparicio et al., 1991). It has been proposed that Sir proteins mediate silencing by deacetylating the histone H3 and H4, compacting chromatin into a more condensed state making it inaccessible to RNA polymerase II (Rusche et al., 2003). Typically, telomeric silencing or TPE is analysed by placing reporter genes immediately proximal to the telomere repeats.

HM loci are flanked by two silencer elements, *E* and *I*, which contribute to establishment of silent chromatin at this locus. The *HMR-E* consists of cis-acting sequences, *A*, *E*, and *B*, that serve as binding sites for trans acting factors Orc1p, Rap1p and Abf1p, respectively. These silencer bound proteins in turn, recruit the Silent Information Regulators (Sir1p, Sir2p, Sir3p, and Sir4p). Sir2p, an evolutionarily conserved NAD-dependent histone deacetylase, begins to deacetylate specific sites on histones H3 and H4 in the nuleosomes. These deacetylated nucleosomes serve as high affinity binding sites for Sir3p and Sir4p and spread along *HMR* locus and establish silenced chromatin or heterochromatin (Fox and McConnell, 2005; Rusche et al., 2003). Therefore, silencer elements serve as recruiters of Sir proteins and can be by-passed if the Sir proteins are directly tethered to this region (Buck and Shore, 1995; Chien et al., 1993; Gotta et al., 1996; Marcand et al., 1996; Moretti and Shore, 2001). These tethering assays have been instrumental in our understanding of the establishment, maintenance and propagation of heterochromatin.

In an attempt to understand the requirements for the establishment of heterochromatin, the Sternglanz laboratory initiated a screen for factors when tethered

could establish silencing. The screen identified many new factors (Andrulis et al., 1998) but also proved a very important point. They obtained multiple factors of the inner nuclear membrane/golgi apparatus as factors that could establish silencing when tethered. The only common factor between these proteins or parts of proteins that they obtained, were that they all contained a domain that would tether the proteins to the nuclear membrane. A series of experiments then directly demonstrated that when the silencer defective *HMR* locus was tethered to the nuclear membrane, it could establish silencing in a Sir protein dependent manner. It was speculated that this silencing was due to the concentration of Sir proteins at the nuclear periphery.

Based on these studies, we designed a genetic screen to identify proteins that might be involved in telomere organization at nuclear periphery.

3.2 Results

3.2.1 Construction of strains for the genetic screen for components involved in the organization of telomeres:

Yeast telomeres are clustered together in a few groups and are sequestered at the nuclear periphery. These foci contain the silent mating type loci, *HMR* and *HML* and together they form the heterochromatin compartment. Any disruption in the organization of this compartment leads to loss of telomeric silencing. We constructed a strain that will report the loss of this organization as loss of silencing.

W303 *hmr Aeb* 3x*UASg TRP1* TEL VIIL *ADE2*

W303: Strain background

hmr ΔAeb defective *HMR E* silencer

3x*UASg* three copies of Gal4 binding sites

TEL VIIL *ADE2* the left telomere of chromosome VII modified to include an *ADE2* gene

1) hmr ΔAeb::* 3x*UASg TRP1: The mating type locus, *HMR* has been modified:

a) The *E* silencer, which has 3 *cis* elements that recruit DNA binding proteins that in turn recruit the silencing proteins, has been mutated to remove the silencer elements, ***E*** and ***B***. These mutations now render the silencer defective and so, silencing at the mating locus, *HMR* is lost. b) Secondly, the defective silencers were replaced with the three copies of upstream activator sequences of Gal10 gene that serve as binding sequences for the Gal4 protein. This allows Gal4p or any protein that contains the Gal4 DNA binding domain to bind here. In such a strain, as the *HMRE* silencer is defective, there is no silencing of the *HMR* locus. C) Thirdly, the endogenous Mat *a* information for mating was replaced with *TRP1*, an auxotrophic marker (Chien et al., 1993). Therefore, as there is no silencing in this strain, the *TRP1* gene is transcribed and allows the strain to grow in medium lacking tryptophan. When silencing is re-established, the strains will be auxotrophic for tryptophan and will require supplementation of the growth medium with tryptophan for survival. Therefore, growth on medium lacking tryptophan indicates loss of silencing and lack of growth indicates establishment of silencing.

2) TEL VIIL *ADE2*: The left arm of chromosome VII is modified to contain *ADE2* gene just upstream of the telomere repeats. Genes which are placed close to the telomeric repeats are silenced due to the repressive chromatin structures that emanate from the ends. Therefore *ADE2* is silenced. When Ade2p is not produced, the adenine biosynthesis stops prematurely, producing an intermediate product P-ribosylamino imidazole which results in accumulation of red coloured pigment. Therefore, cells that are epigenetically repressed are red-sectored and cells that express the Ade2p and are white in colour. This leads to the production of red-sectored colonies. This gives a visual screen for the state of TPE which in turn is necessary for silencing of *TRP1* by Yif1.

3.2.2 Testing our hypothesis in the mutant background:

In order to test our hypothesis that the silencing will be disrupted in strains that lack peripheral anchoring of telomeres, we introduced *yku70* mutation in the strain

discussed above (Table 1; KRY9). Yku70p is required for anchoring the telomeres to the nuclear periphery, and in *yku70* mutants, the telomeres are more internal, the number of telomere clusters increase and the Sirp pool at the telomeres is disrupted, with Sirp found distributed in the nucleoplasm. Therefore, this strain was transformed with Gbd, Gbd-Rap1, Gbd-Sir4 and Gbd-Yif1, and tested for silencing.

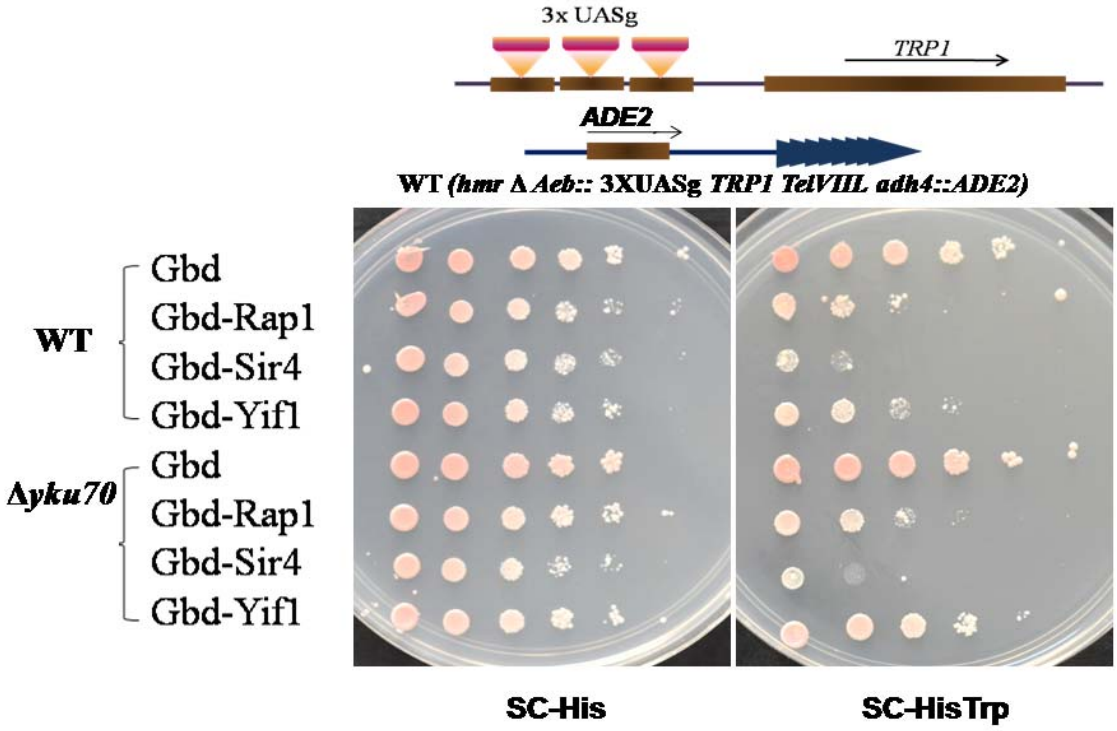

Figure 3: Targeted silencing in WT and *yku70Δ*. Gbd fused proteins were transformed into wildtype (KRY62) and *yku70* (KRY9). Transformants were grown overnight in SC-His broth and 5µl of 10 fold serial dilutions was spotted on SC-His (to select for the plasmid) & SC-HisTrp (to assay silencing).

As shown in Figure 3 and summarized in Table 4, Gbd-Rap1,Gbd-Sir4 and Gbd-Yif1 are able to establish silencing at the modified *HMR* locus and therefore the strains cannot grow on medium lacking tryptophan as seen in rows 2 to 4, whereas Gbd alone does not silence the *TRP1* gene row 1. But in the *yku70* mutant, although Gbd-Rap1 and Gbd-Sir4 are able to silence the *TRP1* gene (rows 6, 7), silencing by Gbd-Yif1 is lost as seen by complete growth on tryptophan drop out plate (row 8). This confirms that targeted silencing by Gbd-Yif1 is dependent on the Sirp at the nuclear periphery.

Table 4: Targeted silencing in wild type and *yku70Δ*

Name of the strain	Transforme plasmid	SC-His Number of cells/ml	SC-HisTrp Number of cells/ml	Silencing	Number of fold repression
Kry62	Gbd	$12X10^7$	$9X10^7$	25.00	~7 fold
	Gbd-Rap1	$2X10^7$	$4X10^3$	98.00	$\sim10^4$ fold
	Gbd-Sir4	$5X10^7$	$5X10^2$	99.80	$\sim10^5$ fold
	Gbd-Yif1	$5X10^7$	$6X10^4$	99.00	$\sim10^3$ fold
yku70:: *KanMx6*	Gbd	$1X10^7$	$1X10^7$	00.00	00.00
	Gbd-Rap1	$1X10^7$	$1 X10^5$	99.00	$\sim10^2$ fold
	Gbd-Sir4	$5X10^7$	$5X10^2$	99.80	$\sim10^5$ fold
	Gbd-Yif1	$1X10^7$	$1 X10^7$	00.00	00.00

3.2.3 An overexpression screen for factors that disrupt silencing by GbdYif1

Our previous experiments show that it is possible to identify proteins involved in the clustering and anchoring of telomeres to the nuclear periphery based on their ability to disrupt silencing of the defective *HMR* locus by Gbd-Yif1. Therefore we set up a genetic screen to identify factors, when over-expressed, would disrupt silencing by Gbd-Yif1. A yeast genomic library expressed from multicopy plasmid Yep13 (kind gift of K. Nasmyth) was transformed into the strain KRY62. Transformants were scored for growth on plates lacking amino acid tryptophan. The parent strain grows poorly on such plates and those that grew robustly were scored as positive. A secondary screen was incorporated, i.e., white colonies. The strain is red to start with due to the repression of the *ADE2* gene at the telomeres. If over-expression of any gene disrupts TPE, the cells will be white. Those white colonies that are also able to grow on medium lacking tryptophan, are likely to have lost the Sirp pool at telomeres. After screening about 15,000 transformants, 25 were short listed. These transformants were restreaked on medium lacking tryptophan to confirm their *TRP+* phenotype. In order to quantify the

extent of de-repression, serial dilution assays were done (see materials and methods). As shown in Figure 4, presence of the plasmids significantly reduced the ability of Gbd-Yif1 to silence *TRP1* expression. Table 5 summarizes the effect of each of these plasmids.

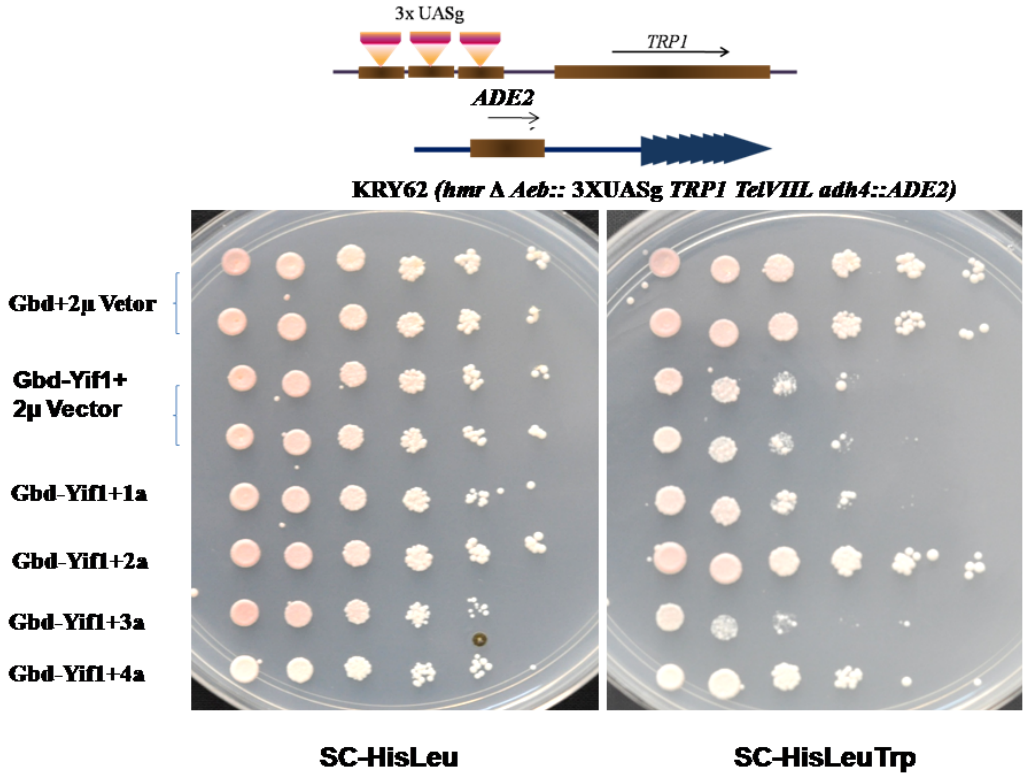

Figure 4: An overexpression screen for factors that disrupt targeted silencing. Overexpression screen was performed by transforming a library of yeast genomic sequences in a multicopy plasmid into a KRY62 containing Gbd-Yif1. Transformants were grown in SC-HisLeu to select Gbd-Yif1 and library plasmids. 5 µl of 10-fold serial dilutions was spotted on SC-HisLeu and SC-HisLeuTrp (to assay silencing). Some of the plasmids reduced the ability of Gbd-Yif1 to silence *TRP1* marker (e.g., 2a, and 4a).

3.2.4 Confirmation that the plasmids were indeed responsible for the de-repression phenotype.

In order to test if the de-repression seen is due to the presence of the plasmids and not due to mutations or other changes in the strain itself, we isolated the plasmid from these strains. These plasmids were now re-introduced into the parent strain;

Table 5: Loss of targeted silencing by Gbd-Yif1 upon overexpression of genomic library plasmids

Name of the strain co-transformed With GbdYif1+genomic library Yep13 plasmid number	Sc-HisLeu Number of cells/ml and color phenotype	SC-HisLeuTrp Number of cells/ml and color phenotype	Silencing (%)
KRY62+Gbd-Yif1+pRS315	$3X10^6$ pink	50 pink	99.99
KRY62+ Gbd-Yif1+2a	$2X10^6$ white	$2\ X10^6$white	00.00
KRY62+ Gbd-Yif1+19a	$5X10^6$ white	$5\ X10^6$white	00.00
KRY62+ Gbd-Yif1+24a	$5X10^4$ white	$4X10^4$ white	20.00
KRY62+ Gbd-Yif1+40a	$2X10^5$ white	$1X10^5$ white	50.00
KRY62+ Gbd-Yif1+49b	$5X10^5$ white	$4X10^5$ white	20.00
KRY62+ Gbd-Yif1+55b	$2X10^5$ white	$1X10^5$ white	50.00
KRY62+ Gbd-Yif1+56a	$2X10^5$ white	$2X10^5$ white	00.00
KRY62+ Gbd-Yif1+61b	$3X10^5$ white	$3X10^5$ white	00.00
KRY62+ Gbd-Yif1+63a	$6X10^5$ white	$5X10^5$ white	16.00
KRY62+ Gbd-Yif1+14a	$3X10^5$ white	$3X10^5$ white	00.00
KRY62+ Gbd-Yif1+44b	$3X10^5$ white	$2X10^5$ white	33.00
KRY62+ Gbd-Yif1+60a	$2X10^5$ white	$1X10^5$ white	50.00
KRY62+ Gbd-Yif1+126a	$1\ X10^5$ white	$1X10^5$ white	00.00
KRY62+ Gbd-Yif1+138a	$7\ X10^5$ white	$6X10^5$ white	14.00
KRY62+ Gbd-Yif1+172b	$1X10^4$ white	$1X10^4$ white	00.00

silencing assays were performed by spotting serial dilutions on plates lacking tryptophan in the growth media, and compared with parent strain containing an empty cloning vector in them (Figure 5). As shown in Figure 5, repression of *TRP1* at *hmr* locus was disrupted by over-expression of 2a in presence of Gbd-Yif1, whereas the empty cloning vector continued to repress suggesting that this derepression is due the presence of the plasmids. Effects of 43a, 44a were more subtle.

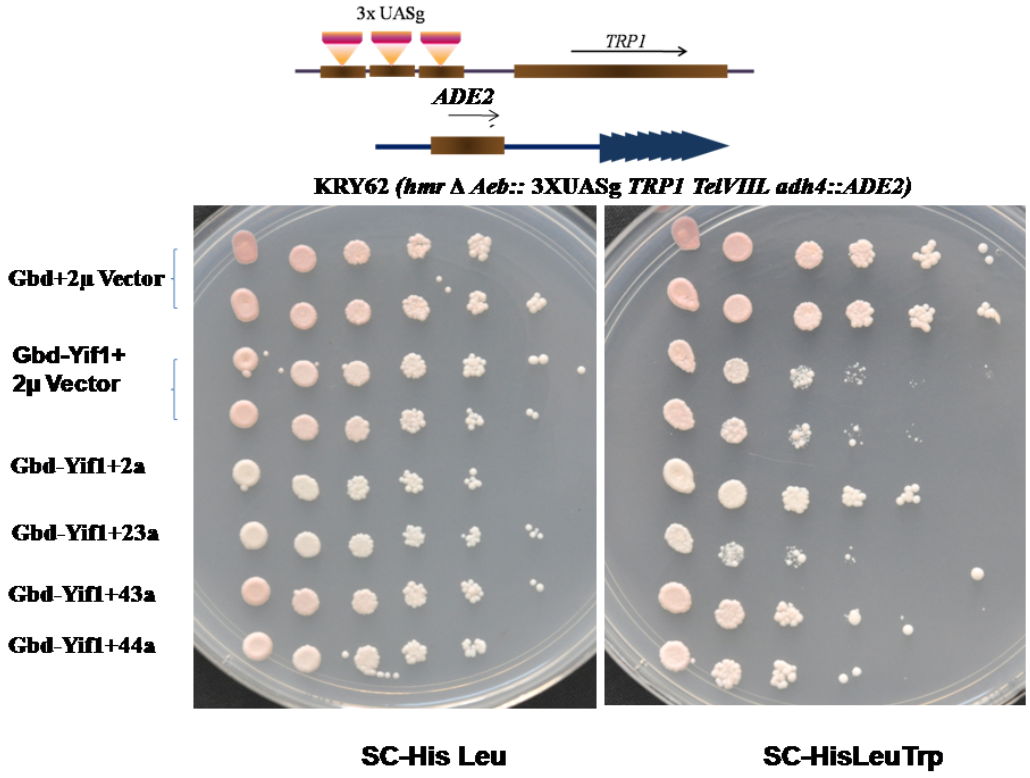

Figure 5: Confirmation of plasmids responsible for the derepression of *TRP1*. Plasmids obtained in the screen were re-transformed into a parent strain KRY62 with Gbd-Yif1 and library plasmids to confirm the derepression of *TRP1*. Silencing assays were performed by spotting 5 µl of 10-fold serial dilutions was spotted on SC-HisLeu and SC-HisLeuTrp.

3.2.5 Sequencing of plasmids obtained in the screen.

In order to identify the genes responsible for the disruption of silencing, we sequenced them (Table 6). Out of the various sequences obtained, we chose to study plasmid 2a, for two reasons: plasmid 2a significantly disrupts targeted silencing and secondly, it contains *EST2*, the telomerase enzyme and we wished to see if the telomere

organization was dependent on telomerase component. *EST2* could be one of the targets for anchoring telomeres to the periphery or could be involved in clustering by bringing together telomeres. 2a plasmid also contains another full length gene, *NKP2*, an uncharacterized, non-essential kinetochore protein that is thought to be involved in kinetochore formation. We can't rule out that *NKP2* may indirectly influence telomere clustering by interfering with the clustering of centromeres. 2a plasmid sequence also contains unknown ORF YLR317W and *TAD3*, a subunit of tRNA-specific adenosine-34 deaminase, which converts adenosine to inosine at the wobble position. To delineate which of these is responsible for the observed phenotype, we subcloned both *EST2* and *NKP2* on multicopy vectors (see materials and methods). Both *EST2* and *NKP2* were tested for silencing phenotype.

Table 6: List of library plasmids and their sequences

Name of the genomic library plasmid	DNA fragment	Chromosome number	Number of genes	Nuclear / cytoplasmic protein encoded genes
2a	**764622-768636**	**XII**	**5**	***NKP2,EST2* and *BUD6***
19a	**82515-85426**	**XV**	**2**	**Malate dehydrogenase**
24a	**694585-696045**	**XVI**	**1**	**Transketolase(cytoplasmic)**
40a	**463350-463689**	**IV**	**2**	**GAL3(nuclear)**
49b	**602856-603056**	**X**	**2**	**PRP16 (nuclear)**
60a	**462021-465055**	**IV**	**2**	**Trp1 encoded gene(cytoplasm)**
138a	**905398-907822**	**XV**	**1**	**MTR10(nuclear)**

3.3.1 Effect of *EST2* overexpression on targeted silencing

The *Saccharomyces cerevisiae* telomerase contains the catalytic subunit Est2 which is a reverse transcriptase and an RNA subunit encoded by *TLC1* gene; together they form the catalytic core of telomerase (Counter et al., 1997; Greider and Blackburn, 1987; Singer and Gottschling, 1994; Taggart et al., 2002). Additional proteins like Est1, Est3 and Cdc13 are required for telomere maintenance. From previous studies, it was established that mutation in telomerase components such as *EST2*, *TLC1*, *EST1*, *EST3* and *CDC13* leads to progressively shortening of telomeres and eventually cells senesce (Lendvay et al., 1996; Lundblad and Szostak, 1989).

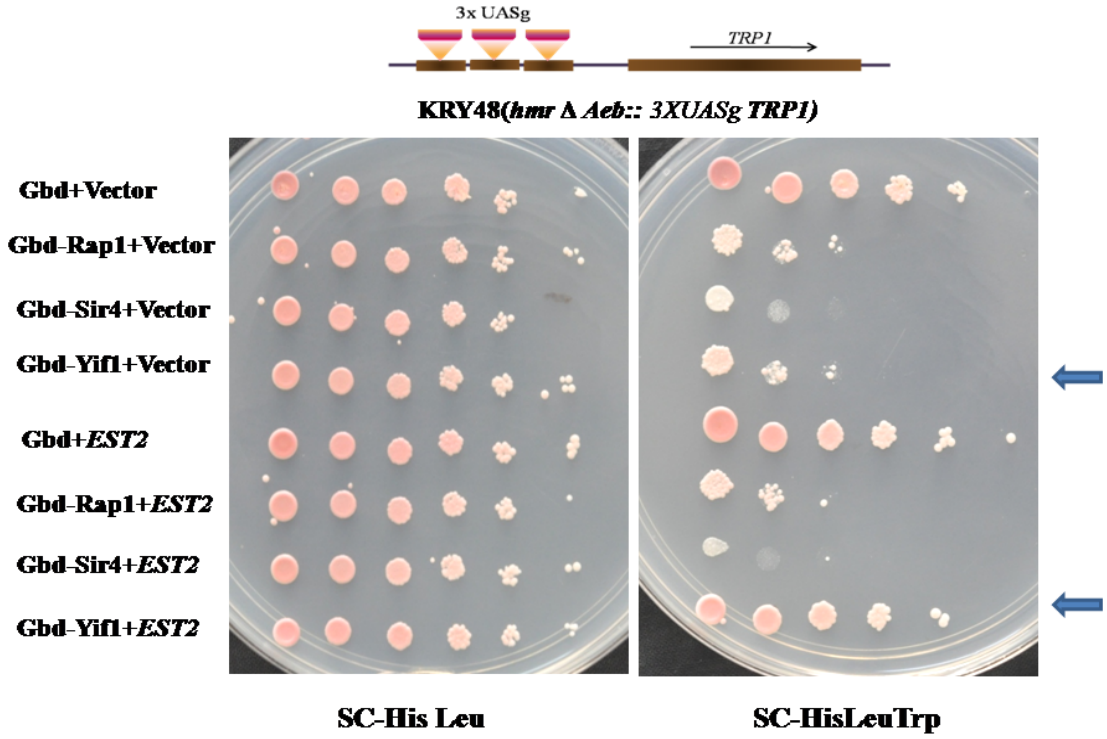

Figure 6: *EST2* overexpression disrupts targeted silencing by GbdYif1 at *HMR* locus. KRY48 was transformed with Gbd, Gbd-Rap1, Gbd-Sir4 and Gbd-Yif1 along with either CKM6 (empty vector) or *EST2* (multi copy) plasmid. 5 µl of 10 fold serial dilutions was spotted on SC-His Leu (to select the plasmids) and SC-His Leu Trp (to assay silencing).

We tested whether *EST2* overexpression causes loss in targeted gene silencing. We co-transformed the KRY48 with empty vector or *EST2* multicopy plasmid and Gbd, Gbd-Rap1, Gbd-Sir4 and Gbd-Yif1. Transformants were initially selected on histidine and

leucine synthetic deficient agar plates to retain both the plasmids in strain KRY48. These transformants were tested for loss of targeted silencing mediated by Gbd fused proteins upon overexpression of *EST2*.

Silencing assay results as shown in Figure 6 suggest that the overexpression of *EST2* leads to loss in targeted silencing mediated by Gbd-Yif1. This loss in silencing is similar to overexpression of library plasmid 2a, seen as better growth of these (row 8) than transformants with empty vector (row 4) on tryptophan drop out agar plates. This result confirms that *EST2* overexpression leads to loss in targeted silencing mediated by Gbd-Yif1.

3.3.2 Effect of *EST2* overexpression at telomeres

As overexpression of *EST*2 causes significant loss in targeted silencing mediated by Gbd-Yif1, we tested if silencing at the telomeres was also affected. We used the yeast strain KRY12 in which *URA3* gene is inserted at the *ADH4* locus that is immediately adjacent to the telomere repeat sequences on the left arm of chromosome VII (Gottschling et al., 1990). The transcriptional silencing is initiated at the telomeres by Sir complex recruited by the telomere binding protein Rap1 and Yku complex (Gasser and Cockel, 2001). The Sir complex proteins spread from the telomere end inwards along the chromosome and hence the *URA3* gene is silenced or subjected to telomere position effect (TPE).

In order to check the effect of *EST2* overexpression on the telomere silencing, we used KRY12 strain transformed with empty vector, library plasmid 2a and high copy *EST2* and were initially selected on leucine synthetic drop out plates to retain the plasmid in the strain. Transformants were grown in selective media for overnight and 10 fold serial dilution was made and spotted on 5- Fluoro orotic acid (5-FOA) containing agar medium. The repression of *URA3* gene can be detected by growth on medium containing 5-FOA, whereas expression of *URA3* gene leads to conversion of 5-FOA into the toxic uracil analog 5-fluorouracil, therefore, strains expressing *URA3* cannot grow in this medium. As shown in Figure 7, a significant reduction in survival rates on

5-FOA medium was observed upon overexpression of *EST2* indicating that telomeric silencing was compromised upon *EST2* overexpression.

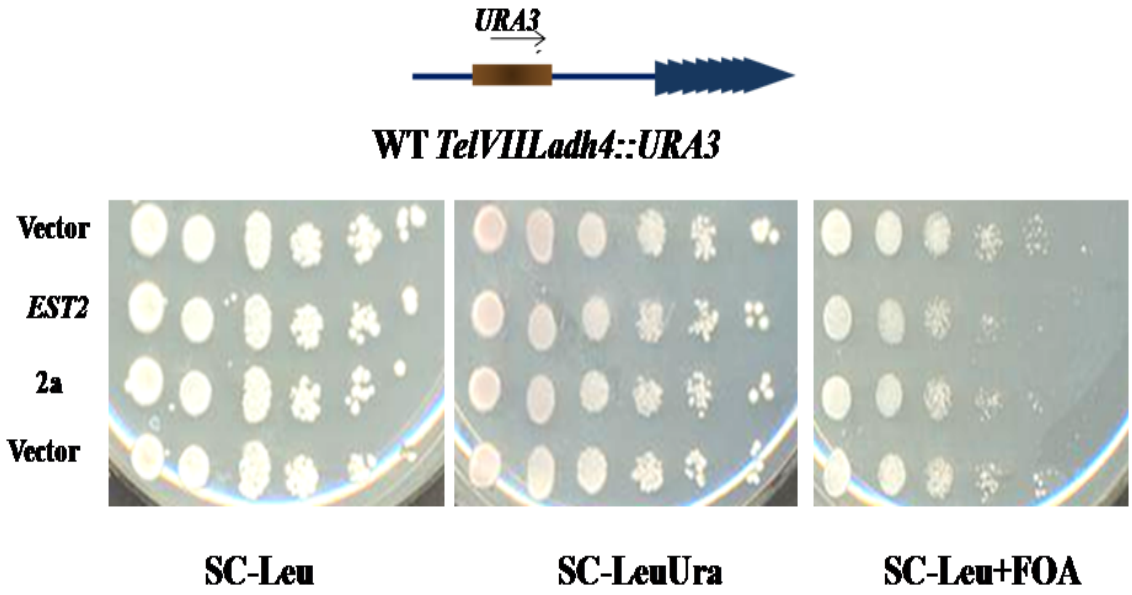

Figure 7: Telomere position effect upon overexpression of *EST2* plasmid. KRY 12 (*Tel VIIL-URA3*) was transformed with CKM6 (empty vector), *EST2* and library plasmid 2a. The transformants were grown in SC-Leu broth and 5ul of 10 fold serial dilutions was spotted on SC-Leu, SC-Leu Ura (control) and SC-Leu+5-FOA (silencing).

3.3.3 Immuno- localization of Sir4 on *EST2* overexpression

Loss in TPE could be due to many reasons. One of them might be loss of subnuclear distribution of telomeres. In order to check if the sub-nuclear organization was disturbed by overexpression of *EST2*, we performed indirect immunofluorescence experiments in the diploid strain (KRY109) containing 13x Myc epitope at the C-terminal of Sir4p to localize the Sir4p in the nucleus (as described in (Gotta et al., 1996).

We also costained the cells with DAPI and Nsp1 a nuclear pore complex protein, to delineate the nucleus. In wildtype cells that express vector alone, Sir4 appears as 4 to 6 condensed spots within the nucleus. In wildtype cells, overexpressing EST2, the condensed spots of Sir4 are more diffuse and the nucleus shows a lot of Sir4 staining,

these results show that Sir4 localization is affected upon *EST2* overexpression (Figure 8).

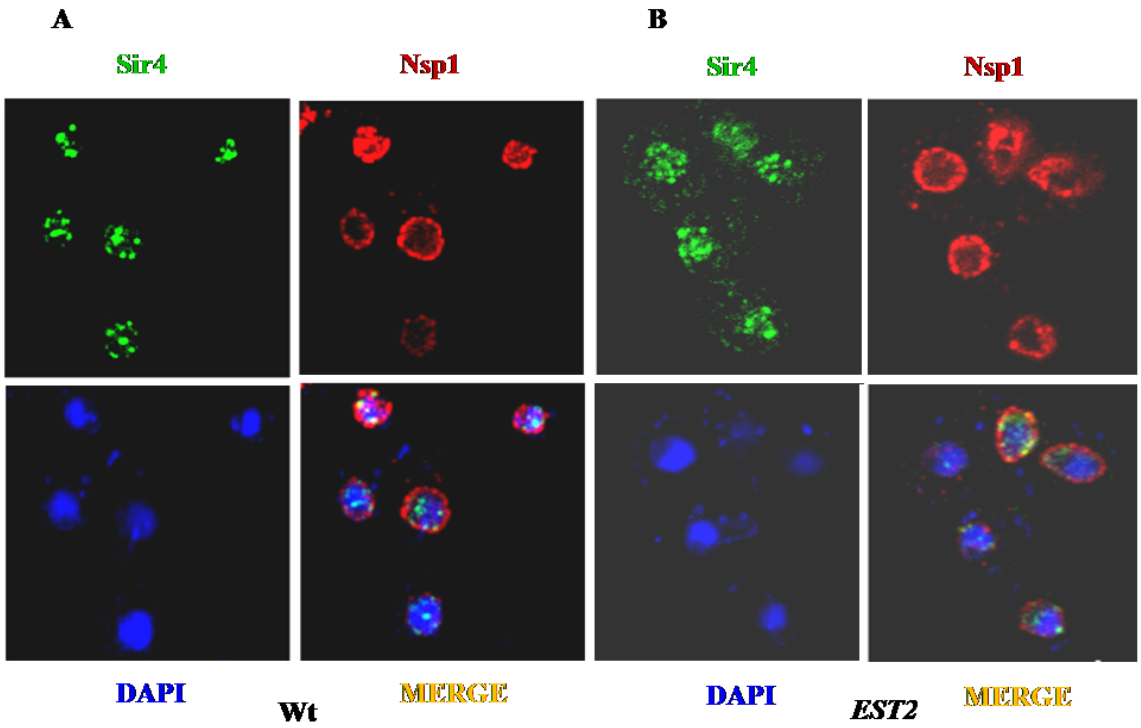

Figure 8: Localization of Sir4p in WT upon *EST2* overexpression. Immunolocalization of Sir4p in WT (KRY109) transformed with either empty plasmid (panel A) or *EST2* multi copy plasmid (panel B). Sir4 (green) represents the clustered telomeres and Nsp1p (red) stains the nuclear pore complex and DNA by DAPI (blue) (panel A). This clustered telomere spots were altered in *EST2* overexpression (panel B).

3.3.4 Effect of *NKP2* overexpression on targeted silencing

Based on genome wide knockout and protein localization studies in yeast, we know that Nkp2 is a non- essential, kinetochore protein and is possibly localized to the spindle pole body embedded in the nuclear periphery. In order to see if the protein has any role in telomere organization, we tested Sir4 localization upon overexpression of *NKP2*.

We first checked whether *NKP2* overexpression causes loss in silencing. We tested silencing by co-transforming with vector or *NKP2* multicopy plasmid and Gbd,

Gbd-RAP1, Gbd-Sir4 and Gbd-Yif1. These transformants were grown in synthetic deficient histidine and leucine liquid broth overnight and 10-fold serial dilution was made and spotted on tryptophan deficient medium to test for loss of targeted silencing mediated by Gal4 fused to Rap1, Sir4 and Yif1 upon overexpression of *NKP2*.

Targeted silencing results as shown in Figure 9 suggest that the overexpression of *NKP2* leads to a ten-fold loss in targeted silencing mediated by Gbd-Yif1. This loss in silencing is reproducible but less than the overexpression of library plasmid 2a (seen as better growth of transformants row 8 than transformants with empty vector in row 4 on tryptophan drop out agar plates). This result confirms that *NKP2* overexpression leads to loss in targeted silencing mediated by Gbd-Yif1, but is not the main contributor from 2a.

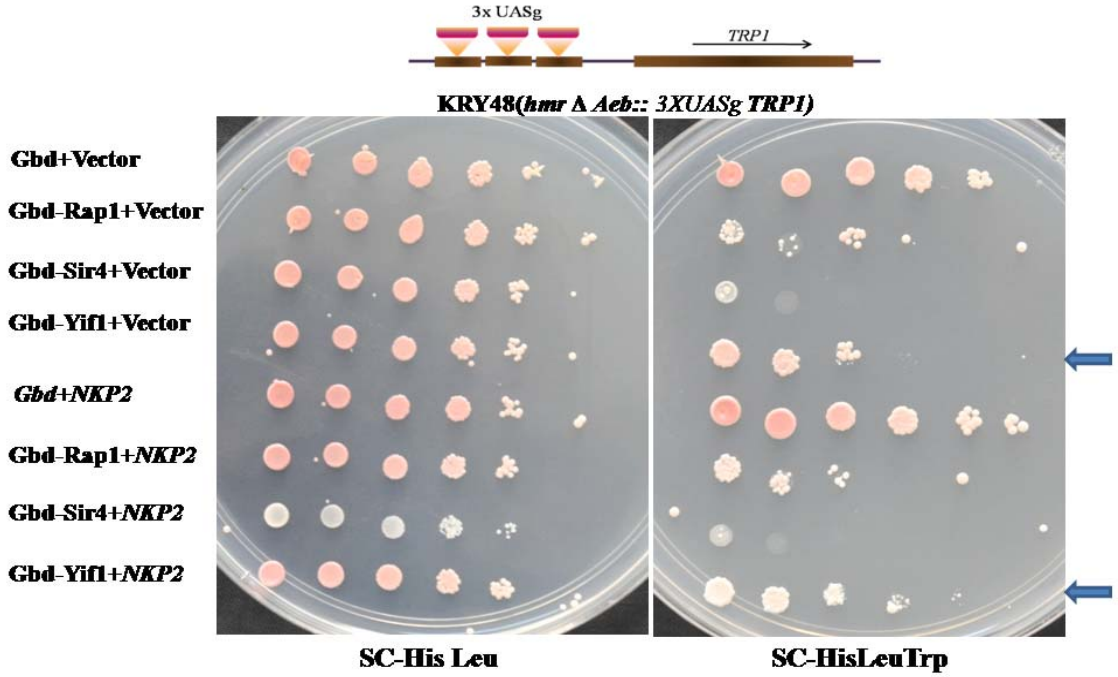

Figure 9: *NKP2* overexpression disrupts targeted silencing at *HMR* locus. KRY48 (*hmrΔAeb*::*3XUASg TRP1*) was transformed with Gbd, Gbd-Rap1, Gbd-Sir4 or Gbd-Yif1 along with either empty vector CKM6 or *NKP2* (multicopy) plasmid. 5 µl of 10 fold serial dilutions was spotted on SC-His Leu (growth) and SC-His Leu Trp (silencing).

3.3.5 Effect of *NKP2* overexpression at telomeres

In budding yeast *Saccharomyces cerevisiae*, gene silencing occurs at *HM* loci, telomeres and rDNA locus, whereas in *Schizosaccharomyces pombe* and other higher organisms silencing also occurs at the centromeres. In budding yeast, nearly 124bp size centromere regions are occupied by kinetochore complex and act as molecular machines to connect the microtubules to segregate chromosomes accurately during mitosis. Kinetochores are tethered to the SPB throughout the cell cycle except for few minutes during S phase of cell cycle (Jaspersen and Winey, 2004; Sazer, 2005). In higher organisms, centromeres and telomeres are specialized structures that share common function of heritably repressing chromatin in an epigenetic manner. The nuclear periphery facilitates the silencing by clustering telomere repeats and in turn sequestering the silencer proteins. As overexpression of *NKP*2 causes loss in targeted silencing mediated by Gbd-Yif1, we tested the effect on telomere silencing of overexpression of *NKP2*. We used KRY12 described in the previous section (section 3.3.2) for this purpose.

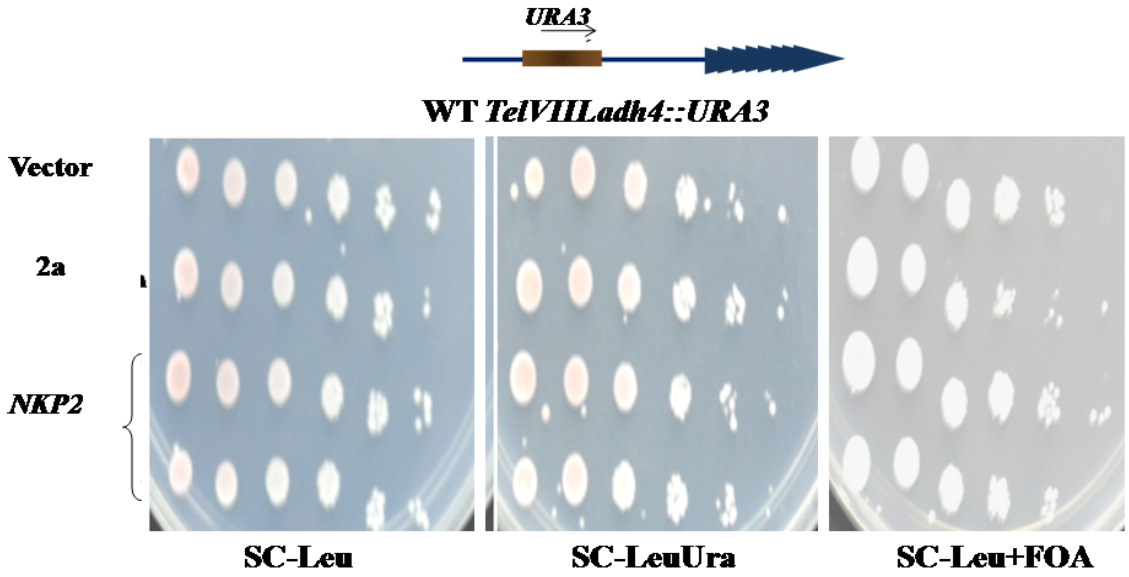

Figure 10: Telomere position effect upon overexpression of *NKP2* plasmids. KRY 12 (*Tel VIIL-URA3*) strain was transformed with CKM6 (empty vector), 2µ *NKP2* plasmid and library plasmid 2a. The transformants grown in SC-Leu broth and 5ul of 10 fold serial dilutions was spotted on SC-Leu, SC-Leu Ura (control) and SC-Leu+5-FOA (to check loss in TPE).

In order to check the effect of *NKP2* overexpression on the telomere silencing, we used KRY12 strain transformed with empty vector, library plasmid 2a and high copy *NKP2* plasmid and the plasmids were selected on leucine deficient medium. The transformants were tested for silencing of the *URA3* reporter gene at the telomere. Transformants were grown in selective media overnight and 10 fold serial dilutions was made and spotted on 5- Fluoro orotic acid (5-FOA) containing agar medium to test the telomere position effect (TPE). As shown in Figure 10, the levels of telomeric silencing were compared in the transformants with empty vector, *NKP2* and library plasmid 2a on 5-FOA plates. However upon overexpression of *NKP2*, we could not detect any reduction in silencing at telomeres. These results suggest that overexpression of *NKP2* shows loss in targeted silencing at *HMR* but not telomere silencing.

3.3.6 Immuno- localization of Sir4p on *NKP2* overexpression

We tested the localization of Sir4p (as described earlier) when *NKP2* was overexpressed. Sir4p was detected with anti-Myc antibody (green) in column 1. The nuclear membrane was stained with antibody to Nsp1p, a nuclear pore complex protein and is shown in (red) column 2. DNA was counterstained with DAPI and is shown in blue colour in column 3. As seen in Figure 11, the localization of Sir4p was not affected upon overexpression of *NKP2*. This result suggests that, overexpression of NKP2 leads to loss of targeted silencing but does not delocalize the Sir protein near the nuclear periphery.

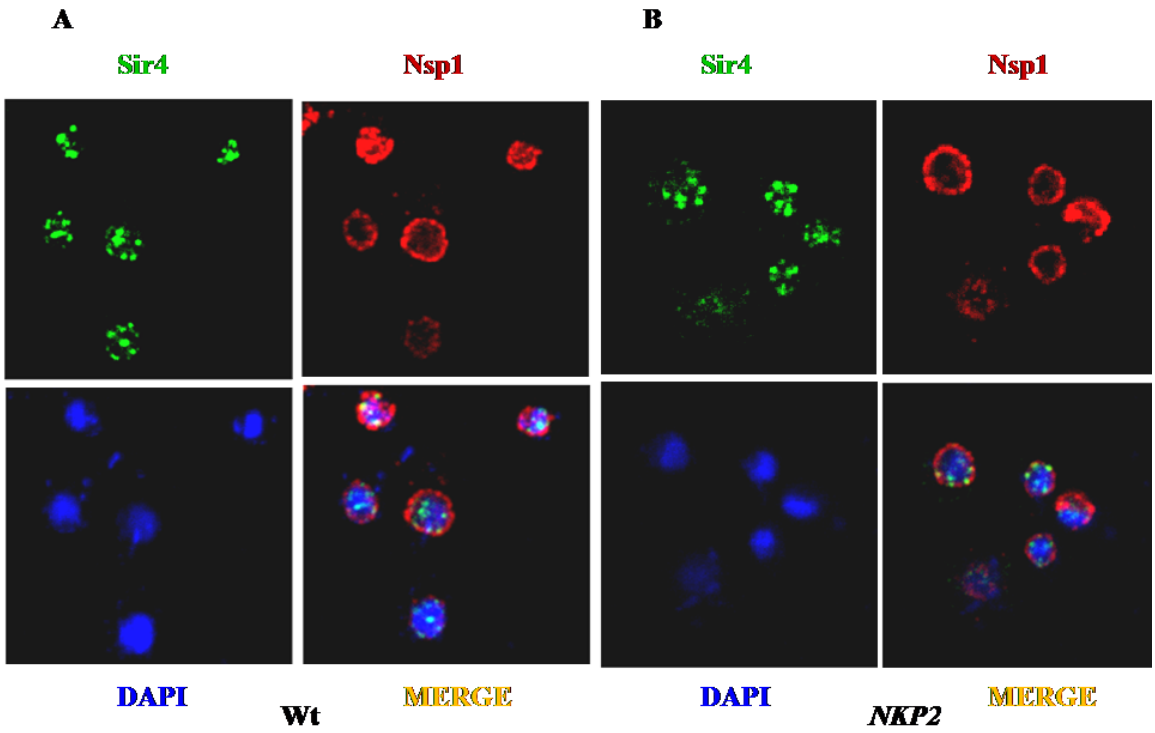

Figure 11: Localization of Sir4p in WT upon *NKP2* overexpression. Immunolocalization of Sir4p in WT (KRY109) transformed with either empty plasmid (panel A) or *EST2* multi copy plasmid (panel B). Sir4 (green) represents the clustered telomeres and Nsp1p (red) stains the nuclear pore complex, DNA was stained by DAPI (blue) (panel A). These clustered telomeres were not altered in NKP2 overexpression (panel B).

3.4 Discussion

Clustering of many telomeres and colocalization of the silent mating type loci with these clusters at the nuclear periphery of the yeast nucleus favours gene silencing by harbouring higher concentration of silencer proteins in its vicinity. These clustered telomeres are maintained by two partially redundant pathways that depend on Yku70/Yku80 heterodimer and Esc1, both of which interact with the structural component of silent chromatin, Sir4, and together tether the telomeres to nuclear

periphery. Disruption of any of these components leads to delocalization of telomeres from nuclear periphery and leads to loss in silencing as well (Laroche et al., 1998).

In a screen to identify other components in this pathway, we identified *EST2* and *NKP2* genes. *EST2* overexpression leads to loss in silencing at *HMR* and telomeres whereas *NKP2* shows only loss of targeted silencing at *HMR* locus. When this work was in progress, Gasser and co-workers showed that *EST2* indeed acts as a tether for telomeres (Schober et al., 2009). It was shown that Est2 acts via Mps3 and its tethering function is cell cycle dependent S phase. Therefore, we did not pursue this further. However, *NKP2* appeared like an interesting candidate for two reasons: it affected tethered silencing by Gbd-Yif1 which is critically dependent on telomeres being clustered at the periphery. It did not affect the natural TPE which is not dependent entirely on clustering. Even though the perturbation by *NKP2* was modest, we performed a few more experiments to test whether *NKP2* had any role in tethering or gene silencing.

Chapter - 4

Characterization of Nkp2

4.1 Introduction

Kinetochores are macromolecular machines that are specialized protein structure assemblies on centromeric DNA and couple chromosomes to the dynamic spindle during cell division (Cheeseman and Desai, 2008; Santaguida and Musacchio, 2009). Transfer of genetic material to daughter cells during cell division requires the proper partitioning of chromosomes mediated by the kinetochore. Although kinetochore function is conserved from yeast to mammals, the size and sequence of the centromeric DNA are highly variable (Henikoff et al., 2001). In *Saccharomyces cerevisiae,* the centromeric sequences have been defined that are sufficient to mediate the kinetochore assembly but, in fission yeast and multicellular organisms, centromeres consist of megabases of DNA. Despite their variation in size and sequence composition, epigenetic aspects of centromeres are highly conserved and are essential for assembly of kinetochore (Buhler and Gasser, 2009; Mythreye and Bloom, 2003; Tanaka et al., 1999). Failure of kinetochore assembly on centromere leads to improper microtubule attachment and can result in chromosome loss. In higher organisms, during mitotic division, such failures can drive tumour formation and in meiosis affect the fertility of the organism (Weaver and Cleveland, 2007).

In *Saccharomyces cerevisiae*, kinetochore complex are composed of approximately 40 different proteins; these kinetochore proteins associate with each other and perform their function by connecting centromere and microtubules to segregate accurately the genetic material to the daughter cells during cell division (Cheeseman et al., 2002). Recently, the organization of yeast kinetochores has been better defined by biochemically purifying the subcomplex within the kinetochore (Akiyoshi et al., 2010; Cheeseman et al., 2001; Janke et al., 2001; Janke et al., 2002; Li et al., 2002). However, the physical interactions between these proteins are yet to be established and the organization of these subcomplexes also needs to be elucidated.

Previously, it was reported that, in *Schizosaccharomyces pombe* and multicellular organisms, centromere proximal regions of chromosomes are silenced. In contrast, the relation between heterochromatin proteins and kinetochore function in the budding yeast remains largely unexplored. The Sir1 heterochromatin protein is a

component of centromeric chromatin and contributes to the mitotic chromosome stability (Sharp et al., 2003). Sir1 binds to Cac1, a subunit of chromatin assembly factor-I (*CAF-I*) and helps to retain the Cac1 at the centromeres, thereby retaining Caf1 at the centromeric chromatin. This function is independent of other Sir proteins (Sharp et al., 2003). In order to find out if there were additional interactions between proteins that bind to the centromere and heterochromatin, we first tested if Nkp2 has any role in heterochromatin establishment at *HMR* and telomeres by generating null mutants of *nkp2*.

4.2 Results

4.2.1. Targeted silencing in *nkp2Δ*

In order to examine the role of Nkp2 on silencing, we constructed a *nkp2* mutant (described in materials and methods). This strain was crossed to KRY28 (*hmraeB::*1X*UASgURA3*) to obtain KRY311 which contain (*nkp2*::*TRP1 hmr*ΔaeB::1XUASg*URA3).* To check targeted silencing, we transformed the plasmids encoding Gbd, Gbd-Rap1, Gbd-Sir4 and Gbd-Yif1 in wild type and *nkp2* mutant. Transformants were grown on histidine drop-out liquid broth overnight and 10 fold serial dilutions was spotted on uracil deficient agar plates to check the targeted silencing.

In wild type, Gbd-Sir4 plasmid establishes silencing at the modified *hmr* loci and no growth in uracil deficient agar plate was detected whereas, Gbd-Rap1 and Gbd-Yif1 show little effect on silencing (Figure 12). However in *nkp2* mutant, we observed the opposite results; Gbd-Rap1 showed no growth in uracil deficient plate. These two results are inconsistent with each other and are unlikely to represent true loss in silencing. These results indicated that loss of growth on uracil deficient plates might mean there might be a spontaneous loss of the *URA3* marker from *HMR* locus, which might indicate increased genome instability.

Panel A

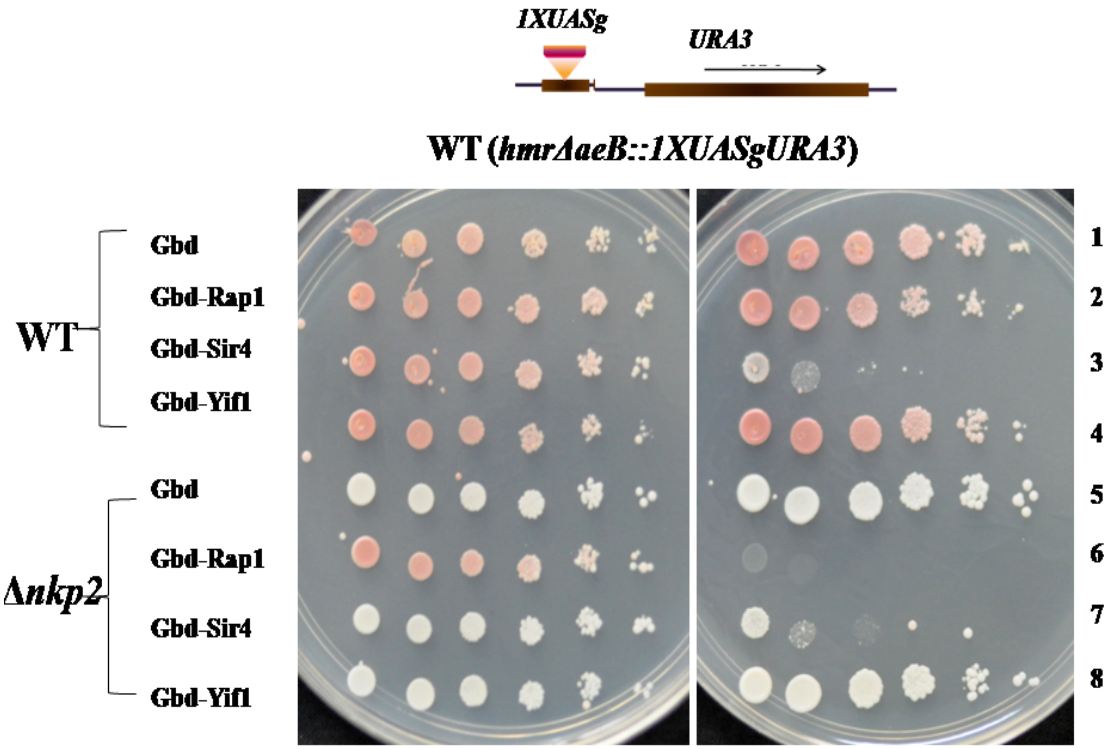

Panel B

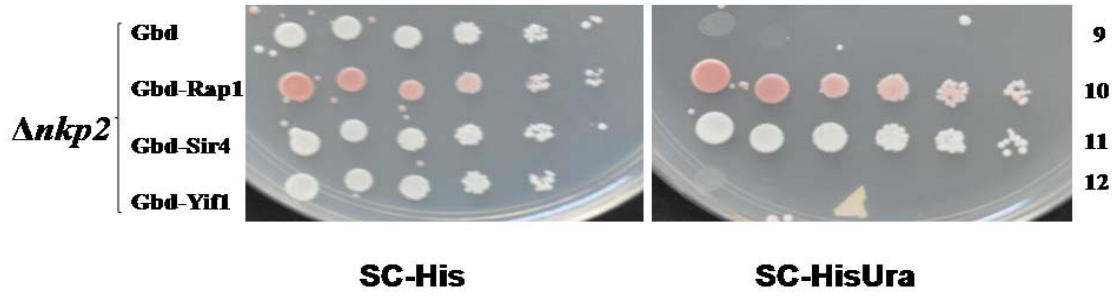

Figure 12: Targeted silencing does not affected in *nkp2Δ*. KRY28 (*hmrΔaeb::1XUASgURA3*) and KRY311 (*nkp2 hmrΔaeb::1XUASgURA3)* were transformed with Gbd, Gbd-Rap1, Gbd-Sir4 and Gbd-Yif1. Transformants were grown in SC-His broth and 5µl of 10-fold serial dilutions was spotted on SC-His (to select the plasmid) & SC-His Ura (to assay silencing).

4.2.2. Telomere silencing in *nkp2Δ*

Simultaneously, we also constructed *nkp2* mutant strains to assay TPE at *URA3* locus on the left telomere of chromosome VII. Gene silencing at telomeres was measured by growth on 5-FOA plates. Six different *nkp2* segregants were inoculated in synthetic complete broth and 10 fold serial dilutions were made and spotted on 5-FOA. Plates were incubated at 30ºC for 2 days. Among six *nkp2* mutants, two of them showed more resistance than wild type strain. Again this was inconsistent, not all *nkp2* mutants behaved identically (Figure 13).

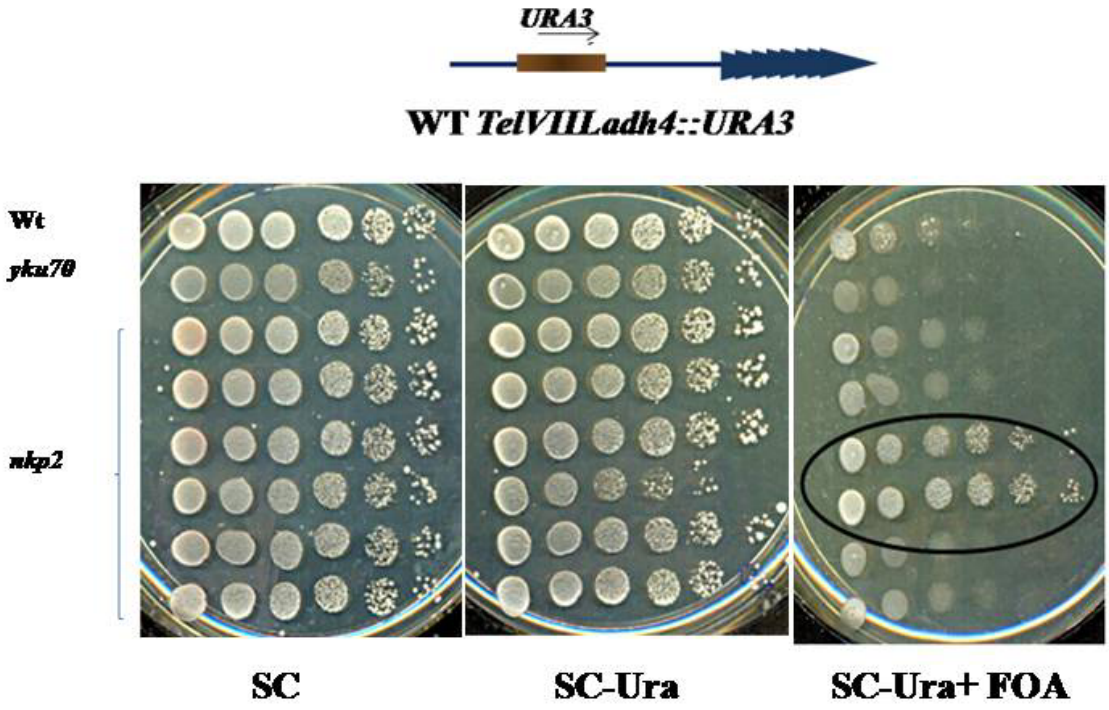

Figure 13: Telomere position effect in *nkp2Δ*. WT (*Tel VIIL-URA3*) and *nkp2* (*nkp2*::*his5+ Tel VIIL-URA3*) were grown in SC-Leu broth and 5ul of 10 fold serial dilutions was spotted on SC, SC- Ura (control) and SC+5-FOA (to check loss in TPE).

These results were puzzling and because not all *nkp2* mutants behaved identically, it rules out a silencing defect. If the growth on uracil (Figure12) or 5-FOA (Figure 13) is not due to silencing, then the other possibility is that they are losing the

URA3 gene. As these are haploid, it is not possible to lose the chromosome and survive. Therefore we reasoned that maybe these strains have uneven number of chromosomes.

In the process of construction of *nkp2* mutant with defective *hmr* strain, we crossed wild type strain with the *hmr::URA3* with *nkp2* mutant and random sporulation was done to isolate the *nkp2* mutant with defective *hmr* strain. It is possible we obtained some strains with extra chromosomes and were losing those at an elevated rate. For eg., it is possible that two chromosome VIIL may be present in the cell with one modified telomere and one wild type and the cell was losing one of them, hence we see either URA plus (retain modified chromosome) or URA minus (lose the modified chromosome).

4.2.3 Abnormal segregation of markers in *nkp2* homozygous strain

To test this possibility more directly, we constructed 2 different *nkp2* mutant strains with different auxotrophic marker KRY277 (*nkp2::his5+)* and KRY311 (*nkp2::TRP1 hmraeB*::*1XUASgURA3*). We crossed these strains and sporulated. We constructed a diploid *nkp2* homozygous strain with one *nkp2* replaced with *his5+* and the other with *TRP1*. This was made by crossing *nkp2*::*his5+*(*Mat α*) with *nkp2*::*TRP1* with *URA3* reporter gene at the defective *hmr* loci (*Mat a*), diploids were selected on tryptophan and histidine dropout medium. Diploid cells were kept on non-fermentable carbon source *i.e.,* potassium acetate for spore formation. After 3 days spores were checked under microscope and the formation of tetrads was similar to wild type diploid strain. Spores were digested with zymolyase and random spore analysis was performed to score the segregants with auxotrophic markers. We observed that ~25% of segregants (73 out of 300 segregants analyzed) grew on both tryptophan and histidine dropout medium and also showed a specific mating type, either *Mat a* or *Mat α*. This is unexpected, as a haploid can have only one of the two *nkp2* chromosomes. We reasoned this could be due to improper segregation of chromosomes: these strains may contain uneven number of chromosomes and might carry additional chromosome XII, and just one of Chromosome III, therefore can mate. These experiments together suggested that

nkp2 mutants do not have any effect on silencing but might affect chromosome segregation.

4.2.4 Homozygous *NKP2* deleted cells were able to mate with haploid strain.

The previous experiments show that there is some chromosome missegregation in *nkp2* mutants. To test this further, we did southern blots to check the *nkp2* locus status. We performed genomic southern to check the *nkp2* loci in a strain with one copy of chromosome III i.e., either *MAT a* or *MAT α* locus. *NKP2* gene is present on right

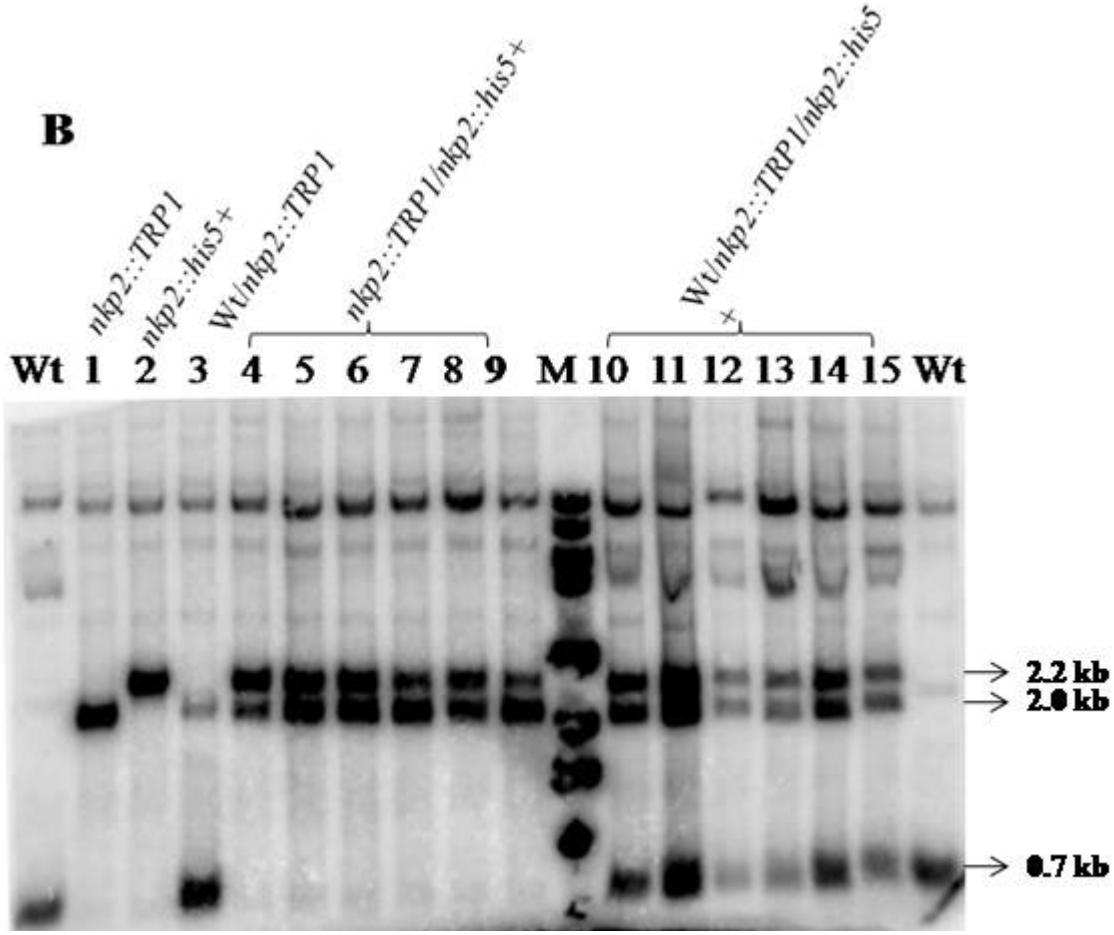

Figure 14: Southern blot analysis of *nkp2Δ with mating behavior in diploid cells*. Southern blot was performed with homozygous *nkp2* diploid strain and triploid strain. The genomic DNA isolated and digested with *XhoI* and *SalI* double digest transfer to nylon membrane and probe with *NKP2*. Wild type copy of *NKP2* gives ~0.7 kb where as *NKP2* gene replaced with *TRP1* marker gives ~1.9 kb *and his5+* gives about 2.2 kb fragments. From lane 4-9 are diploid cells which shows the mating type either Mat a or Mat α, these diploid cells were mated with wild type haploid to make triploid from lane 10-15.

arm of chromosome XII. Genomic DNA was digested with two enzymes *XhoI* and *SalI*, and probed with *NKP2* gene fragment. Wildtype gives about 0.7kb fragment whereas *NKP2* gene replaced with either *TRP1*or *his5*+ gives approximately 1.9 kb or 2.2 kb respectively. We found that the *nkp2::his5*+ / *nkp2::TRP1* contained two copies of *nkp2* locus (Figure 14, lane 4-9) and lost one of the chromosome III. Next we mated this strain with an authentic haploid strain. The resultant strain contains 3 *nkp2* loci: 2 of the mutant marked loci from the diploid parent and one from the haploid carrying wild type *NKP2* (Figure 14, lane 10-15).

The southern blot clearly indicates that these strains contain 2 *nkp2* loci to begin with and then mate with wild type to produce a strain with 3 *NKP2* loci. However, this does not say if the strain was a true diploid or was disomic for the chromosome number XII which contains *NKP2*. To answer this question, we performed a sporulation test. We sporulated the haploids that mate with haploid wild type strain (lanes 4-9 in Figure 14). Diploids with 2 *nkp2* copies can give a large number of viable spores. Triploid on the other hand cannot (lanes 10-15). We dissected the *nkp2* diploid and so called triploid spores and tested the viability, the viability from diploid cells was about 98% and segregated into a 2:2 *his5*+:*TRP1* whereas so called triploid, the viability was decreased to below 50%.

Southern blot and tetrad dissection results indicated that the *nkp2*::*his5*+/*nkp2*::*TRP1* is a diploid that can mate. This means that there is a high rate of loss of chromosome III in *nkp2* mutant leading to the production of monosomy at chromosome III. We tested this more directly by performing specific chromosome loss assay for chromosome III.

We performed a plate based mating assay to test if diploids of *nkp2* undergo mating. To this end, we grew cultures wild type and *nkp2* mutant overnight, equal numbers of cells are mixed with fixed number of mating tester *MAT a* or *MAT α*. These cultures were grown overnight and 10 fold serial dilutions were made and cells were spotted on synthetic deficient media without amino acids. In the mating assays, *nkp2* mutant cells show more growth on synthetic deficient medium; this is because *nkp2*

mutant loses chromosome III more frequently than wild type. All these results together suggest that, chromosome loss was prominent in *nkp2* mutant as seen in Figure 15.

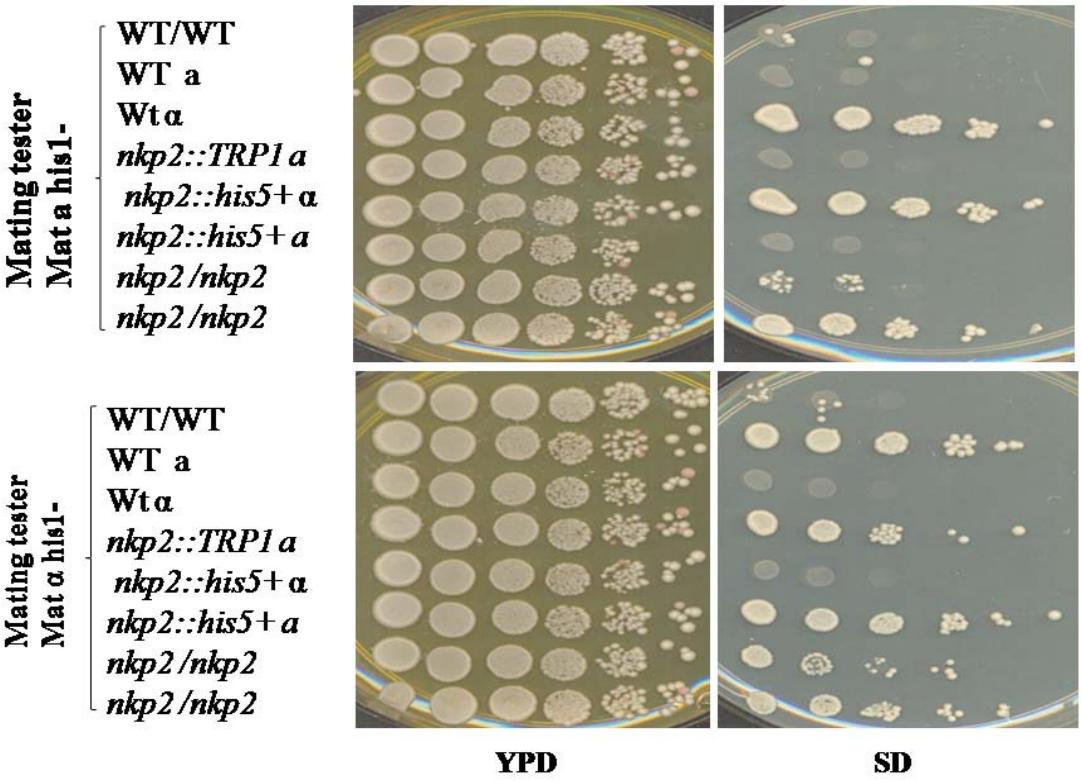

Figure 15: Mating assay in *nkp2* homozygous diploid cells. Mating assays were performed with *nkp2* homozygous diploid. Cells grown in YPD were mixed with either *MAT a* or *MAT α* and incubated for overnight. 5µl of 10-fold serial dilutions was spotted on YPD (to select the experimental strain and mating tester) & SD (to select those cells which had mated with the mating tester).

As the plate-based assay indicated that *nkp2* mutants indeed tend to mate frequently, we quantified this phenotype to get a measure of the extent of loss of chromosome III. Diploid cells contain *MAT a* and *MAT α* information on two copies of chromosome III. Wild type and *nkp2* mutant diploid cells were grown overnight and equal number of cells are mixed with the mating tester strain either *MAT a* or *MAT α,* and placed on nitrocellulose membrane for 4 hours on YPD at 30ºC. These cells were washed in phosphate buffer and plated on synthetic deficient plates for growth. In this assay, diploid cells which have lost any one of the chromosome III, either *MAT a* or *MAT α,* can mate with the opposite mating tester strain (Figure 15). For example if

diploid cell loses *MAT a* marked chromosome III, it can mate with mating tester strain *MAT a* and vice versa (Table 7). *nkp2* homozygous mutant shows about four fold increase in loss of chromosome III compared to the wild type strain .

Table7: Quantitative mating assay in wild type and *nkp2Δ*

Name of the strain	Total number of colonies screened	Mated colonies	Total percentage of Mated colonies (%)
WT	$2X10^6$	600	0..03
nkp2	$2X10^6$	2230	0.11

4.2.5. Chromosome loss upon overexpression of *NKP2*

All these results suggest that Nkp2 may have role in chromosome segregation but not in silencing. As Nkp2 is a kinetochore protein, we decided to test the role of Nkp2 in chromosome loss upon overexpression. We performed the colony colour assay to measure the chromosome instability. The wild type strain carrying a cloned ochre-suppressing form of a tRNA gene, *SUP11*, serves as a marker on artificial chromosome. To measure chromosome loss, strain carrying an artificial chromosome with a cloned ochre-suppressing form of a tRNA gene, *SUP11*, was used. Strain carrying artificial chromosome are *ADE2+* (due to the suppression of the non-sense mutation in the *ade2* gene) and white in colour whereas loss of the artificial chromosome causes colonies to appear red. To perform loss assays, we transformed the plasmid encoding multiple copies of *NKP2* and empty vector to check chromosome loss in wild type strain. Initially, transformants were selected on leucine, adenine deficient selective media to retain the *SUP11* and then plated on leucine drop out agar plates. To quantify the loss of chromosome, we initially plated approximately 3,500 cells, grew them for 3 days at

30ºC and stored at 4ºC for 6 days to assess the colour. As shown in Figure 16, we found that a few colonies lost the *SUP11* chromosome and became red in colour upon overexpression of *NKP2*. These results suggest that overexpression of *NKP2* has small enhancing effect of *SUP11* loss.

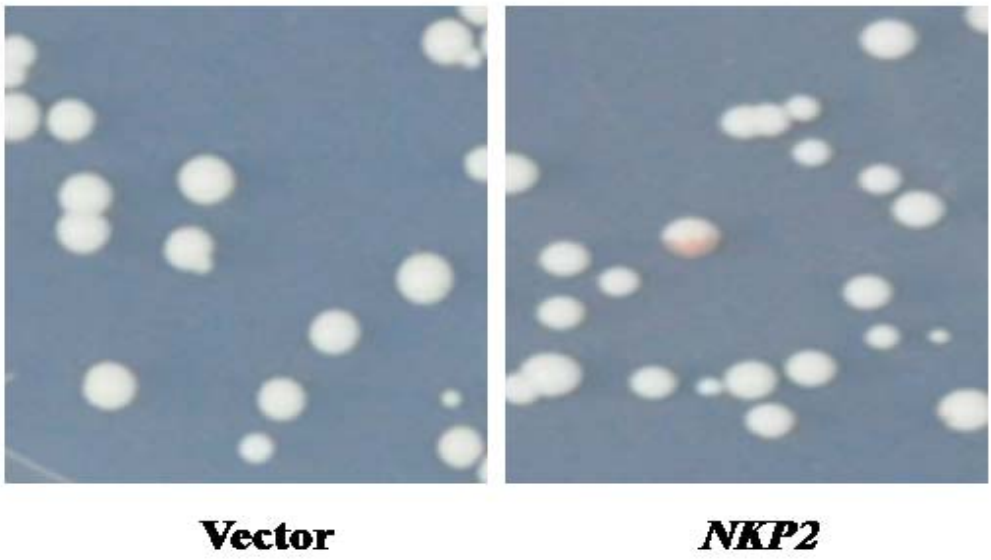

Figure 16: Artificial chromosome loss (*SUP11*) upon overexpression of *NKP2*. Wild type cells with artificial chromosome *SUP11* was transformed with either empty vector or *NKP2* plasmids. Plate about 3,500 cells on Leucine dropout agar plates to access the colour.

4.2.6. Chromosome loss in *nkp2*Δ

The results presented earlier suggest that *nkp2* mutants are defective in chromosome transmission. It has been shown that incorrect kinetochore assembly or kinetochore-microtubule attachment can result in loss or gain of chromosomes (Raghuraman et al., 2001). During mitosis, in the somatic cells of higher organisms, such failure can cause tumour formation and in meiosis, defective chromosome segregation leads to aneuploidy (Weaver et al., 2007). We tested the chromosome loss in *nkp2* mutant more directly using an artificial chromosome loss.

We performed the colony colour assay described above in *nkp2* mutants to measure chromosome instability. We constructed the *nkp2* mutant strain carrying the *SUP11* artificial chromosome by crossing *nkp2* mutant with a wild type strain (kind gift

of Marston). We used *ctf3* mutant as positive control as Ctf3 is a kinetochore protein and is involved in correct segregation of chromosomes. Initially colonies were selected on adenine drop out broth overnight to select for *SUP11* and approximately, 3,500 cells

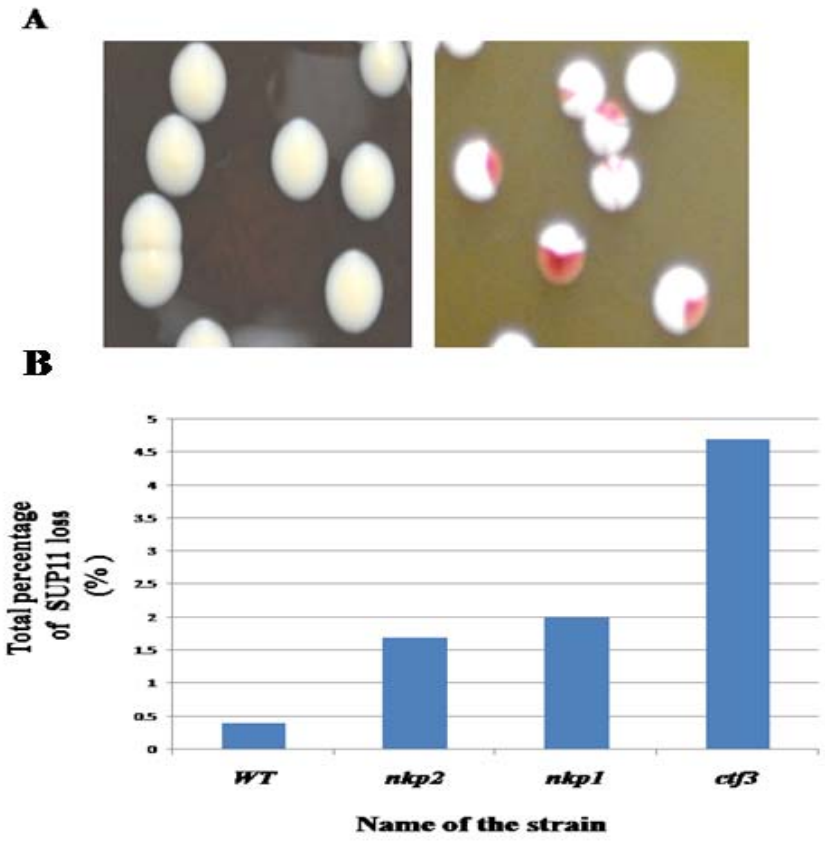

Table 8: Artificial chromosome loss in Ctf19 kinetochore mutants

Name of the strain	SUP11 chromosome loss	Total percentage of SUP11 loss (%)
WT	15	0.4
nkp2	60	1.7
nkp1	72	2.0
ctf3	164	4.7

Figure 17: Artificial chromosome loss was elevated in *nkp2Δ*. 3,500 wild type, *nkp2*, *nkp1* and *ctf3* cells with artificial chromosome *SUP11* cells were plated on YPD agar plates to score the half sector colonies. Panel B shows graphical representation of artificial chromosome loss (*SUP11*) and Table 8 represents with numbers and percentages.

were plated on rich media agar plates, these agar plates were incubated at 30ºC for 3days and shifted to 4ºC for one week. The percentage of sectored colonies, which were at least half red indicating loss in the first division after plating were scored. We found that *nkp2* shows significant loss of *SUP11* compared to wild type (Figure17/Table 8). We also included *nkp1* mutant; it's a kinetochore protein that is thought to interact with Nkp2 protein. *ctf3* mutants show more significant loss than the *nkp2* mutant, whereas *nkp1* is comparable to *nkp2* (Figure 18). These results suggest that Ctf19 components are required for accurate chromosome transmission during mitosis.

4.2.7 Tetrad analysis shows gene conversion events

In order to study the segregation of chromosomes more systematically, we dissected the tetrads from *nkp2* homozygous diploids and looked at each meiotic event

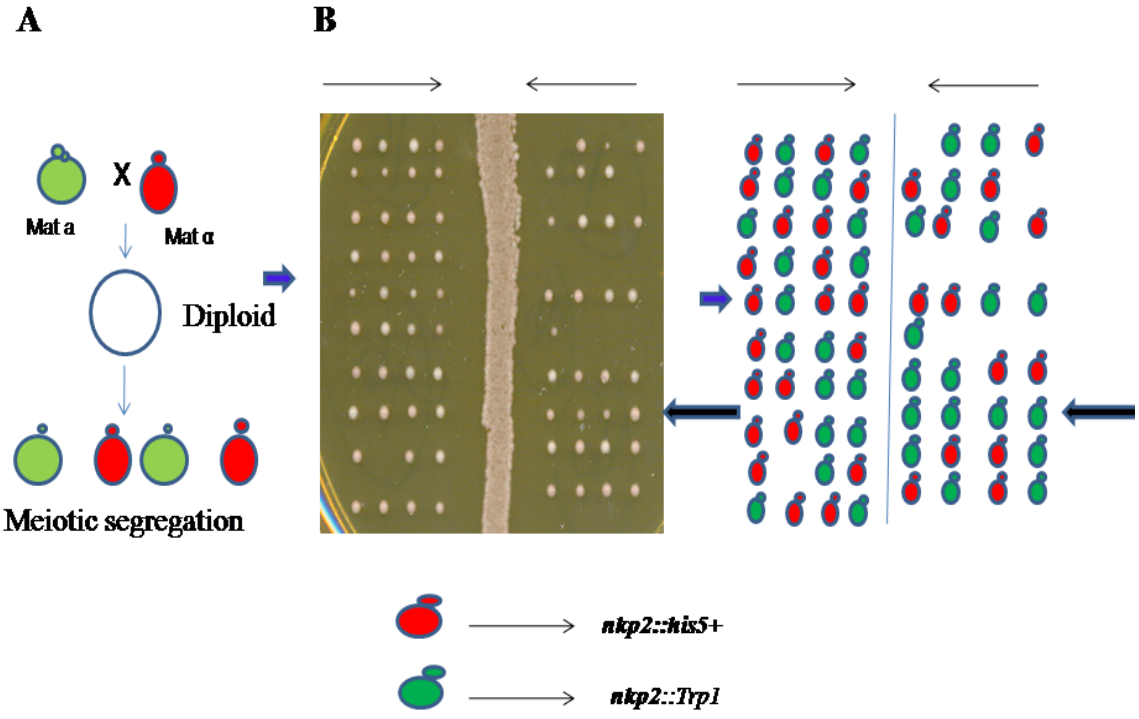

Figure 18: Tetrad analysis shows gene conversion events in *nkp2Δ* homozygous diploid. Panel (A) is a pictorial representation of the meiotic segregation of wild type strain. Panel (B) shows the spores obtained from dissecting of *nkp2* homozygous diploid.

Table 9: Tetrad analysis of *nkp2Δ*

Name of the strain	Total number of tetrad analyzed	3:1 segregation of either *his5+:TRP1* or *TRP1:his5+*	4:0 segregation of eeither *his5+:TRP1* or *TRP1:his5+*
WT	**100**	**0**	**0**
nkp2	**100**	**13**	**7**

for the segregation of *nkp2* and *MAT* locus. We dissected ~100 tetrads and each tetrad segregated 2:2 with respect to *his5+* and *TRP1* cells and the *MAT* locus (a and α). Among the 100 tetrads, few of them showed 3 *his5+* and 1 *TRP1* and in a few tetrads, all 4 were *TRP1* or *his5+* (Figure 18 and Table 9). Both these patterns of segregation represent gene conversion events that took place post meiotically (3:1, a classic single event during meiosis II stage); or in case of 4:0, it could also be a mitotic gene conversion event that took place just prior to meiosis, leading to loss of heterozygosity.

4.3 Discussion

In our study, we observed that chromosome loss was seen rather than loss in silencing at the *HMR* locus in *nkp2* mutant. We observed slightly elevated levels of chromosome loss upon *NKP2* overexpression. However, we saw an even more elevated chromosome loss in *nkp2* deletion. These results are consistent with the idea that any defect in the kinetochore components is detrimental to proper chromosome segregation. These data also indicate that Nkp2 function is required for proper segregation of chromosomes.

Chapter - 5

Investigation of molecular basis of Nkp2 function

5.1 Introduction

Studies in budding yeast have contributed immensely to the defining of pathways involved in genome maintenance and integrity of genetic material (Paques and Haber, 1999; Shrivastav et al., 2008). There are several mechanisms by which a wild type allele could become non-functional, but there are two pathways that predominate to inactivate the wild type allele from diploid cells, i.e., loss of part or the entire chromosome or a recombination event takes place within the wild type allele and non-functional allele, which replace the wild type allele with the mutant allele. This process is known as loss of heterozygosity (LOH) events (Carr and Gottschling, 2008).

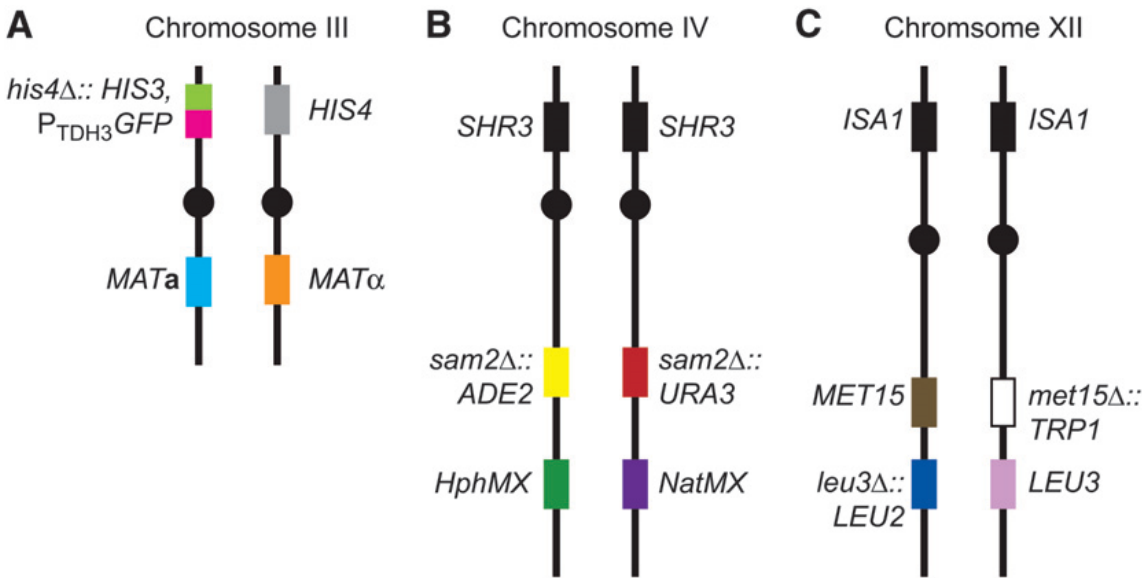

Figure 19: Schematic representation of multiple heterozygous marker strain. The multiple heterozygous markers (MHM) strain is to study loss of Heterozygosity (LOH) on three chromosomes. Chromosomes III, IV and XII were each marked with two pairs of selectable heterozygous markers adapted from Gottschling group, (Andersen et al., 2008).

Studies in budding yeast, *Saccharomyces cerevisiae*, has provided more details about genome instability i.e. spontaneous loss of heterozygosity, than has been possible in other organisms (Acuna et al., 1994; Barbera and Petes, 2006; Esposito and Bruschi, 1993; Hiraoka et al., 2000; McMurray and Gottschling, 2003). In yeast, the genomic changes that occur in each diploid cell is determined primarily through mitotic

recombination which could either be reciprocal recombination (loss of heterozygosity occurs in both cells) or non reciprocal recombination (LOH occurs in one cell and other remains heterozygous) (Acuna et al., 1994; Carr and Gottschling, 2008). Recent screens specifically examine LOH events which are focused on chromosome loss rather than recombination events in diploid cells. Previously, Gottschling lab, had constructed a strain with heterozygous markers at three different chromosomes to analyse the loss of heterozygosity either qualitatively or quantitatively (Figure 19) (Andersen et al., 2008).

5.2 Results

5.2.1 Loss of heterozygosity in *nkp2Δ*

In order to investigate the molecular mechanism of chromosome loss we used multi heterozygous marker (MHM) chromosomes (kind gift of Gottschling). Multiple markers are inserted at different chromosomal regions especially on two large chromosomes IV, XII and at the smallest chromosome III (Figure 19). In a diploid cell, at chromosome III, on the left arm of one homologue, *HIS4* gene was replaced with *HIS3*; the heterozygous strain is positive for histidine biosynthesis. If any of the chromosome arms is deleted or modified by gene conversion, then the strain becomes histidine negative because it has only one each of HIS3 and HIS4. In chromosome IV, the nonessential gene *SAM2* was deleted and replaced with two different markers on the two homologues, *ADE2* and *URA3.* Other drug resistance markers (hygromycin and nourseothrecin) are inserted distal to the modified *SAM2* locus. The loss of one arm can be scored as a colour change: when heterozygous strain retains the *ADE2* gene it will be white in colour, loss of *ADE2* produce colonies with red colour. Additionally, *URA3* can be used to measure change in genotype. Chromosome XII has 2 markers both on the right arm of the chromosome. The first is the *MET15* marker. *MET15*- cells produce black coloured colonies on plates containing lead nitrate. The strain is heterozygous for *MET15* at chromosome XII. As the cells have only one functional copy of *MET15*, any loss of that chromosome will produce Met- cells that will appear with black sectors on

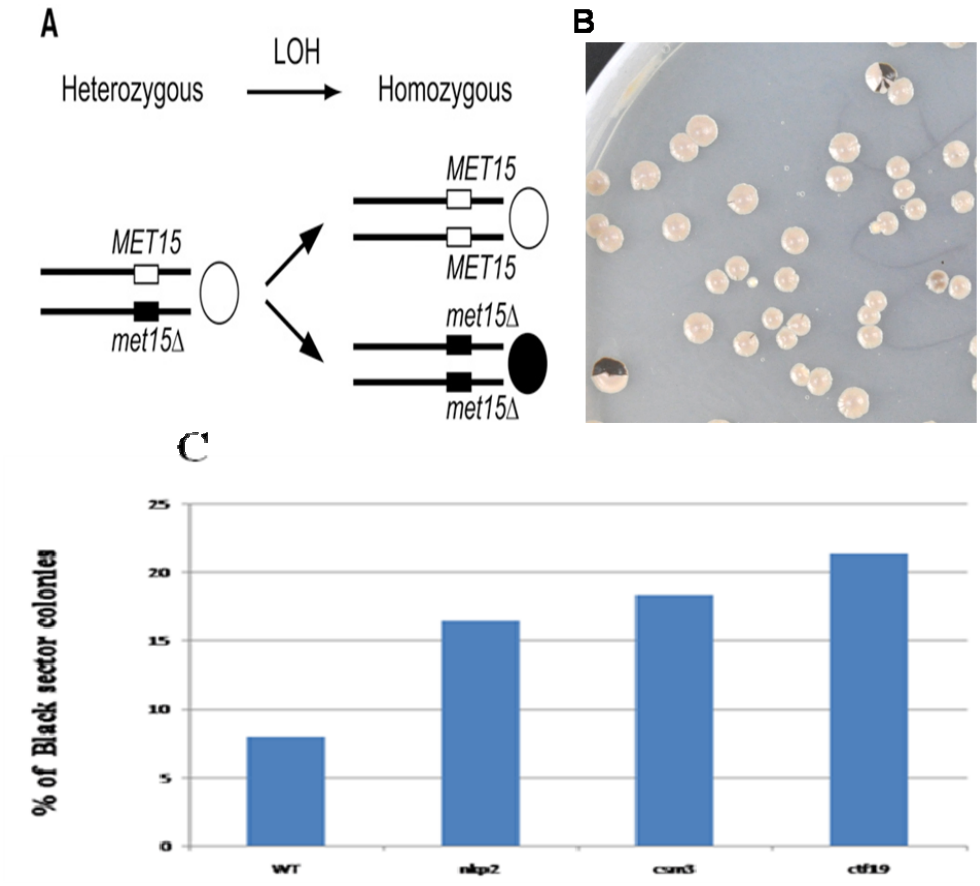

Table10: Black sectored colonies in MHM strains

Name of the strain	Total number of colonies screened	Black sector colonies	Total percentage of black sector colonies (%)
WT	4000	322	8.0
nkp2	4000	662	16.5
csm3	4000	735	18.35
ctf19	4000	854	21.35

Figure 20: Loss of Heterozygosity at *MET15* loci. (A) Schematic representation of loss of heterozygosity (LOH) at chromosome XII. LOH events in heterozygous cells (*MET15*/ *met15Δ*) that become homozygous (*met15Δ*/*met15Δ*) and (*MET15*/*MET15*) result in black and white colonies. (B) In the presence of lead nitrate colonies formed black half sectored lacking *MET15*. (C) Graphical representation of black half sector colonies in *nkp2* mutant is twofold higher than wild type, Table 10 with numbers and percentages of black sectored colonies.
Similarly, the chromosome also contains leu3::*LEU2*/*LEU3*+; again loss of any one of these chromosomes will leads to Leu- phenotype. These multiple heterozygous markers thus give two phenotypes; one is black /white and the other is leucine positive/negative colonies.

We used this strain to address the mechanism of chromosome instability seen in *nkp2* mutant. We constructed *nkp2* mutant in multi heterozygous marker (MHM) strain. The *csm3* and *ctf19* MHM strains were used as a positive control for LOH at chromosome III, IV and XII. The wild type (KRY525), *nkp2* (KRY532), *csm3* (KRY526) and *ctf19* (KRY528) were initially selected for all markers, grown in liquid cultures overnight at 30ºC and about 4000 colonies plated on lead nitrate containing rich media and incubated for 5 days at 30ºC and plates were transferred to 4ºC for 4 days. Colonies were screened for black sectors on lead nitrate plates. We found that about 8% of the cells form black sector colonies in wild type strain whereas in *nkp2* it was about 17%, in *csm3* the black sector colonies were similar at 18% whereas in *ctf19* mutants a slightly more elevated level of 21% was observed (Figure 20 and Table 10). The half sector colonies in wild type, *nkp2* and *csm3* mutants were patched on lead nitrate agar plates to screen for other multiple heterozygous markers i.e., half of the colony is white and other half is black to test the recombination events.

Similarly, we screened for red sector colonies at the chromosome IV, the chromosome IV is marked with two different auxotrophic markers *ADE2* and *URA3*. The heterozygous colonies were white in colour whereas loss of *ADE2* gene from the chromosome IV leads to formation of red colonies. In wild type cells the red sectored colonies formed was about 0.3%, in *nkp2* red sector colonies about 1% and *csm3* is about 0.9% (Figure 21 and Table 11).

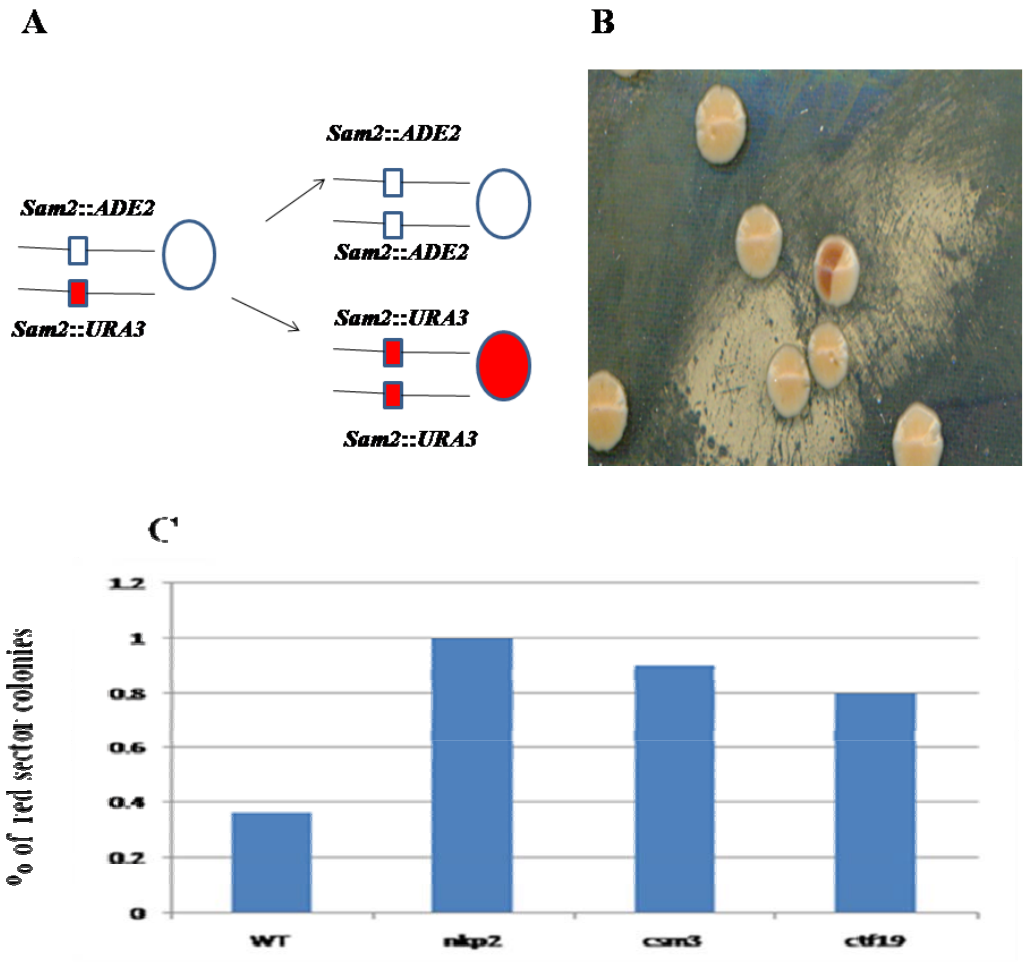

Table 11: Red sectored colonies in MHM strains

Name of the strain	Total number of colonies screened	Red sector colonies	Total percentage of Red sector colonies (%)
WT	4000	15	0.37
nkp2	4000	41	1.02
csm3	4000	36	0.9
ctf19	4000	32	0.8

Figure 21: Loss of Heterozygosity at chromosome IV in MHM strain. (A) Schematic representation of loss of heterozygosity (LOH) at chromosome IV. LOH events in heterozygous cells (*ADE2*/*URA3*) that become homozygous (*URA3*/*URA3*) and (*ADE2*/*ADE2*) results in red and white colonies. (B) About 4000 cells were spread on YPD. Heterozygous for *ADE2* appears white colour colony while cells lacking *ADE2* are red. During mitotic growth cells lost *ADE2*

leading to formation of Red/White half sector colonies. (C) Graphical representation of red sector colonies in *nkp2* mutant is twofold higher than wild type and Table 11 represents numbers and percentages of red sectored colonies.

Finally, we checked for LOH at chromosome III in wild type, *nkp2*, *csm3* and *ctf19* strains. Initially cells were selected on histidine drop out media and were subjected

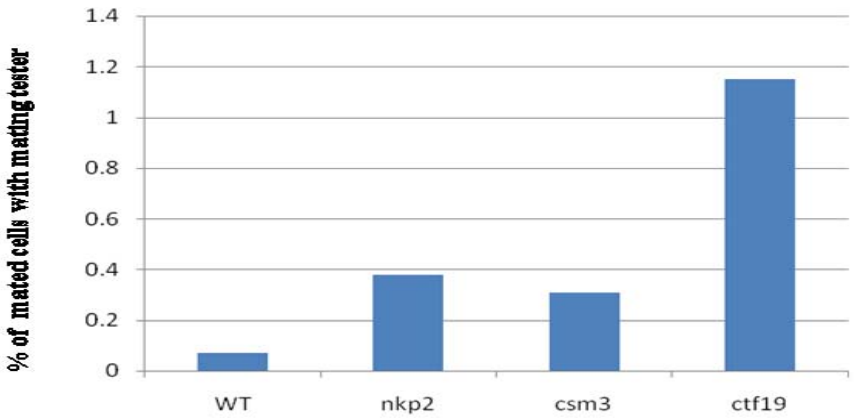

Table12: Quantitative mating assay in MHM strains

Name of the strain	Total number of colonies screened	Mated colonies	Total percentage of Mated colonies (%)
WT	$2X10^6$	1493	0..07
nkp2	$2X10^6$	7627	0.38
csm3	$2X10^6$	6143	0.31
ctf19	$2X10^6$	23045	1.15

Figure 22: Loss of Heterozygosity at chromosome III in MHM strain. Graphical representation of loss of heterozygosity (LOH) at chromosome III. LOH events at *MAT* loci by loss of *MAT a* chromosome arm from the diploid cell able to mate with mating tester PT-1 *Mat a* and Table 12 represents the numbers and percentages.

mating assay. Diploids do not mate. However, loss of either one of the chromosome III will allow cells to mate appropriately. A filter based mating assay was performed for 4 hrs and then plated on SC-His Lys to select for MHM strain and on SD plates for mated cells. The total number of cells plated is obtained from SC-His Lys plates. The fraction of SD+ over SC-His Lys gives the fraction of mated cells (Figure 22). In this assay, *nkp2* and *csm3* showed approximately a five-fold increase over the wild type whereas *ctf19* showed 20-fold increase (Table 12).

From the three assays described here, we conclude that *nkp2* mutants show elevated LOH levels compared to wild type. Although *nkp2* was not identified in the screen carried out by Gottschling and colleagues (Andersen et al., 2008), we find that LOH events, at least with respect to chromosome IV and XII LOH was comparable to *csm3* and *ctf19* which was identified in the screen. At chromosome III the events in *nkp2* was bit lower than *ctf19*.

5.2.2 LOH events in *nkp2* are predominantly due to nonreciprocal recombination on chromosomes XII and IV

To identify the nature of recombination events at chromosome IV and XII, The MHM strain was designed to distinguish between reciprocal or non reciprocal events. The crossing over takes place in a LOH strain to become half sector colonies with homozygous for two halves of the cells, in contrast, nonreciprocal LOH events produces one cell that retains heterozygosity whereas the other half becomes homozygous. To determine whether a LOH event occurred by reciprocal or non-reciprocal mechanism, one of the *MET15* gene is deleted from diploid cell to create heterozygosity for *MET15*/*met15:: TRP1*. When black/white half sectored colony were analysed the black half was Met- and Trp+ and white half was Met+ and Trp-, indicating that LOH events was reciprocal. In non reciprocal events the black half was Met- and Trp+ and white half of the colony was Met+ and Trp+. The reciprocal events are more at *MET15* locus at chromosome XII in wild type strain whereas in kinetochore mutants, the fraction of reciprocal events was significantly decreased relative to wild type. Whereas, non reciprocal events were about 63% in *nkp2* mutant, in wild type nonreciprocal events are

about 35%. These results suggest that in kinetochore mutants the ratio are reversed and the alternate mechanism of LOH was favoured.

5.3 Discussion

We tested the gene conversion events more directly by using multiple heterozygous marker strain. We observed that loss of heterozygosity was significantly increased in *nkp2* mutant relative to wild type at three different chromosomes. We tested the mechanism of gene conversion events in *nkp2* both quantitatively and qualitatively. As large fraction of LOH was due to non-reciprocal events it, the 3:1 segregation we observed in the meiotic segregation of *nkp2/nkp2* diploids could reflect this increase LOH events.

Chapter - 6

Role of Nkp2 in genome stability & maintenance

6.1 Introduction

Accurate transmission of the replicated genome during cell division is crucial for cell viability, proliferation and development. In eukaryotes, after replication, the sister chromatids are physically connected by cohesion. Upon entry into mitosis, replicated chromosomes are compacted. Concomitantly, chromosomes assemble a special structure called kinetochore to connect centromeric DNA to the spindle microtubules. During prometaphase, kinetochores interact with the microtubules. By metaphase, all chromosomes become bioriented, each microtubule from opposite the spindle pole attaches to the sister kinetochores. However, during the progression from prometaphase to metaphase, some chromosomes are inappropriately attached or spindles are connected at one side of the sister kinetochore. To avoid gain or loss of genetic information, the kinetochore monitors the state of attachment and activates the signalling pathway where mitotic spindle checkpoint proteins play a role to prevent the onset of anaphase in the presence of incorrectly attached or unattached kinetochores. Once the bi-orientation occurs for all the chromosomes, the sister chromatids are separated by degradation of the cohesion molecule by the separase and sister chromatids move to opposite poles of the cell during anaphase. During telophase, chromosomes are decondensed and two exact copies of the replicated genome are distributed into daughter cells.

Kinetochore is a biological molecular motor composed of multi-protein complex. Electron micrograph images reveal that the less dense inner and outer kinetochore sub-complexes are connected with central kinetochore sub-complex (McEwen et al., 2007). Initial efforts to define kinetochore organization were hampered by the low abundance of constituent proteins and because some of these proteins are required for cell viability. The identification of kinetochore proteins was first accomplished in vertebrates by using autoantibodies that recognized three major kinetochore proteins CENP-A, CENP-B and CENP-C (Earnshaw and Rothfield, 1985). After few years, the first yeast kinetochore proteins were identified (Baker et al., 1989; Cai and Davis, 1990; Cai and Davis, 1989; Lechner and Carbon, 1991). However, the subsequent dissection of kinetochore in vertebrates was difficult, because kinetochores remain tightly bound to the centromeric DNA, making metazoan kinetochores hard to enrich in solution (Earnshaw et al., 1984). In contrast, *Saccharomyces cerevisiae*

kinetochores are easily detached as individual proteins and subcomplexes from centromeres and spindle microtubule during cell extraction (De Wulf et al., 2003). Genetic screens for mutations that affect chromosome stability in *Saccharomyces cerevisiase* along with biochemical efforts were initiated. These mutations lie in genes that are required for a variety of processes contributing to accurate and efficient distribution of replicated chromosomes (Hieter et al., 1985; Koshland and Hieter, 1987).

The budding yeast kinetochore associates with centromere DNA during replication and hierarchical assembly of inner, outer and central kinetochore subcomplexes in a few minutes follows (Tanaka et al., 2005). Central kinetochore subcomplex consists of distinct and evolutionary conserved proteins. For example, Ctf19, Mcm21, Mcm16 and Ctf3 of vertebrates have been localized to the inner kinetochore subcomplex whereas, in budding yeast; the position of these components relative to centromere is still not known (Foltz et al., 2006; Kouprina et al., 1993; Okada et al., 2006).

In our study we observed that *nkp2*Δ resulted in chromosome missegregation and gene conversion events. Recently, Marston's group proposed a model for Ctf19 subcomplex with Nkp2 as a part of this complex. Recent studies have identified the role of some central kinetochore subcomplex components in genome stability. Some of the *ctf19* subcomplex mutants show genome instability by chromosome loss assay. All these data strengthen our view that the kinetochores are assembled, organized and functionally integrated to achieve accurate chromosome segregation.

We focused on the Ctf19 subcomplex components, how these proteins are organized along with Nkp2 into the higher order central kinetochore subcomplex structure, as well as how they function to achieve proper chromosome segregation. For this, we tested if *nkp2*Δ has elevated or lowered chromosome missegregation with the Ctf19 subcomplex components by making double mutants and testing their chromosome loss levels. To map the genetic interaction of Nkp2 with Ctf19 subcomplex components, we performed a chromosome loss assay in *nkp2* with individual double mutant of Ctf19 subcomplex components.

6.2 Results

6.2.1 Genome instability in Ctf19 complex mutants

To further study the function of Nkp2, we performed colour-based colony sector assay in double mutants of *nkp2* with other *ctf19* complex components using the artificial chromosome, *SUP11*, described in the earlier section. We scored the sectored colonies; those were at least half red colonies indicating loss of chromosome in the first few generation after plating. We constructed a double mutant carrying a *nkp2*Δ and mutation of individual *ctf19* components by crossing *nkp2*Δ carrying the *SUP11* artificial chromosome with individual *ctf19* mutants. We tested the chromosome loss in *ctf19* complex double mutant with *nkp2*, initially selected them on adenine deficient medium to retain the artificial chromosome and plated them on rich media to quantify the sectored colonies. During cell division, missegregation of artificial chromosome leads to formation of sectored colonies. This could be due to abnormal attachment of spindle microtubules, defect or dissolution in cohesion leading to missegregation of artificial chromosomes.

Strikingly, we observed that double mutants of *nkp2 nkp1*, *nkp2 mcm22* and *nkp2 mcm17* sectored heavily and show elevated levels of chromosome loss than either single mutant. These results suggest that *nkp2* interacts with *nkp1*, *mcm22* and *mcm17*. The chromosome loss assay results corroborate with the protein-protein interactions that were seen in these Ctf19 components (Fernius and Marston, 2009). In other *ctf19* components like *ctf19*, *mcm21*, *mcm16, iml3* and *ctf3,* single mutants show high rate of chromosome loss where as double mutants with *nkp2*Δ suppresses the chromosome loss phenotype (Figure 23). These results indicated that the Nkp2 shows negative genetic interaction with *ctf19*, *mcm21*, *mcm16*, *iml3* and *ctf3*.

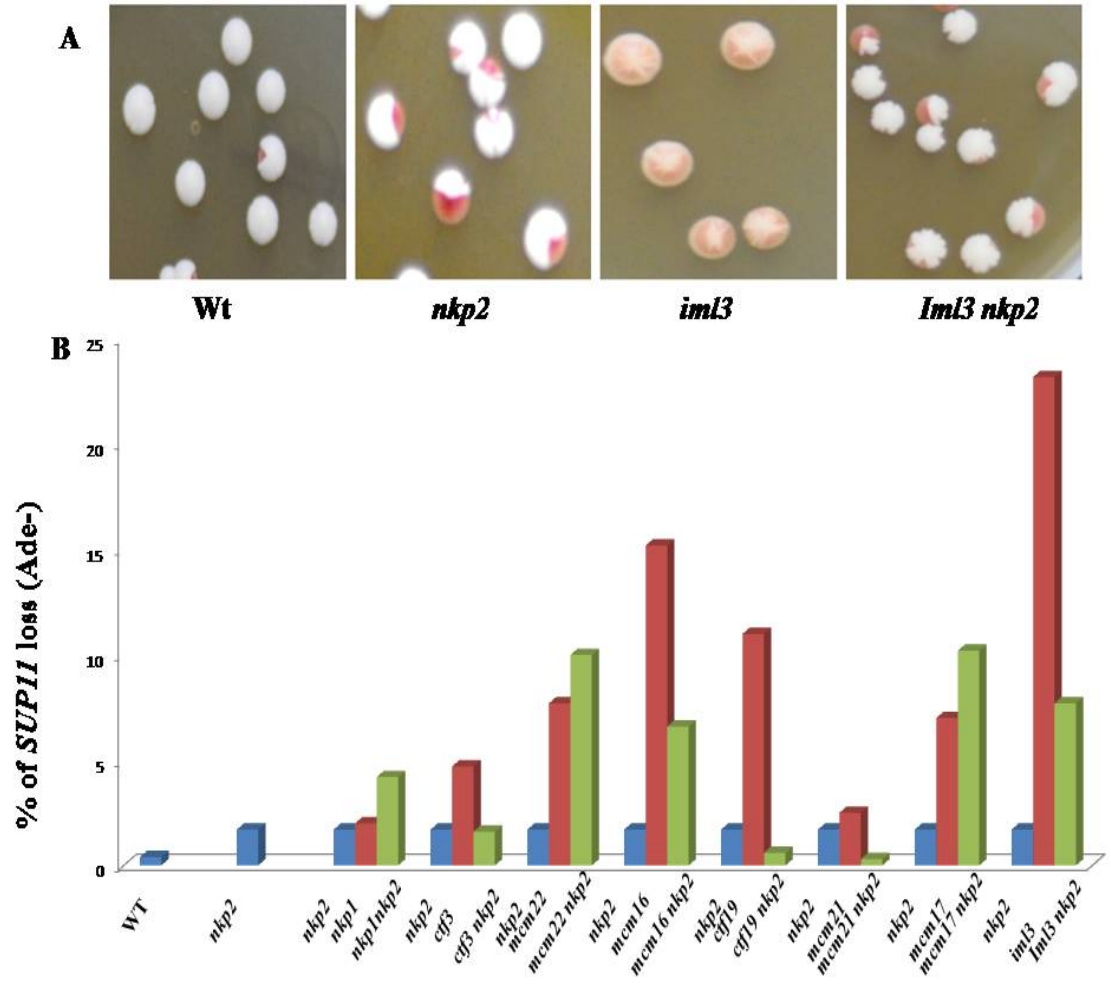

Figure 23: Chromosome loss was elevated and suppressed in *ctf19* double mutants. *ctf19* double mutant with artificial chromosome *SUP11* were grown in SC-Ade broth to select *SUP11*. Spread about ~4,000 cells on YPD agar plates to score half sector colonies. Panel A shows the *SUP11* chromosome loss with half sectored colonies. Panel B shows graphical representation of *ctf19* double mutant; *nkp2* with *ctf19* individual mutant represent as green bars whereas, red bars represents single mutant of each *ctf19* component and blue represents *nkp2*.

Table13: Chromosome loss (*SUP11*) in *ctf19* double mutants

Name of the strain	Artificial chromosome loss	Total percentage of *SUP11* loss (%)
Wt	**16**	**0.4**
nkp2	**68**	**1.7**
nkp1	**80**	**2.0**
nkp1 nkp2	**168**	**4.2**
ctf3	**188**	**4.7**
ctf3 nkp2	**64**	**1.6**
mcm22	**311**	**7.7**
mcm22 nkp2	**403**	**10.0**
mcm16	**558**	**15.2**
mcm16 nkp2	**265**	**6.6**
ctf19	**320**	**11.0**
ctf19 nkp2	**30**	**0.6**
mcm21	**120**	**2.5**
mcm21 nkp2	**18**	**0.3**
iml3	**926**	**23.2**
iml3 nkp2	**306**	**7.7**

6.2.2 Quantitative mating assay in Ctf19 complex mutants

To confirm the chromosome loss phenotype observed in colour-based colony sector assay we assessed the loss of chromosomes III in a homozygous diploid mutant strain by quantitative mating assays discussed earlier. We tested homozygous mutants of *ctf19* individual components and in combination with the *nkp2* deletion. Initially, we grew them in rich media overnight and harvested the cells and about 2 X 10^6 cells were

mixed with 1 X10^8 cells of mating tester Mat a or Mat α on nylon membrane and placed them on YPD agar at 30ºC for 4 hours, washed and plated multiple YPD agar plates.

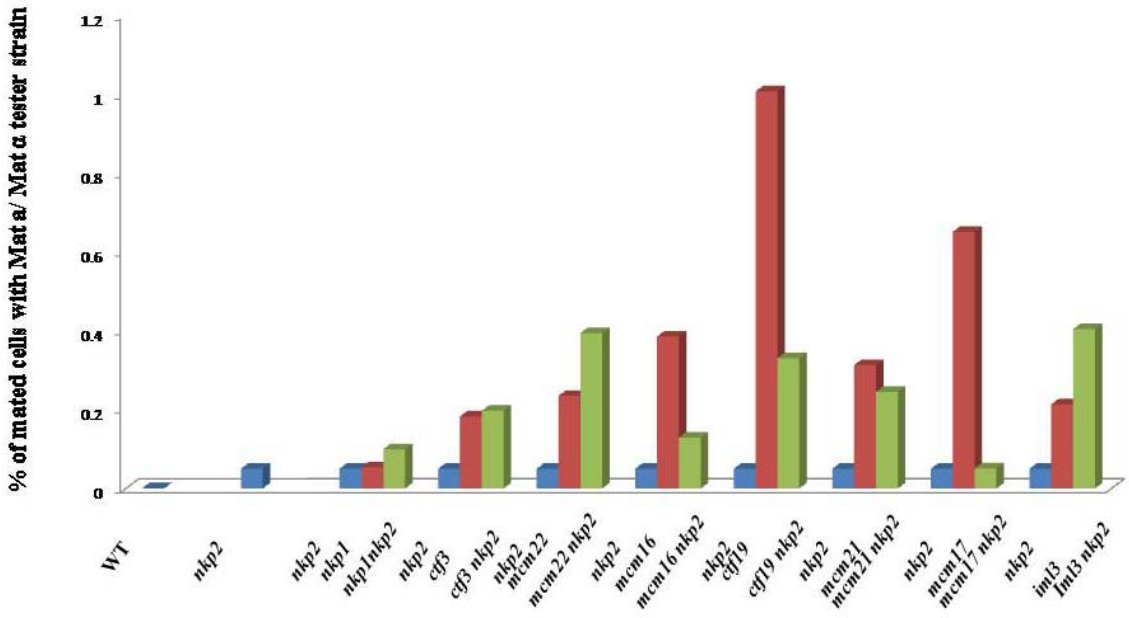

Figure 24: Quantitative mating assay in *ctf19* double mutant. Mating assay performed in *nkp2* double mutant with *ctf19* individual components. Green bars represent double mutants of *ctf19* component with *nkp2*Δ and red bar represents the individual mutant of *ctf19*Δ, blue is *nkp2*Δ.

As expected wild type diploid cells consisting of heterozygous information of Mat a and Mat α were not able to mate with any of the mating tester whereas, in single mutants of *ctf19* homozygous mutants shows increased chromosome III loss as compared with wild type as scored by increased mating. We tested the chromosome III loss in double mutant by quantitative mating assay. We found elevated chromosome loss in double mutants of *nkp1 nkp2*, *nkp2 mcm22*, *nkp2 ctf3* and *nkp2 iml3* whereas individual single mutants showed less severe chromosome loss. In other double mutants like, *nkp2 mcm17*, *nkp2 mcm16*, *nkp2 mcm21* and *nkp2 ctf19* chromosome III loss was suppressed (Figure 24).

Table 14: Quantitative mating assay in *ctf19 double mutants*

Name of the strain	Artificial chromosome loss	Total percentage of *SUP11* loss (%)
Wt	32	0.0008
nkp2	1,992	0.0498
nkp1	2,147	0.0536
nkp1 nkp2	3,972	0.0993
ctf3	7,290	0.1824
ctf3 nkp2	7,880	0.1970
mcm22	9,380	0.2345
mcm22 nkp2	15,740	0.3937
mcm16	15,400	0.3850
mcm16 nkp2	5,160	0.1290
ctf19	40,250	1.0062
ctf19 nkp2	13,185	0.3296
mcm21	12,505	0.3126
mcm21 nkp2	9,790	0.2447
iml3	8,530	0.2132
iml3 nkp2	16,160	0.4040

The two chromosome loss assays corroborate with each other and establish that the Nkp2 shows positive genetic interaction with Nkp1, Mcm22 and Iml3 and negative genetic interaction with other components of Ctf19 complex such as Mcm16, Mcm17, Mcm22, Ctf3 and Ctf19. Previous reports had shown that Ctf3, Mcm22 and Mcm16 interact with each other and establish kinetochore protein assembly in a Ctf19 dependent manner (Measday et al., 2002; Pot et al., 2003).

6.2.3. Nkp2 is involved in separation of sister homologs during meiosis

In order to test the role of Nkp2 in the establishment and maintenance of cohesin at centromere regions we constructed a strain of *nkp2* mutant with an array of Lac operators that were integrated close to the centromere of chromosome IV. We targeted green fluorescent protein (GFP) to bind the tandem array of Lac operators. To follow chromosome segregation, we marked both the copies of a chromosome in a diploid cell

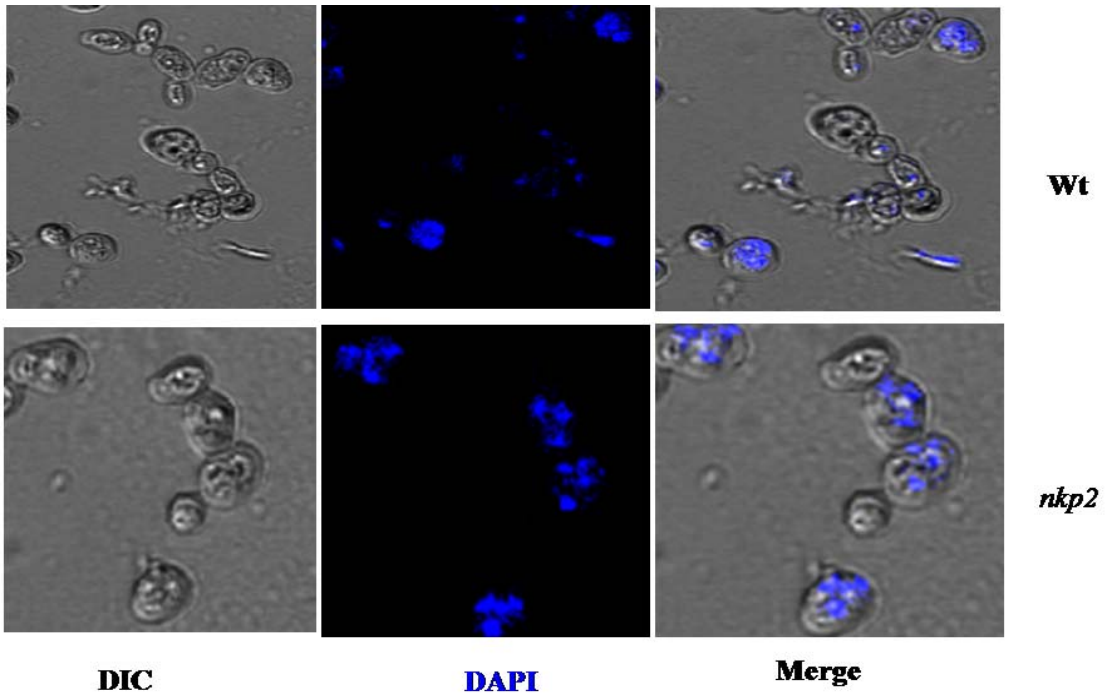

Figure 25: *nkp2Δ* undergoes meiosis much earlier than wild type. Wild type and *nkp2* mutants were grown them in sporulation medium for 24 hours. Harvested the spores and tested the tetrad formation by staining the nucleus with DAPI (Blue).

to determine the chromosome segregation during mitosis and meiosis (Straight et al., 1996). We analyzed the mitotic segregation of GFP-marked chromosome IV in wild type and *nkp2*Δ; *nkp2*Δ shows equal segregation of GFP spots in dividing cells, showing that *nkp2* segregates normally as wild type but in mutants like *mcm17* and *iml3* significant number of cells undergoes non-disjunction (Fernius and Marston, 2009). These results suggest that *nkp2* mutant does not show the non-disjunction of replicated chromatin. To examine the role of Nkp2 during meiosis, we tested wild type and *nkp2*

mutant for entry into meiosis in a time dependent manner. For this we released the cells from the presporulation medium into a sporulation medium and harvested the cells at every 2 hour intervals. We observed that *nkp2* shows tetrad formation much earlier than wild type strain (Figure 25).

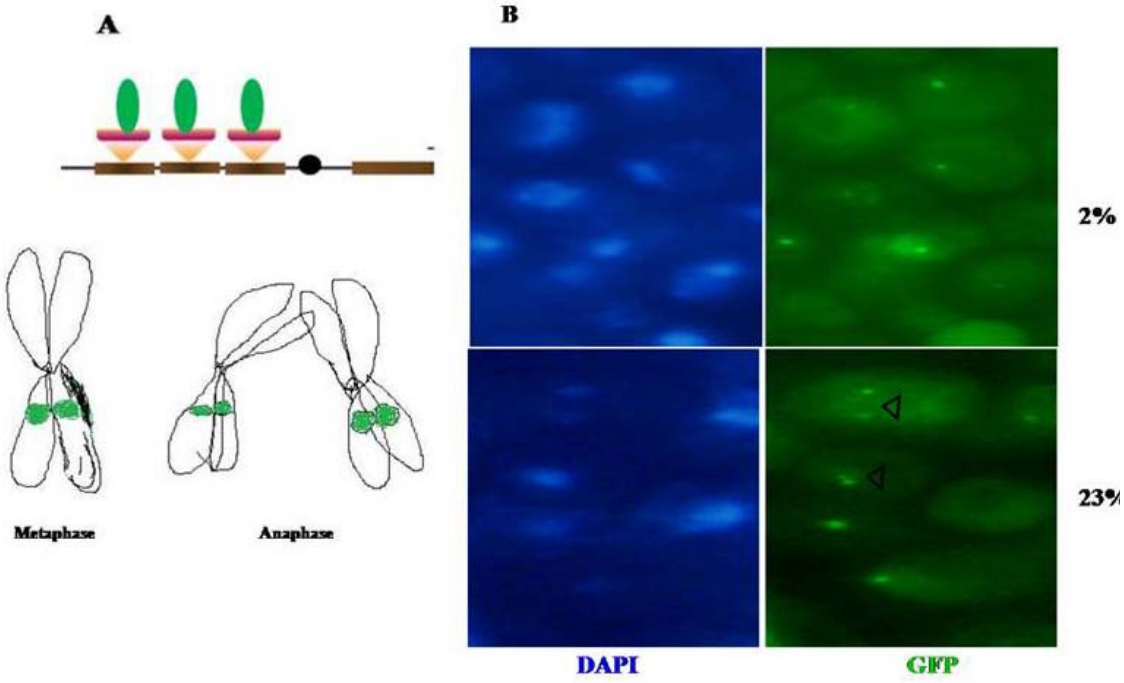

Figure 26: Separation of homologs is much earlier in *nkp2Δ* than wild type. Panel A: Schematic representation of how sister chromatids that are held together separate upon cohesion degradation. In panel B, WT and *nkp2*Δ strains with sister chromatids marked with GFP. Sister homologs of both strains were imaged at the same time point after introduction in sporualtion medium. Separated sisters appear as two GFP spots. *nkp2*Δ shows many cells with 2 spots, whereas wild type shows single GFP spot.

We further confirmed the early meiosis seen in *nkp2* mutant by testing the homologue separation during anaphase I. For this we harvested the cells from sporulation media at every one hour interval and analyzed the meiotic segregation of GFP-marked chromosome in wild type and *nkp2*. We found that in *nkp2* mutants, at 8 hour time point, homologs are separated in about 23% of the cells whereas, in wild type, the homologue separation is about 2% (Figure 26), a ten-fold increase. This result suggests that in *nkp2* homologs are separated much faster than wild type. This might be

because of cohesion on chromosome arms is lost during meiosis I thereby triggering the segregation of homologs to the opposite spindle poles. However, cohesion around centomeric region is maintained until anaphase II. Loss of centromere cohesion during meiosis II triggers the segregation of sister chromatids (Nasmyth, 2005; Nasmyth and Haering, 2005). We further tested the marked GFP during meiosis II, we observed that ~98% of the cells with four GFP spots are segregated in tetranucleate spore, but the meiosis II is also much faster than wild type. All these observations suggest that, in *nkp2* mutant, during meiosis, chromosome arm cohesion might dissolve much earlier than wild type and enters and completes meiosis II much earlier than wild type.

6.3 Discussion

Transmission of genetic material requires a kinetochore that is is functionally active and connects the spindle microtubule to the centromeric DNA. The replicated chromosome segregates accurately into daughter cells from mother cell through attachment to the microtubule. During cell division a variety of processes depends on the kinetochore components which connect the centromere region to the microtubules. Previously it was shown that the central Ctf19 subcomplex proteins are required for a variety of processes contributing to accurate transmission of replicated chromosomes, connectiong centromere to the spindles, kinetochore assembly with other kinetochore subcomplex and cohesion of chromatids during cell division (Cleland 2003 et al.,). We tested chromosome stability of *nkp2* in combination with individual subcomplex components. From these, it was evident that *nkp2 nkp1*, *nkp2 mcm22* and *nkp2 mcm17* double mutants show enhanced chromosome loss whereas, with other components of subcomplex, namely, *iml3, ctf19, mcm21* and *mcm16,* suppressed the chromosome loss phenotype.

There many ways in which Nkp2 may enhance or reduce chromosome loss in *ctf19* mutants. Lack of Nkp2 might cause severe defect in attachment of microtubules or lack of tension at the microtubules activate the spindle checkpoint proteins in mutants of *iml3*, *ctf19,* and *mcm16*. The spindle checkpoint delays metaphase, and promotes bi-orientation of microtubules and segregates the chromosomes accurately, therefore the

phenotype was suppressed. Secondly, instead of bipolar attachment, microtubules from same spindle pole attaches to the sister kinetochore in monopolar attachment and these monopolar attachments are sensed by spindle check point proteins like Mad1, Mad2 and Mad3, and prevent the misegregation of artificial chromosome until spindles are properly attached to the kinetochore, and once the bi-orientation of spindles occurs for all chromosomes, the sister chromatids are separated. We found that moderate chromosome loss was seen in *nkp1*, *nkp2*, *mcm17* and *mcm22* single mutants. However, the rate of non essential chromosome (*SUP11*) loss was enhanced upon removal of Nkp2 in *nkp1*, *mcm22* and *mcm17* as compared with either of the single mutants. This observation suggests that the removal of Nkp2 in *nkp1*, *mcm22* and *mcm17* might cause distortion of central kinetochore complex that could not be sensed or repaired by the spindle check point proteins.

From the quantitative mating assay, we found that *nkp1 nkp2; iml3 nkp2* and *mcm22 nkp2* double mutants exhibited increased chromosome III loss as compared with either of single mutants where as in other double mutants like *mcm16 nkp2*; *mcm17 nkp2*; *mcm21 nkp2* and *ctf19 nkp2* chromosome III loss was reduced. However *nkp2 ctf3* double mutant exhibited equivalent chromosome loss as *ctf3* single mutant. These results from artificial chromosome loss and quantitative mating assays suggest that the lack of Nkp2 enhanced chromosome loss possibly by defect in check point arrest where as reduced chromosome loss was seen due to proficient checkpoint arrest. The rate of chromosome loss was equivalent in a *ctf3 nkp2,* double deletion strain to the rate of chromosome loss in either *ctf3* or *nkp2,* suggesting that Ctf3 and Nkp2 might function together in Ctf19 complex.

The rate of chromosome loss was significantly reduced in double deletion strains of *nkp2 ctf19* (reduced to 10 fold), *nkp2 mcm21* (2 fold), *mcm16 nkp2* (2 fold) as compared to the rate of chromosome loss in *ctf19*, *mcm21* and mcm16 single deletion strains. These observations suggest that removal of Nkp2 might cause severe distortion of COMA (Ctf19, Okp1, Mcm21 and Ame1) core complex and Ctf3 subcomplex (includes Ctf3, Mcm16 and Mcm22) and this could be sensed by checkpoint proteins and prevent the mis-segregation of chromosome until the mitotic spindles are properly aligned. The single mutants may not be able to create enough signal for the activation of

the spindle checkpoint. However in *mcm22 nkp2 and nkp1 nkp2* double mutant strains 1.5-2 folds increased in chromosome loss was observed and this might be due to removal of Nkp2 having increased defect in kinetochore function.

In case of *iml3* and *mcm17* we see different trends in chromosome loss between the two assays for chromosome loss employed. The *iml3 nkp2* double deletion strain shows 3-fold reduction in artificial chromosome loss assay and 2-fold increase in chromosome III loss assay. *mcm17 nkp2*, on the other hand, shows a 1.5 fold increase in the artificial chromosome loos assay and a 12 fold reduction in the chromosome III loss assay. These differences could be due to the different sizes of these two different chromosomes. It has been reported earlier that chromosome size is an important determinant in the efficiency of chromosome segregation (Murray et al., 1986). We believe that these differences could be due to differential contribution of these proteins to the kinetochore structure and loss of these proteins affects each chromosome slightly differently.

Further we examined the chromosome segregation during meiosis in *nkp2* mutant. We found that, Nkp2 is involved in sister homolog separation during meiosis I, removal of Nkp2 cause early meiosis I and sister homolog separates much faster than wild type. These data suggest that Nkp2 might be involved in assembly and maintenance of cohesion at centromeric regions.

Chapter - 7

Subcellular localization of Nkp2 in Ctf19 complex mutants

7.1 Introduction

Kinetochores are protein assemblies that couple chromosome region to dynamic microtubules, required for accurate and efficient segregation of chromosomes during cell division in all eukaryotes (Maiato et al., 2004). Kinetochore is a multiprotein subcomplex consisting of about 65 proteins that are assembled into about 10 subcomplexes and are organized as building blocks as inner, central and outer kinetochore (Cheeseman et al., 2002; De Wulf et al., 2003; Westermann et al., 2003). From genome wide protein mapping, localization studies and biochemical assays it was inferred that Nkp2 is part of central kinetochore subcomplex (Cheeseman et al., 2002).

From the affinity purification, the Ctf19 complex consisting of Ctf19, Okp1, Mcm21 and Ame1, referred as COMA subcomplex, were isolated as a biochemically stable complex. Other proteins like Nkp2, Nkp1, Ctf3, Mcm16, Mcm17, Mcm22 and Iml3 are thought to be peripheral components (Akiyoshi et al., 2010; Fernius and Marston, 2009; Hornung et al., 2011). Previously, it was reported that the some of the Ctf19 vertebrate homologs have been localized to the centromere of humans and chicken (Foltz et al., 2006; Okada et al., 2006). In budding yeast, the position of these components relative to the centromere is not clear. All budding yeast central kinetochore complexes such as CTF19 and MIND assemble onto centromere through CBF3 inner kinetochore complex in a COMA–dependent manner. However the Ctf3 subcomplex (Ctf3, Mcm16 and Mcm22) and Mcm17/Iml3 proteins are recruited independent of each other to COMA. Nkp1 & Nkp2 function at the kinetochore as a component of the Ctf19 but the mode of recruitment was not known. Localization studies have shown that the inner kinetochore component Ndc10 (helps in centromere attachment to the spindle pole body) colocalized with the Ctf19 and the localization of Nkp2 was shown to be similar as in other component of Ctf19 subcomplex (Cheeseman et al., 2002; Measday et al., 2002; Ortiz et al., 1999). To gain additional in vivo evidence, Nkp2 localization was tested in mutants of individual Ctf19 complex with respect to spindle pole body component Mps3.

Results

7.2.1 Functional analysis of Nkp2 in cell cycle dependent manner

In order to investigate the functional role of Nkp2 at each stage of cell cycle we constructed a strain with 13 copies of myc epitope tagged at C-terminus of endogenous Nkp2. Firstly; we tested the protein expression levels of Nkp2 in a cell cycle dependent manner by western blots. For this, total protein was isolated from the tagged strain which was arrested at different cell cycle stages such as G1- phase by α factor, S-phase with hydroxyurea, metaphase mitotic arrest by nocodozole.

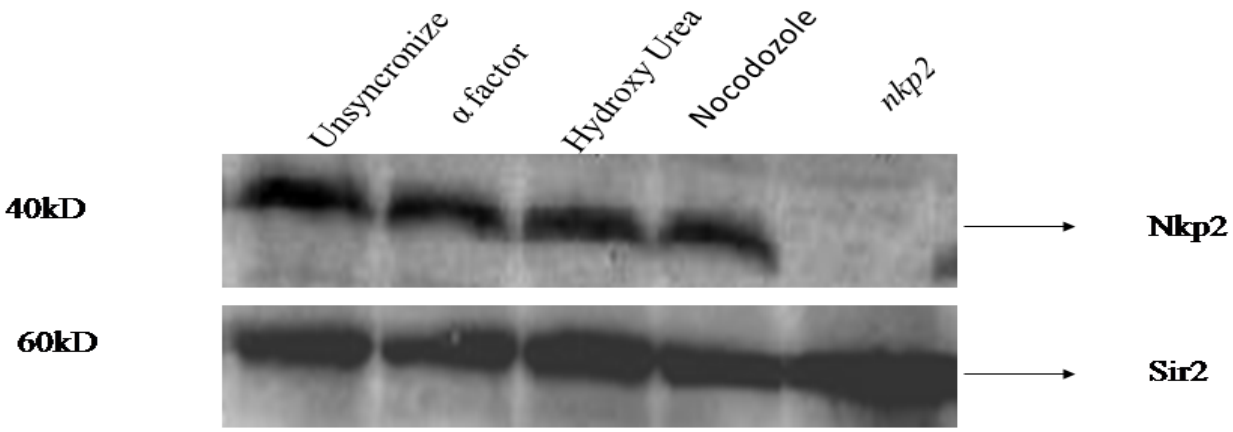

Figure 27: Similar levels of Nkp2 protein expressed in various stages of cell cycle. Equal amount of protein was loaded and probed with anti-myc antibody to detect the Nkp2 tagged myc and loading consistency checked with anti-Sir2 polyclonal antibody.

Equal amount of proteins from different cell cycle arrested cultures and *nkp2* mutant were separated on 15% SDS-PAGE and subjected to western analysis with anti-myc antibody for detecting the Nkp2 and poly-clonal antibody for Sir2 to check for equal loading of proteins. Nkp2 protein was detected at about 40 kDa and Sir2 at 60 kDa respectively (Figure 27). Furthermore, the western blot shows that the Nkp2 protein levels are similar at all stages of cell cycle during G1, S and mitotic phase. Sir2 protein is shown as a loading control in each lane equal amount of protein was loaded (Figure 27).

7.2.2 Immuno-localization of Nkp2 during different cell cycle stages

We next examined localization of Nkp2 at different cell cycle stages. We performed immunolocalization of wild type strain to localize Nkp2 in a cell cycle dependent manner. The nuclear rim was stained with antibodies to Nsp1p, a nuclear pore complex protein. Nsp1p was visualized with alexa fluor (green) and Nkp2 with Cy3 (red). DNA was counterstained with DAPI. Figure 28 shows the localization of Nkp2 is cell cycle dependent manner. During G1 and S-phase single distinct Nkp2 spot (open arrows) observed at the nuclear rim whereas, in mitotic cells, Nkp2 spot moved more interior from the nuclear periphery.

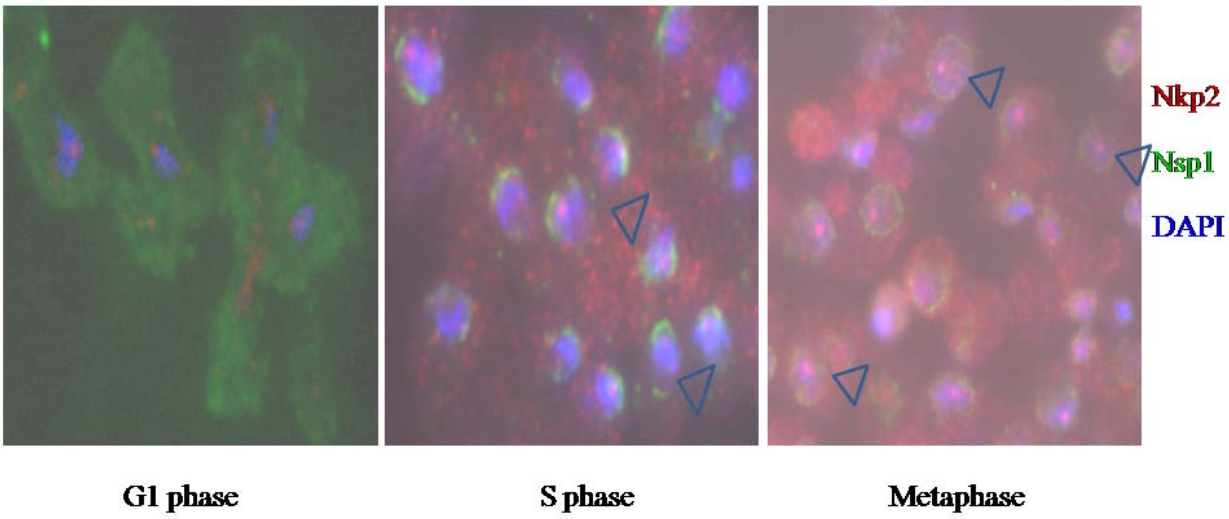

Figure 28: Cell cycle dependent localization of Nkp2. Localization of Nkp2 was performed in cells arrested at various stages of cell cycle. Nkp2 was seen at the nuclear rim during G1 and S phase whereas, in metaphase arrest Nkp2 delocalized from the nuclear periphery.

We find that Nkp2 protein levels are similar throughout the cell cycle but the localization of Nkp2 depended on cell cycle stages. At G1 and S phase Nkp2 is present at the nuclear rim. Previously, it was shown that Nkp2 colocalized with spindle pole body, which is embedded in the nuclear rim throughout the cell cycle (Huh et al., 2003).

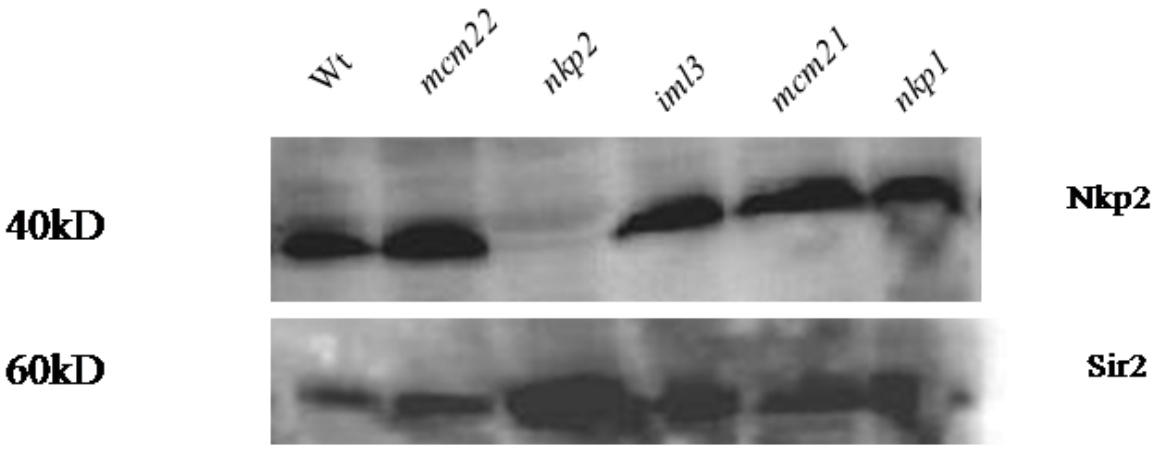

Figure 29: Nkp2 expression levels are similar in other *ctf19* mutants. Total proteins were extracted from wild type and different *ctf19* mutant with *MYC* tagged *NKP2*. Equal amount of proteins were loaded on SDS-PAGE and subjected to immunobloting with anti-myc antibody to detect the Nkp2 and anti-Sir2 polyclonal antibody to detect the Sir2 for equal loading. A similar level of expression of Nkp2 was seen in *ctf19* mutant.

In order to test if the localization of Nkp2 is affected in *ctf19* mutants, we constructed a strain carrying myc-tagged Nkp2 and HA tagged Mps3, a spindle pole body component to further confirm and mark the SPB. In this strain, we introduced individual *ctf19* complex mutants and tested the localization of Nkp2 and Mps3. Initially, we examined the protein levels of Nkp2. We found that protein levels of Nkp2 are stable and similar in *ctf19* mutants as seen in wild type (Figure 29).

7.2.3 Localization of Nkp2 in Ctf19 complex mutants

We next tested if the localization of Nkp2 was affected in any of the *ctf19* mutants. For this, cells were fixed and immunostaining was performed on these strains. Nkp2 was visualized with a Cy3 (red) conjugate and Mps3 with alexa fluor 453 (green). DNA was counter stained with DAPI in blue. As expected in wild type, Nkp2 shows distinct single focus within the nucleus and this focus colocalized with Mps3. This observation suggests that, Nkp2 colocalizes with spindle pole body. Similarly, the

localization of Nkp2 was seen at the spindle pole body in mutants like *iml3*, *mcm17* and *nkp1* (Figure 30). That is, single distinct foci of Nkp2 colocalized with Mps3, suggesting that Nkp2 localization did not require functional Iml3 or Mcm17 or Nkp1. However, in mutants like *mcm16* and *ctf3* there are multiple foci spread throughout nucleus (Figure 31). These results suggest that the localization of Nkp2 to the spindle pole body was dependent on Ctf3 and Mcm16.

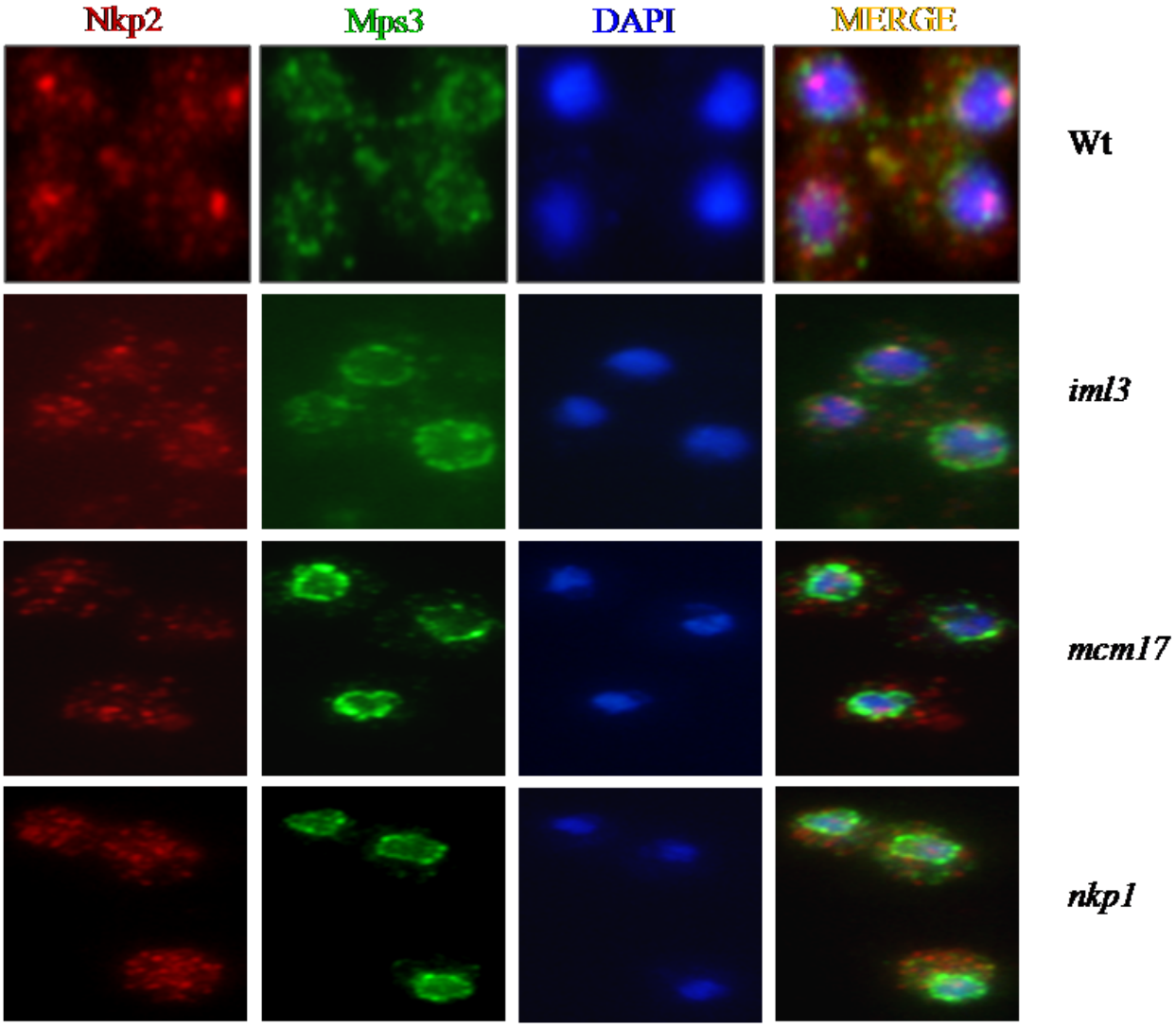

Figure 30: Immunofluorescence analysis for localization of Nkp2 in *iml3*, *mcm17* and *nkp1*. Immunolocalization of Nkp2 in wild type, *iml3*, and *mcm17* and *nkp1* mutant. Nkp2 (red) single spots observed and Mps3 (green) stains the spindle pole body and DNA (DAPI).

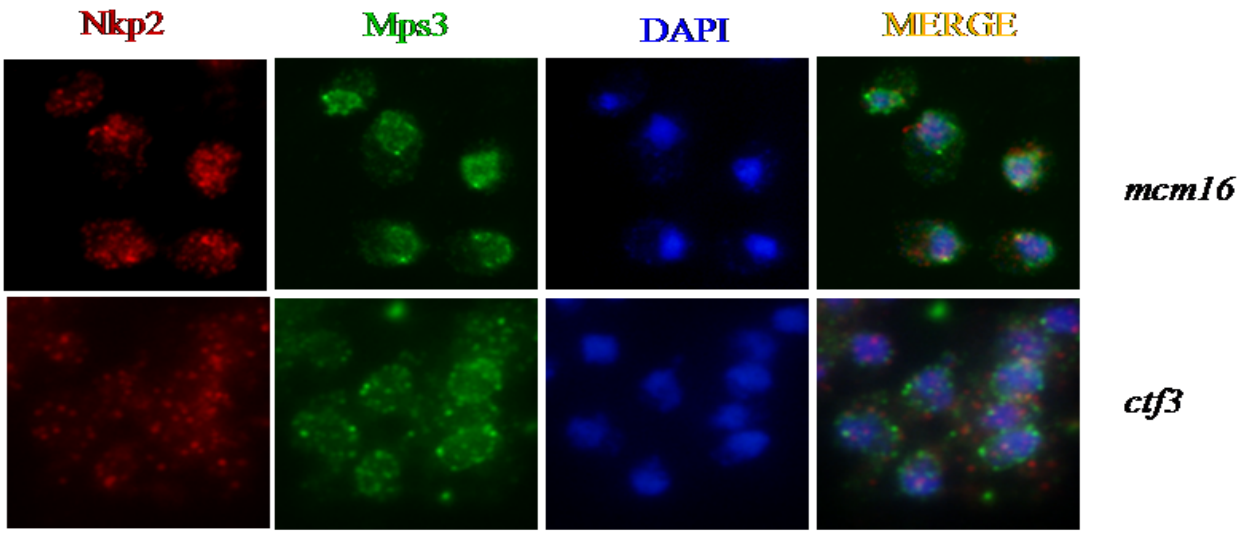

Figure 31: Immunostaining of Nkp2 and Mps3 in *mcm16* and *ctf3*. Immunolocalization of Nkp2 in *mcm16* and *ctf3* mutant. Nkp2 (red) multiple spots were observed. Mps3 (green) stain with the spindle pole body and DNA by DAPI (blue).

In *ctf19* and *mcm21* mutants localization of Nkp2 was severely affected, where Nkp2 protein was not seen in nucleus, even though the proteins levels of Nkp2 were stable and similar as wild type (Figure 32, Figure 30). Previously, it was reported that Ctf19 and Mcm21 interact with Nkp2 by affinity purification. Our results suggests that the Nkp2 nuclear localization was affected in COMA subcomplex mutants, these proteins might be necessary for assembly of Nkp2 in Ctf19 central kinetochore complex.

We next tested localization of Nkp2 in *mcm22* mutant, where multiple foci of Nkp2 were seen within the nucleus and Mps3 localization also affected in this mutant. We also counter stained the nuclear membrane with Nsp1 to test if the spots were nuclear. Nkp2 is found in multiple foci that are scattered throughout the nucleus. The scattering of kinetochores is a consequence of the improper attachment of chromosomes to spindle microtubules (He et al., 2000; Janke et al., 2001; Wigge and Kilmartin, 2001). Our results taken together suggest that Mcm22, Ctf3 and Mcm16 are required for organization of central kinetochore component, Nkp2.

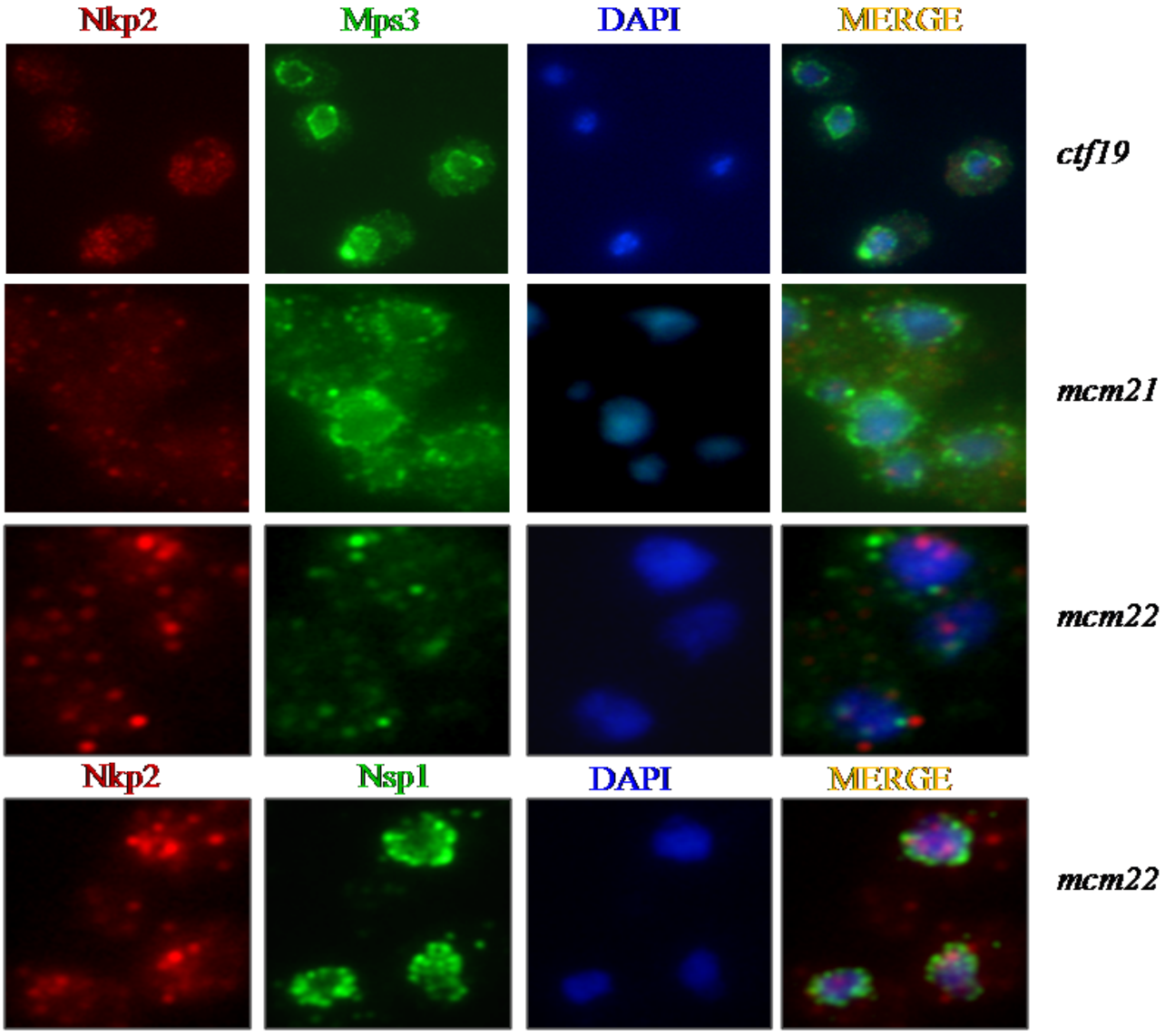

Figure 32: Scattered localization of Nkp2 and Mps3 in *mcm22*. Immunolocalization of Nkp2 in *ctf19*, *mcm21* and mcm22 mutant. Nkp2 (red) spots are scattered throughout the nucleus. Mps3 (green) stain the spindle pole body and DNA by DAPI (blue). In *mcm22* mutant, Nsp1 (green) stain the nuclear membrane in down panel.

7.3 Discussion

The Nkp2 protein levels are stable and similar throughout the cell cycle. But, the localization of Nkp2 is more interior in the nucleus during metaphase arrest. This observation suggests that kinetochore protein moves and is localized to interior of the nucleus during metaphase, where chromosomes are aligned on mitotic plate. We tested the Nkp2 protein stability in *ctf19* mutant components; Nkp2 protein was stable and similar in all *ctf19* mutants. However, the localization of Nkp2 is affected in some of the *ctf19* mutants. For example, localization of Nkp2 was affected and 3-5 distinct foci were seen in *mcm16* and *ctf3*. Whereas, in mutants like *ctf19* and *mcm21,* components of COMA, the Nkp2 localization to the nucleus was affected, however Nkp2 protein expression is similar as wild type. We tested Nkp2 localization in *mcm22* mutant where the Nkp2 is scattered throughout the nucleus and more bright spots are visible, where as in wild type only 1-2 distinct foci was seen. In *mcm22*, we observed that localization of Mps3 was also affected. This observation suggests that Mcm22 affects the assembly of other components in the spindle pole body as well. In summary our results show that Ctf3 and Mcm16 are required to align and assemble Nkp2 within the Ctf19 complex.

Chapter - 8

Overall Discussion

8.1 *EST2* overexpression disrupts silencing at telomeres and *HMR* locus

In budding yeast, the sixty four telomere ends from a diploid cell are clustered together into a few foci and co-localize with HM loci at the nuclear periphery. Organization of this sub-compartment within the nucleus consisting of heterochromatin regions favours gene silencing at nuclear periphery by harbouring higher concentration of silencer proteins in its vicinity (Gotta et al., 1996). These clustered telomeres are maintained by two partially redundant pathways that depend on Yku70/Yku80 heterodimer and Esc1, a nuclear envelope protein which interacts with the structural component of silent chromatin, Sir4, and together tether the telomeres to nuclear periphery. Disruption of any of these components leads to delocalization of telomeres from nuclear periphery and leads to loss in silencing as well (Andrulis et al., 1998; Hediger et al., 2002; Laroche et al., 1998). However, how Yku70/Yku80 complex supports anchoring of telomeres are not understood. We do not know the molecular mechanism involved in clustering of telomeres. Our goal was to identify the molecular principles that guide, establish and maintain the telomere organization.

From previous studies, it had been reported that the clustering and peripheral localization of telomeres promotes silencing of ectopic loci when targeted to the nuclear periphery where Sir proteins are concentrated at nuclear periphery (Andrulis et al., 1998). We designed a screen for factors that disrupt the targeted silencing to identify factors that contribute to telomere clustering and anchoring. Our screen was designed to identify factors when overexpressed, will disrupt silencing by Gbd-Yif1, a protein used for targeting modified *HMR* locus to the nuclear periphery. This screen identified a plasmid containing a fragment of chromosome XII. This region contained two full length genes, *NKP2* and *EST2*.

We tested targeted silencing upon overexpression of *EST2* and *NKP2.* We observed that targeted silencing was lost upon overexpression of *EST2*. Our studies also showed that there was disruption of telomeric silencing and there was concomitant disruption of Sir protein organization upon overexpression of *EST2*. When we tested the overexpression of *NKP2* on telomeric silencing and Sir protein organization, we found

that the effects on telomere silencing were minimal and there was no perturbation of Sir protein clusters. Therefore from the first part of our study we concluded that *EST2* affects telomere organization. During the course of this study, it was shown by the laboratory of Susan Gasser that *EST2* indeed anchors telomeres in a cell cycle stage dependent manner (Schober et al., 2009).

8.2 *nkp2* shows chromosome loss rather than gene silencing

Genetic analysis shows that small but reproducible loss in targeted silencing is observed at *HMR* locus upon overexpression of *NKP2*. Further, in order to test if *NKP2* has any role in gene silencing, we deleted *nkp2* and assayed gene silencing. Our gene silencing data shows that *nkp2* mutant does not have a role in telomere organization but rather showed spontaneous loss of markers from *HMR* locus and telomere regions. Although we set out to identify proteins that are involved in telomere clustering at the nuclear periphery, our screen identified *NKP2* as protector of genome stability.

To study directly the function of *NKP2* in genome stability, we examined chromosome loss in the *nkp2*Δ homozygous diploid marked with two different selectable markers (*his5*+ and *TRP1*). We tested and quantified the segregation of the *NKP2* locus by random sporulation. We observed that about one fourth of segregants retained both the *his5*+ and *TRP1* genes and also showed a specific mating type, either Mat a or Mat α. This is unexpected, as a haploid can have only one copy of the two *nkp2* chromosome. Our finding suggests that there is improper segregation of chromosomes: these could be haploids that carry an additional chromosome XII or alternatively, they could be diploids that have lost one of chromosome III and can mate. We further confirmed the presence of the two *nkp2* loci by genomic southern and found that it retained both the copies of *nkp2* and was able to mate with haploids. We dissected these "triploid" spores and examined that the viability and found that it goes down to half compared to *nkp2* diploid spores, suggesting that the parents were true diploids that

showed elevated loss of chromosome III. Does *nkp2* mutation lead to production of monosomy at chromosome III? We tested this directly by performing quantitative mating assay on diploids. From this experiment, we observed that about four-fold increase in chromosome III loss compared to the wild type. We examined the chromosome loss in *nkp2* mutant more directly using an artificial chromosome loss assay. We found that *nkp2* shows significant loss of artificial chromosome (*SUP11*) compared to wild type. These data firmly establish that loss of *nkp2* leads to chromosome instability. Even though multiple genome-wide screens have been performed for chromosome loss, *nkp2* was never identified in any of these screens. Therefore, we set out o further characterize the function of *NKP2*.

8.3. Gene conversion events in *nkp2Δ*

It has been previously shown that incorrect kinetochore assembly or kinetochore-microtubule attachment can result in loss or gain of chromosomes (Raghuraman et al., 2001). We tested segregation of chromosomes more systematically in meiosis where gene conversion events are rare. In the first set of experiments we tested the segregation of the *nkp2* locus using the homozygous mutant spores containing *nkp2* marked with two different auxotrophic markers *his5+* and *TRP1*. We observed in the *nkp2* mutant a few spores with 3*his5+* and 1*TRP1* and a few tetrads with all 4 *TRP1* or *his5+*. These patterns of segregation suggest that gene conversion events took place either mitotically just prior to meiosis or gene conversion events took place post meiotically. We further tested the role of *nkp2* in meiosis at additional chromosomal loci marked with different auxotrophic markers (either *ADE2* or *URA3* at *LYS2* locus) in a *nkp2* diploid. We observed that gene conversions were seen more at chromosome XII but not at chromosome II. These results raise the possibility that such conversions are more pronounced in larger chromosomes (chromosome XII is the largest chromosome) which tend to have more recombination events. In summary, our results support the idea that there are increased gene conversion events in the absence of Nkp2 during mitosis.

8.4 Non reciprocal events are more in *nkp2Δ*

Cancer is generally considered as an age-associated disease that is driven by spontaneous genetic changes in somatic cells (DePinho, 2000). One of the early steps in cancer progression is that the mutation rate is higher than normal. This mutator phenotype increases the likelihood of subsequent genetic events (Loeb, 1991; Loeb et al., 2003). There are several mechanisms by which the functional allele becomes non-functional in a heterozygous diploid, but the two predominant pathways to inactivate the wild type allele from diploid cells are loss of part or entire chromosome or alternatively, recombination events that take place between non-functional allele and wild type allele replacing the functional allele with the non-functional allele. These genetic changes within the diploid cells are known as loss of heterozygosity (LOH) (Carr and Gottschling, 2008).

Budding yeast, *Saccharomyces cerevisiae*, has provided more details about spontaneous genetic changes than have been possible in other organisms (Acuna et al., 1994; Barbera and Petes, 2006; Esposito and Bruschi, 1993; Hiraoka et al., 2000; McMurray and Gottschling, 2003). In yeast, there are methods to identify the genetic changes in which LOH events occurs primarily through mitotic recombination in each cell. In addition, LOH events can be categorized as reciprocal or nonreciprocal and these studies facilitate a better mechanistic understanding of LOH events. Using these assays we have shown that loss of heterozygosity was significantly elevated in *nkp2* mutant relative to wild type at three different chromosomes marked with multiple auxotrophic markers. We found about 2-4 fold increase in chromosome loss at chromosome XII, IV and III. It has been reported previously, that *ctf19*Δ, a component of Ctf19 central kinetochore subcomplex, shows elevated loss of heterozygosity that is similar as *nkp2* mutant. We further tested the mechanism of recombination events in *nkp2* mutants to see if they were either reciprocal or nonreciprocal events. Our analysis reveals nonreciprocal events were more prevalent in *nkp2* whereas in wild type LOH is predominantly reciprocal. High level of nonreciprocal events at chromosome XII and high incidence of chromosome III loss were seen in *nkp2* mutant. Previously, it was shown that nonreciprocal LOH events at MET15 and increase in chromosome III loss take place in *ctf19* and *mcm21*. As Mcm21 and Ctf19 are components of the central

kinetochore subcomplex COMA, (De Wulf et al., 2003) it implies that disruption of kinetochore structure is indeed responsible for elevated LOH at chromosome XII and high frequency of chromosome III loss. Our results reveal that, *nkp2* mutant also shows increased nonreciprocal loss of heterozygosity (LOH) events and increased chromosome III loss similar to *ctf19* and *mcm21.* Nkp2 is a peripheral component of Ctf19 complex and moreover it interacts physically with Ctf19 and Mcm21. These results together show that Ctf19 complex structure is required to maintain the genome stability and additionally, Nkp2 function is important for its integrity.

We further tested the missegregation of chromosomes by direct observation of chromosomes in mitosis and meiosis. During mitosis, we observed that marked chromosomes with LacI-GFP are segregated normally in *nkp2* mutant as wild type unlike in mutants like *iml3* and *mcm17* mutants where a significant number of cells undergo non-disjunction (Fernius and Marston, 2009). We tested the chromosome segregation in meiosis in *nkp2* mutant. We found that *nkp2* mutant undergoes metaphase to anaphase transition much earlier than wild type during meiosis I. This implies that without *nkp2,* cohesion at the chromosome arms might be dissolved earlier and therefore enters anaphase I much earlier than wild type. We further followed this in meiosis II to see if similar phenotype was observed. We observed that about ~98% of the cells with four GFP spots are segregated in tetranucleate spore of *nkp2* mutants, as seen in wild type. However, meiosis II is also much faster than wild type. All these observations indicate that the Nkp2 is involved in chromosome segregation during mitosis and in meiosis.

8.5 Genome instability in Ctf19 complex mutants

In eukaryotes, replicated genome is transmitted accurately from mother cell to daughter cell during mitosis and meiosis. During cell division, replication of genetic material is coupled physically with chromosome segregation machinery such as kinetochores, which are assembled at the centromeric DNA, and these are connected to the spindle microtubules to execute effective segregation. During metaphase, some chromosomes are inappropriately attached or microtubules are connected at one side of the sister kinetochore from the spindle pole body (SPB). We tested the genetic

interactions among components of *ctf19* complex and *nkp2* mutants with respect to chromosome stability in budding yeast. We measured chromosome loss in *nkp2* mutant in combination with deletions of individual components of *ctf19* in the colour based artificial chromosome loss assay and also the quantitative mating assay.

From the chromosome loss assay and quantitative mating assay results we find that double mutants of *nkp2 nkp1*, *nkp2 mcm22*, *nkp2 iml3* and *nkp2 mcm17* primarily increased rate of chromosome loss than either single mutant whereas chromosome loss was lowered in *nkp2* with other components of *ctf19* double mutants such as *mcm16, mcm21, ctf3 and ctf19*. Our findings suggest that double mutants of *ctf19* components with *nkp2* may cause severe defect in organization of kinetochore thereby leading to loss of chromosome.

8.6 Functional analysis of Nkp2 with other components of Ctf19 complex

To examine the activities of Nkp2 kinetochore protein, we tested the expression of Nkp2 in a cell cycle-dependent manner. We found that expression of Nkp2 are similar in all stages of cell cycle such as G1, S and metaphase of mitosis but the localization of Nkp2 is dependent on cell cycle stages. At G1 and S phase, Nkp2 is present at the nuclear rim whereas, in metaphase Nkp2 moved interior from the nuclear rim. Previously, it was shown that Nkp2 colocalized with spindle pole body which is embedded in the nuclear rim throughout the cell cycle (Huh et al., 2003). We have investigated the localization of Nkp2 in Ctf19 complex mutants. We found that the localization of Nkp2 was similar in mutants like *nkp1*, *mcm17* and *iml3* as seen in wild type. However, the localization of Nkp2 is affected in some of the *ctf19* mutants. We find that Nkp2 nuclear localization was severely affected in *ctf19* and *mcm21,* with the protein being dispersed throughout the cell, even though protein levels of Nkp2 are stable and similar as in wild type. In contrast in *mcm16, ctf3* and *mcm22* mutants the Nkp2 was scattered throughout nucleus, i.e., the protein is nuclear but not localized to the spindle pole body, with multiple spots of Nkp2 detected in the nuclear interior. These results show that assembly of Nkp2 within the central kinetochore Ctf19 complex is dependent on other components of the subcomplex.

Table 15: Interaction summary of Ctf19 components with Nkp2

Name of the strain	Chromosome loss	Localization of Nkp2
Wt	–	**Single spot localize with SPB**
nkp2	↑	–
nkp1	↑	**Single spot localize with SPB**
nkp1 nkp2	↑↑	–
ctf3	↑↑	**Multiple spots within nucleus**
ctf3 nkp2	↓	–
mcm22	↑↑	**Multiple spots within nucleus**
mcm22 nkp2	↑↑↑	–
mcm16	↑↑↑↑	**Multiple spots within nucleus**
mcm16 nkp2	↓↓↓	–
ctf19	↑↑↑↑↑	**Dispersed more in cytoplasm to nucleus**
ctf19 nkp2	↓↓↓↓	–
mcm21	↑↑	**Dispersed more in cytoplasm to nucleus**
mcm21 nkp2	↓↓↓↓	–
mcm17	↑↑↑	**Single spot localize with SPB**
mcm17 nkp2	↑↑↓↓	–
iml3	↑↑↑↑	**Single spot localize with SPB**
Iml3 nkp2	↑↑↓↓	–

Conclusions:

The faithful transmission of genetic material from mother cell to daughter cell requires the chromosome segregation machinery including the proper attachment of the large proteinaceous structures termed the kinetochore to the spindle pole body. This kinetochore is composed of more than 60 different proteins which function together to direct the kinetochore assembly and generate attachment between chromosomal DNA and spindle microtubules and regulate chromosome segregation. The functions of individual components in this machinery are not very clear. Our results show that Nkp2 is involved in chromosome segregation during cell division i.e., mitosis and meiosis. Although multiple screens have been carried out to exhaustively identify the proteins and pathways involved in this process, Nkp2 was not identified. However, when we took up a focussed study to address Nkp2 function, we discovered that it is involved in kinetochore function and is required for proper segregation of chromosomes. Additionally, we have been able to map interactions using both cell biological and genetic means. This effort has revealed important clues to the function of Nkp2 and possibly other kinetochore components. For eg, in general, synthetic lethality and two-hybrid screens have been used to study inter-protein interactions. However, using a chromosome loss assay to study the interactions has provided clues for interactions between the kinetochore components. In an effort to understand if Nkp2 is functionally redundant with other Ctf19 components, we estimated the rate of chromosome loss in double deletion strains of *nkp2* with each of viable *ctf19* deletions strain by non-essential chromosome loss and quantitative mating assays. We found that the chromosome loss was enhanced or suppressed in double deletion strains of *ctf19* components possibly due to alterations in response to checkpoints. This underscores the importance of using phenotype based assays to understand protein function within large complexes. Our data with Nkp2 localization in *ctf3, mcm16 and mcm22* suggest that nuclear localization was affected and kinetochores were distributed as 3-4 foci scattered throughout the nucleus. The scattering of Nkp2 is a consequence of partial detachment of chromosomes from microtubules. In *ctf19* and *mcm21* deletion strains Nkp2 was dispersed more in cytoplasm rather than nucleus. These results suggest that Nkp2 assembly into the kinetochores depends on Ctf3, Mcm16 and Mcm22. Previously, it was

reported that Ctf3, Mcm16 and Mcm22 together form a Ctf3 subcomplex (Measday et al., 2002). Our phenotype based assays and localization studies add Nkp2 to Ctf3 subcomplex, and suggest that together they form a larger complex within the Ctf19 complex.

Future Prospects:

Our work has generated multiple tools to study the inter protein interactions within the kinetochore complex. We have studied the effect of other kinetochore component mutations on Nkp2 function. The converse experiments where localization of other components in *nkp2* mutants has to be undertaken. That will give additional information on the protein-protein interactions within the kinetochore and also complement the information on the mechanistic basis of chromosome loss in these strains.

Appendix

A 1.1 Construction of *EST2* clone in Yeplac181 vector (CKM205)

EST2 gene was sub cloned into Yeplac181, 2µ vector carrying *LEU2* and ampicilin resistance markers. 2a genomic library plasmid was digested with *BamHI* and *SalI* restriction enzymes and DNA fragment of size 3.8 kb bp containing full length *EST2* gene along with its promoter region was ligated into *BamHI* and *SalI* digested Yeplac181 (CKM6) vector listed in Table 2. The resulting plasmid was confirmed by digesting with *BamHI* and *SalI* restriction enzymes. Yeplac181 vector backbone contains one *BamHI* site at the polycloning region and insert contains one *SalI* site. Therefore, upon digestion, the clones give two fragments of size 5.7 kbp and 3.8 kb as seen in Figure A1.C.

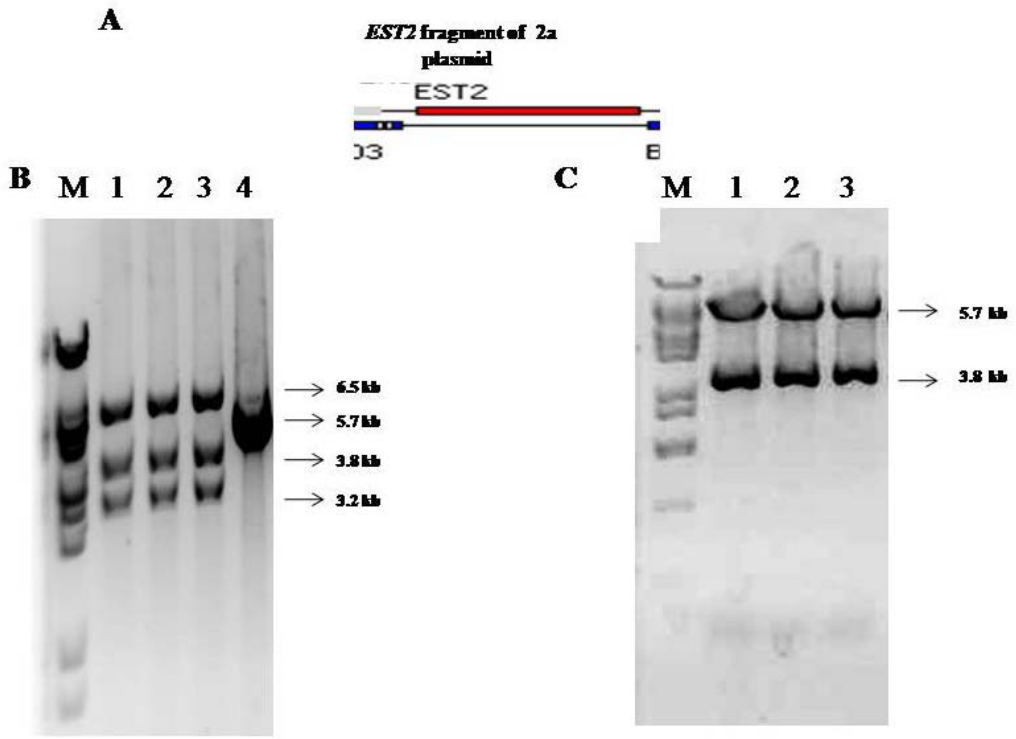

Figure A1: Confirmation of *EST2* clone in Yeplac181 vector. A). *EST2* insert from 2a library plasmid. B). Gel eluted DNA fragments *BamHI* & *SalI* digested YEplac181 plasmid of size 5.7 Kb in lane 4 and *BamHI* & *SalI* released DNA fragment of size 3.8 kb containing *EST2* gene along with its promoter from *2a* genomic library plasmid in lane 1-3. C). Confirmation of *EST2* clone by digesting with *BamHI & SalI* enzymes that releases three fragments of size 5.7 kb and 3.8 kb.

A 1.2 Construction of *NKP2* clone in Yeplac181 vector (CKM204)

NKP2 gene was cloned in multi copy Yeplac181 vector. *NKP2* PCR product digested with *EcoRI* & *HindIII* and 1.1 kb DNA fragment containing *NKP2* gene (453bps) and its promoter region (700bp) was cloned into *EcoRI* & *HindIII* digested Yeplac181 vector. The resulted plasmid (CKM204) was confirmed by digesting with *EcoRI* & *Hind III* restriction enzyme. Yeplac181 vector backbone contains *EcoRI* & *Hind III* sites at poly cloning region flanking the *NKP2* insert and the insert does not contain sites for these enzymes. Therefore upon digestion with *EcoRI* & *HindIII* enzymes, the clone gives two fragments of size 5.7 kb and 1.1 kb as seen in Figure A2.

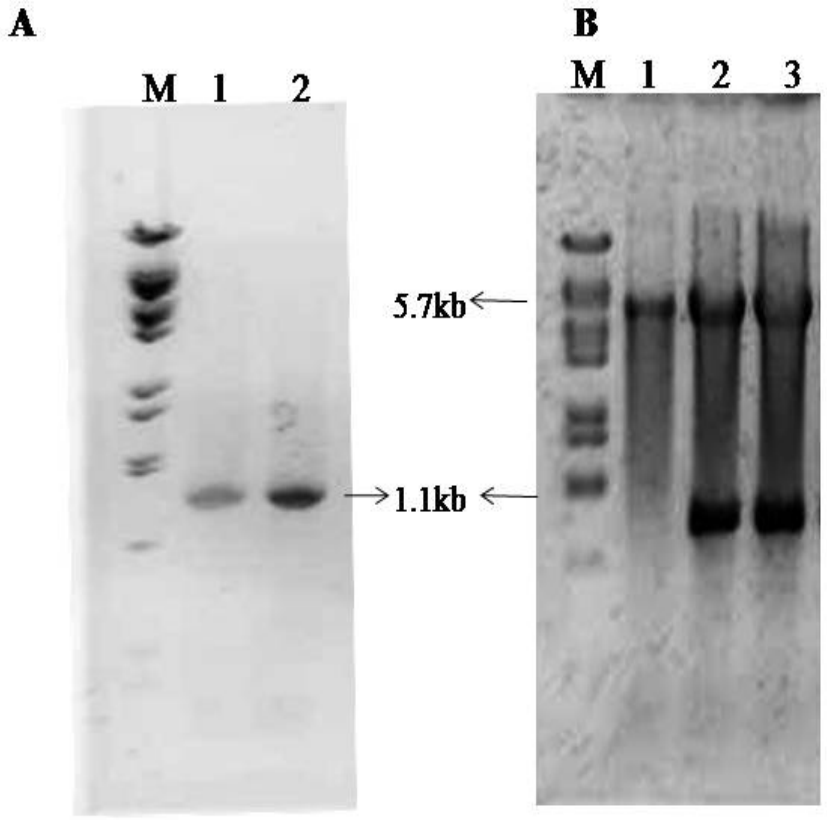

Figure A2: Confirmation of *NKP2* clone in Yeplac181 vector (CKM204). *NKP2* PCR product and YEplac181 empty vector were digested with *EcoRI & HindIII* restriction enzymes. Panel A shows *NKP2* PCR product digestion gives single fragment of size 1.1kb (insert containing *NKP2* gene with promoter) whereas empty vector digested with same *EcoRI & HindIII* to become linear. In panel B Lane 1 is empty vector showing single band of size 5.7kb. Lane 2 & 3 are *NKP2* clones showing fragment of size 1.1 kb.

A 2.1 Construction of *nkp2::his5+*

PCR amplification of DNA fragment for *NKP2* gene deletion. *nkp2* null mutant was constructed by knocking off complete gene with *his5+* marker by using PCR based homologous recombination method (Longtine et al., 1998). The forward primer for deleting *NKP2* gene was designed by selecting 30 bp just upstream of start codon and reverse primer by taking 30 bp sequences downstream of stop codon. The sequences of the primers used are listed in Table 3. Plasmid E337 (listed in Table 2) is used as template for amplifying *his5+* marker. The Figure A3.A shows the DNA fragment of size 1403 bp amplified by PCR. This DNA was transformed into competent yeast cells by LiAc method. It gets integrated into the genome by homologous recombination. The transformants were selected on histidine dropped out medium. Then single colonies were picked up and the genomic DNA was extracted by phenol:chloroform:isoamylalcohol (25:24:1) method.

Screening PCR for *nkp2* null mutant. Screening PCR was done for *nkp2* null mutant by using the forward primer (around 19 bp) that gets annealed within the deletion module and the reverse primer (19 nt) that anneals with the unaltered downstream region of the *NKP2* gene. The sequences of the primers are given in Table 3. The diagnostic PCR product of around 565 bp in Figure A3.B shows that *NKP2* gene has been replaced by *his5+* marker by homologous recombination.

Southern confirmation for *nkp2* null mutant. Genomic southern was done for further confirmation of *nkp2* null mutant. Genomic DNA from yeast strains that showed positive for *NKP2* knockout in screening PCR was isolated by zymolyase method. This genomic DNA was subjected to 6hrs restriction digestion with *XhoI & SalI* enzymes that gives 0.7 kb fragment at *NKP2* locus in WT strain and 2.2 kb fragment in *nkp2* null mutant. The digested genomic DNA was run on 0.8% Agarose gel and transferred to nylon membrane. The bands were detected by southern hybridization of the blot with alpha p-32 radiolabelled *NKP2* probe. *NKP2* probe was made by digesting the multi copy *2a* library plasmid (CKM204) with *SalI & XhoI* restriction enzymes. The DNA fragment of size 654 bp having part of C-terminus of *NKP2* gene and its downstream region, was taken as template and radiolabelled using BRIT random radiolabelling kit.

The blot was washed and exposed to autoradiogram. Figure A3.C shows the presence of 2.2 kb band confirming that the particular yeast strain is *nkp2* null mutant.

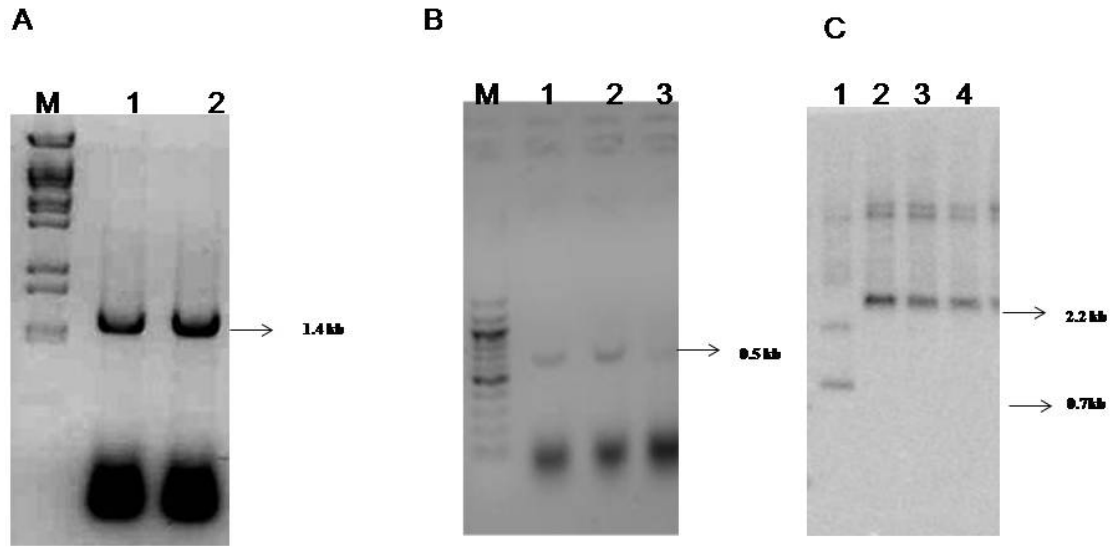

Figure A3: Construction of *nkp2::his5+*. A) PCR product of size 1.4 kb used for replacing *NKP2* gene with *his5+* marker. B). Screening PCR product of size 0.56 kb in lanes 1-3 shows that *NKP2* gene has been replaced with *his5+*marker in these strains. C). Genomic southern confirmation for *nkp2::his5+* mutants. 2.2 kb band in lane 2-4 represents wild type strain and 0.7 kb band in lane 1 confirms *nkp2::his5+* mutant.

A 2.2 Construction of *nkp2::KanMx6 and nkp2::TRP1*

nkp2 knockout with *KanMx6* and *TRP1* markers was done by following the same method used for knocking out *nkp2* gene (Appendix 2.1). The sequences of the primers used for deleting *nkp2* gene are given in Table 3. Plasmids E335 and E336 listed in Table 2 were used as templates to amplify *KanMx6* and *TRP1* markers respectively for replacing *NKP2* gene. The Figure A4.A shows the PCR product of *KanMx6* (1.4 kb) and *TRP1* (1 kb) DNA fragments respectively. This DNA was transformed into yeast strains. The strains transformed with *KanMx6* marker were selected on YPD plate containing

200µg of G418 drug and those with *TRP1* marker were selected on tryptophan dropped out medium.These strains were further confirmed by genomic southern by hybridizing with *NKP2* gene specific probe. The genomic DNA from these strains was digested with *XhoI & SalI* enzyme. WT strain gives band of size 0.7 kb, *nkp2::KanMx6* mutant gives band at 2.2 kb and *nkp2::TRP1* gives band at 1.8 kb. The template for *NKP2* probe was made from *2a* library. The DNA fragment of size 654 bp having part of C-terminus of *NKP2* gene and its downstream region was taken as template and radiolabelled using BRIT random radiolabelling kit. The result of the autoradiogram of southern blot in Figure A4.B & C shows 0.7 kb band in WT strain, 2.2 kb band in *nkp2::KanMx6* mutant and 1.8 kb band in *nkp2::TRP1* mutant confirms that these yeast strains are *nkp2* null mutants.

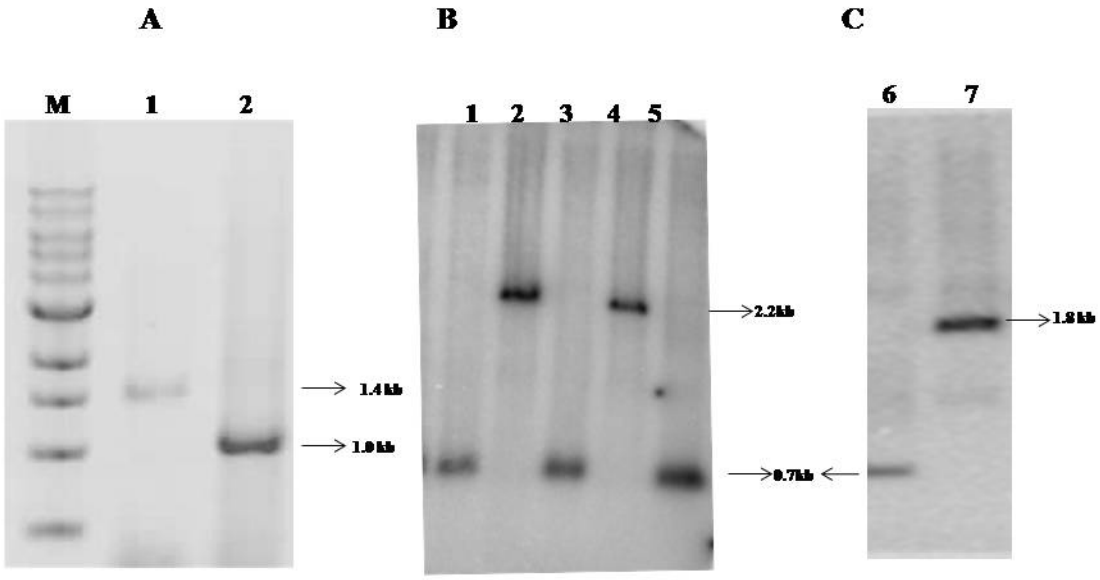

Figure A4: Construction of *nkp2::KanMx6* and *nkp2::TRP1* . A). PCR product of size 1.4 kb used for replacing *NKP2* gene with *KanMx6* marker and PCR product of size 1kb used for replacing *NKP2* gene with *TRP1* marker. B). Genomic southern confirmation of *nkp2::KanMx6* mutant. 2.2 kb band in lane 2 and 4 confirms *nkp2::KanMx6* mutant and C) 1.8 kb band in lane 7 confirms *nkp2::TRP1* mutant. 0.7 kb band in other lanes shows that the genomic DNA in these strains was unaltered at *NKP2* locus.

A 2.3 Construction of *NKP2*-13x-myc strain

Nkp2 was tagged with 13x myc epitope at its C-terminus by PCR based homologous recombination method (Longtine et al., 1998). The forward primer was designed by taking sequence just upstream of the stop codon and in frame so that it does not disrupt the reading frame of the myc epitope and selectable marker *HIS3Mx6* which is going to be inserted in the downstream of the gene. The sequences of the primers are given in Table 3. Plasmid E342 (listed in Table 2) was used as template for PCR to amplify 13x myc-*HIS3Mx6* DNA fragment. Figure A5.A shows the PCR product of 13x myc-*HIS3Mx6* DNA fragment of size 2.2 kbp which is transformed into yeast strain by following high efficiency LiAC transformation protocol. The transformants were selected on histidine dropout medium. The colonies that grew on histidine dropout medium were subjected to screening PCR. The sequences of the primers used for screening PCR are given in Table 3. The diagnostic screening PCR product of 565 bp in Figure A4.B shows that *NKP2* is tagged with myc epitope at its C-tereminus.

These strains were further confirmed by genomic southern by hybridizing with *NKP2* gene specific probe. The genomic DNA from these strains was digested with *XhoI* and *SalI* restriction enzymes by incubating at 37ºC for 6-8hrs. WT strain gives band of size 0.7 kb whereas *NKP2*-13xmyc-*HISMx6* strain gives band of size 2.8 kb at *NKP2* locus. *NKP2* probe was made by digesting the multi copy *2a* library plasmid (CKM202) with *SalI & XhoI* restriction enzymes. The DNA fragment of size 654 bp having part of C-terminus of *NKP2* gene and its downstream region, was taken as template and radiolabelled using BRIT random radiolabelling kit.. The result of the autoradiogram of southern blot in Figure A5.C shows 0.7 kb band in lane 1 represents WT strain and 2.8 kb band in lane 3 confirms that the yeast strain is tagged with 13myc epitope at C-terminus of *NKP2*.

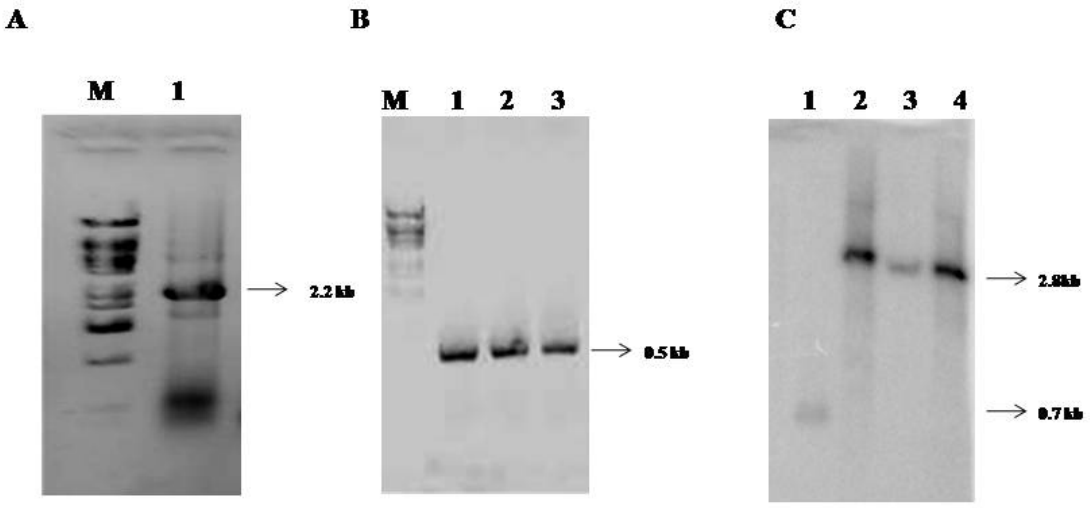

Figure A5: Construction of *NKP2*-13xmyc tag. A). 2.2kp PCR product used for tagging 13x myc at C-terminus of *NKP2* gene. B). Screening PCR product of size 560bp in lanes 1-3 shows that *NKP2* gene has been tagged with 13x myc-*HIS3Mx6* at its C-terminus in these strains. C). Genomic southern confirmation of NKP2-13xmyc-*HIS3Mx6* strain. 0.7 kb band in lane1 represents wild type strain and 2.8 kb band in lane2-4 confirms *NKP2*- 13xmyc-*HIS3Mx6* strain.

References

Bibliography

Abranches, R., Beven, A.F., Aragon-Alcaide, L., and Shaw, P.J. (1998). Transcription sites are not correlated with chromosome territories in wheat nuclei. J Cell Biol *143*, 5-12.

Acuna, G., Wurgler, F.E., and Sengstag, C. (1994). Reciprocal mitotic recombination is the predominant mechanism for the loss of a heterozygous gene in Saccharomyces cerevisiae. Environ Mol Mutagen *24*, 307-316.

Adams, I.R., and Kilmartin, J.V. (2000). Spindle pole body duplication: a model for centrosome duplication? Trends Cell Biol *10*, 329-335.

Akiyoshi, B., Sarangapani, K.K., Powers, A.F., Nelson, C.R., Reichow, S.L., Arellano-Santoyo, H., Gonen, T., Ranish, J.A., Asbury, C.L., and Biggins, S. (2010). Tension directly stabilizes reconstituted kinetochore-microtubule attachments. Nature *468*, 576-579.

Andersen, M.P., Nelson, Z.W., Hetrick, E.D., and Gottschling, D.E. (2008). A genetic screen for increased loss of heterozygosity in Saccharomyces cerevisiae. Genetics *179*, 1179-1195.

Andrulis, E.D., Neiman, A.M., Zappulla, D.C., and Sternglanz, R. (1998). Perinuclear localization of chromatin facilitates transcriptional silencing. Nature *394*, 592-595.

Andrulis, E.D., Zappulla, D.C., Ansari, A., Perrod, S., Laiosa, C.V., Gartenberg, M.R., and Sternglanz, R. (2002). Esc1, a nuclear periphery protein required for Sir4-based plasmid anchoring and partitioning. Mol Cell Biol *22*, 8292-8301.

Aparicio, O.M., Billington, B.L., and Gottschling, D.E. (1991). Modifiers of position effect are shared between telomeric and silent mating-type loci in S. cerevisiae. Cell *66*, 1279-1287.

Apostolou, E., and Thanos, D. (2008). Virus Infection Induces NF-kappaB-dependent interchromosomal associations mediating monoallelic IFN-beta gene expression. Cell *134*, 85-96.

Baker, R.E., Fitzgerald-Hayes, M., and O'Brien, T.C. (1989). Purification of the yeast centromere binding protein CP1 and a mutational analysis of its binding site. J Biol Chem *264*, 10843-10850.

Bank, E.M., Ben-Harush, K., Wiesel-Motiuk, N., Barkan, R., Feinstein, N., Lotan, O., Medalia, O., and Gruenbaum, Y. (2011). A laminopathic mutation disrupting lamin filament assembly causes disease-like phenotypes in Caenorhabditis elegans. Mol Biol Cell *22*, 2716-2728.

Barbera, M.A., and Petes, T.D. (2006). Selection and analysis of spontaneous reciprocal mitotic cross-overs in Saccharomyces cerevisiae. Proc Natl Acad Sci U S A *103*, 12819-12824.

Bertuch, A.A., and Lundblad, V. (2003). Which end: dissecting Ku's function at telomeres and double-strand breaks. Genes Dev *17*, 2347-2350.

Bi, X. (2002). Domains of gene silencing near the left end of chromosome III in Saccharomyces cerevisiae. Genetics *160*, 1401-1407.

Bielas, J.H., Loeb, K.R., Rubin, B.P., True, L.D., and Loeb, L.A. (2006). Human cancers express a mutator phenotype. Proc Natl Acad Sci U S A *103*, 18238-18242.

Blower, M.D., Sullivan, B.A., and Karpen, G.H. (2002). Conserved organization of centromeric chromatin in flies and humans. Dev Cell *2*, 319-330.

Brand, A.H., Breeden, L., Abraham, J., Sternglanz, R., and Nasmyth, K. (1985). Characterization of a "silencer" in yeast: a DNA sequence with properties opposite to those of a transcriptional enhancer. Cell *41*, 41-48.

Brand, A.H., Micklem, G., and Nasmyth, K. (1987). A yeast silencer contains sequences that can promote autonomous plasmid replication and transcriptional activation. Cell *51*, 709-719.

Bryk, M., Banerjee, M., Murphy, M., Knudsen, K.E., Garfinkel, D.J., and Curcio, M.J. (1997). Transcriptional silencing of Ty1 elements in the RDN1 locus of yeast. Genes Dev *11*, 255-269.

Buck, S.W., and Shore, D. (1995). Action of a RAP1 carboxy-terminal silencing domain reveals an underlying competition between HMR and telomeres in yeast. Genes Dev *9*, 370-384.

Buhler, M., and Gasser, S.M. (2009). Silent chromatin at the middle and ends: lessons from yeasts. EMBO J *28*, 2149-2161.

Bupp, J.M., Martin, A.E., Stensrud, E.S., and Jaspersen, S.L. (2007). Telomere anchoring at the nuclear periphery requires the budding yeast Sad1-UNC-84 domain protein Mps3. J Cell Biol *179*, 845-854.

Bystricky, K., Heun, P., Gehlen, L., Langowski, J., and Gasser, S.M. (2004). Long-range compaction and flexibility of interphase chromatin in budding yeast analyzed by high-resolution imaging techniques. Proc Natl Acad Sci U S A *101*, 16495-16500.

Bystricky, K., Laroche, T., van Houwe, G., Blaszczyk, M., and Gasser, S.M. (2005). Chromosome looping in yeast: telomere pairing and coordinated movement reflect anchoring efficiency and territorial organization. J Cell Biol *168*, 375-387.

Cai, M., and Davis, R.W. (1990). Yeast centromere binding protein CBF1, of the helix-loop-helix protein family, is required for chromosome stability and methionine prototrophy. Cell *61*, 437-446.

Cai, M.J., and Davis, R.W. (1989). Purification of a yeast centromere-binding protein that is able to distinguish single base-pair mutations in its recognition site. Mol Cell Biol *9*, 2544-2550.

Capell, B.C., and Collins, F.S. (2006). Human laminopathies: nuclei gone genetically awry. Nat Rev Genet *7*, 940-952.

Carr, L.L., and Gottschling, D.E. (2008). Does age influence loss of heterozygosity? Exp Gerontol *43*, 123-129.

Cheeseman, I.M., Anderson, S., Jwa, M., Green, E.M., Kang, J., Yates, J.R., 3rd, Chan, C.S., Drubin, D.G., and Barnes, G. (2002). Phospho-regulation of kinetochore-microtubule attachments by the Aurora kinase Ipl1p. Cell *111*, 163-172.

Cheeseman, I.M., and Desai, A. (2008). Molecular architecture of the kinetochore-microtubule interface. Nature reviews Molecular cell biology *9*, 33-46.

Cheeseman, I.M., Enquist-Newman, M., Muller-Reichert, T., Drubin, D.G., and Barnes, G. (2001). Mitotic spindle integrity and kinetochore function linked by the Duo1p/Dam1p complex. J Cell Biol *152*, 197-212.

Cheeseman, I.M., Niessen, S., Anderson, S., Hyndman, F., Yates, J.R., 3rd, Oegema, K., and Desai, A. (2004). A conserved protein network controls assembly of the outer kinetochore and its ability to sustain tension. Genes Dev *18*, 2255-2268.

Chen, L., and Widom, J. (2005). Mechanism of transcriptional silencing in yeast. Cell *120*, 37-48.

Chien, C.T., Buck, S., Sternglanz, R., and Shore, D. (1993). Targeting of SIR1 protein establishes transcriptional silencing at HM loci and telomeres in yeast. Cell *75*, 531-541.

Counter, C.M., Meyerson, M., Eaton, E.N., and Weinberg, R.A. (1997). The catalytic subunit of yeast telomerase. Proc Natl Acad Sci U S A *94*, 9202-9207.

Cremer, T., and Cremer, C. (2001). Chromosome territories, nuclear architecture and gene regulation in mammalian cells. Nat Rev Genet *2*, 292-301.

Cremer, T., Cremer, M., Dietzel, S., Muller, S., Solovei, I., and Fakan, S. (2006). Chromosome territories--a functional nuclear landscape. Curr Opin Cell Biol *18*, 307-316.

Csink, A.K., and Henikoff, S. (1998). Large-scale chromosomal movements during interphase progression in Drosophila. J Cell Biol *143*, 13-22.

De Wulf, P., McAinsh, A.D., and Sorger, P.K. (2003). Hierarchical assembly of the budding yeast kinetochore from multiple subcomplexes. Genes Dev *17*, 2902-2921.

Dekker, J., Rippe, K., Dekker, M., and Kleckner, N. (2002). Capturing chromosome conformation. Science *295*, 1306-1311.

DePinho, R.A. (2000). The age of cancer. Nature *408*, 248-254.

Dernburg, A.F., Broman, K.W., Fung, J.C., Marshall, W.F., Philips, J., Agard, D.A., and Sedat, J.W. (1996). Perturbation of nuclear architecture by long-distance chromosome interactions. Cell *85*, 745-759.

Dorn, J.F., Jaqaman, K., Rines, D.R., Jelson, G.S., Sorger, P.K., and Danuser, G. (2005). Yeast kinetochore microtubule dynamics analyzed by high-resolution three-dimensional microscopy. Biophysical journal *89*, 2835-2854.

Draviam, V.M., Xie, S., and Sorger, P.K. (2004). Chromosome segregation and genomic stability. Curr Opin Genet Dev *14*, 120-125.

Duan, Z., Andronescu, M., Schutz, K., McIlwain, S., Kim, Y.J., Lee, C., Shendure, J., Fields, S., Blau, C.A., and Noble, W.S. (2010). A three-dimensional model of the yeast genome. Nature *465*, 363-367.

Dundr, M., and Misteli, T. (2001). Functional architecture in the cell nucleus. Biochem J *356*, 297-310.

Dundr, M., Misteli, T., and Olson, M.O. (2000). The dynamics of postmitotic reassembly of the nucleolus. J Cell Biol *150*, 433-446.

Earnshaw, W.C., Halligan, N., Cooke, C., and Rothfield, N. (1984). The kinetochore is part of the metaphase chromosome scaffold. J Cell Biol *98*, 352-357.

Earnshaw, W.C., and Rothfield, N. (1985). Identification of a family of human centromere proteins using autoimmune sera from patients with scleroderma. Chromosoma *91*, 313-321.

Eckert, C.A., Gravdahl, D.J., and Megee, P.C. (2007). The enhancement of pericentromeric cohesin association by conserved kinetochore components promotes high-fidelity chromosome segregation and is sensitive to microtubule-based tension. Genes Dev *21*, 278-291.

Esposito, M.S., and Bruschi, C.V. (1993). Diploid yeast cells yield homozygous spontaneous mutations. Curr Genet *23*, 430-434.

Fernius, J., and Marston, A.L. (2009). Establishment of cohesion at the pericentromere by the Ctf19 kinetochore subcomplex and the replication fork-associated factor, Csm3. PLoS genetics *5*, e1000629.

Foltz, D.R., Jansen, L.E., Black, B.E., Bailey, A.O., Yates, J.R., 3rd, and Cleveland, D.W. (2006). The human CENP-A centromeric nucleosome-associated complex. Nat Cell Biol *8*, 458-469.

Fox, C.A., and McConnell, K.H. (2005). Toward biochemical understanding of a transcriptionally silenced chromosomal domain in Saccharomyces cerevisiae. J Biol Chem *280*, 8629-8632.

Furuyama, S., and Biggins, S. (2007). Centromere identity is specified by a single centromeric nucleosome in budding yeast. Proc Natl Acad Sci U S A *104*, 14706-14711.

Gartenberg, M.R., Neumann, F.R., Laroche, T., Blaszczyk, M., and Gasser, S.M. (2004). Sir-mediated repression can occur independently of chromosomal and subnuclear contexts. Cell *119*, 955-967.

Ghosh, S.K., Sau, S., Lahiri, S., Lohia, A., and Sinha, P. (2004). The Iml3 protein of the budding yeast is required for the prevention of precocious sister chromatid separation in meiosis I and for sister chromatid disjunction in meiosis II. Curr Genet *46*, 82-91.

Gietz, R.D., and Woods, R.A. (2002). Transformation of yeast by lithium acetate/single-stranded carrier DNA/polyethylene glycol method. Methods Enzymol *350*, 87-96.

Gilson, E., Roberge, M., Giraldo, R., Rhodes, D., and Gasser, S.M. (1993). Distortion of the DNA double helix by RAP1 at silencers and multiple telomeric binding sites. J Mol Biol *231*, 293-310.

Gotta, M., Laroche, T., Formenton, A., Maillet, L., Scherthan, H., and Gasser, S.M. (1996). The clustering of telomeres and colocalization with Rap1, Sir3, and Sir4 proteins in wild-type Saccharomyces cerevisiae. J Cell Biol *134*, 1349-1363.

Gottschling, D.E. (1992). Telomere-proximal DNA in Saccharomyces cerevisiae is refractory to methyltransferase activity in vivo. Proc Natl Acad Sci U S A *89*, 4062-4065.

Gottschling, D.E., Aparicio, O.M., Billington, B.L., and Zakian, V.A. (1990). Position effect at S. cerevisiae telomeres: reversible repression of Pol II transcription. Cell *63*, 751-762.

Grady, W.M. (2004). Genomic instability and colon cancer. Cancer Metastasis Rev *23*, 11-27.

Greider, C.W., and Blackburn, E.H. (1987). The telomere terminal transferase of Tetrahymena is a ribonucleoprotein enzyme with two kinds of primer specificity. Cell *51*, 887-898.

Guacci, V., Hogan, E., and Koshland, D. (1997). Centromere position in budding yeast: evidence for anaphase A. Mol Biol Cell *8*, 957-972.

He, X., Asthana, S., and Sorger, P.K. (2000). Transient sister chromatid separation and elastic deformation of chromosomes during mitosis in budding yeast. Cell *101*, 763-775.

Hediger, F., Neumann, F.R., Van Houwe, G., Dubrana, K., and Gasser, S.M. (2002). Live imaging of telomeres: yKu and Sir proteins define redundant telomere-anchoring pathways in yeast. Curr Biol *12*, 2076-2089.

Henikoff, S., Ahmad, K., and Malik, H.S. (2001). The centromere paradox: stable inheritance with rapidly evolving DNA. Science *293*, 1098-1102.

Hieter, P., Mann, C., Snyder, M., and Davis, R.W. (1985). Mitotic stability of yeast chromosomes: a colony color assay that measures nondisjunction and chromosome loss. Cell *40*, 381-392.

Hiraoka, M., Watanabe, K., Umezu, K., and Maki, H. (2000). Spontaneous loss of heterozygosity in diploid Saccharomyces cerevisiae cells. Genetics *156*, 1531-1548.

Hochstrasser, M., Mathog, D., Gruenbaum, Y., Saumweber, H., and Sedat, J.W. (1986). Spatial organization of chromosomes in the salivary gland nuclei of Drosophila melanogaster. J Cell Biol *102*, 112-123.

Hornung, P., Maier, M., Alushin, G.M., Lander, G.C., Nogales, E., and Westermann, S. (2011). Molecular architecture and connectivity of the budding yeast Mtw1 kinetochore complex. J Mol Biol *405*, 548-559.

Huh, W.K., Falvo, J.V., Gerke, L.C., Carroll, A.S., Howson, R.W., Weissman, J.S., and O'Shea, E.K. (2003). Global analysis of protein localization in budding yeast. Nature *425*, 686-691.

Iborra, F.J., and Cook, P.R. (2002). The interdependence of nuclear structure and function. Curr Opin Cell Biol *14*, 780-785.

Janke, C., Ortiz, J., Lechner, J., Shevchenko, A., Magiera, M.M., Schramm, C., and Schiebel, E. (2001). The budding yeast proteins Spc24p and Spc25p interact with Ndc80p and Nuf2p at the kinetochore and are important for kinetochore clustering and checkpoint control. EMBO J *20*, 777-791.

Janke, C., Ortiz, J., Tanaka, T.U., Lechner, J., and Schiebel, E. (2002). Four new subunits of the Dam1-Duo1 complex reveal novel functions in sister kinetochore biorientation. EMBO J *21*, 181-193.

Jaspersen, S.L., and Winey, M. (2004). The budding yeast spindle pole body: structure, duplication, and function. Annu Rev Cell Dev Biol *20*, 1-28.

Jin, Q.W., Fuchs, J., and Loidl, J. (2000). Centromere clustering is a major determinant of yeast interphase nuclear organization. J Cell Sci *113 (Pt 11)*, 1903-1912.

Joglekar, A.P., Bloom, K., and Salmon, E.D. (2009). In vivo protein architecture of the eukaryotic kinetochore with nanometer scale accuracy. Curr Biol *19*, 694-699.

Kim, S.H., McQueen, P.G., Lichtman, M.K., Shevach, E.M., Parada, L.A., and Misteli, T. (2004). Spatial genome organization during T-cell differentiation. Cytogenet Genome Res *105*, 292-301.

Koshland, D., and Hieter, P. (1987). Visual assay for chromosome ploidy. Methods Enzymol *155*, 351-372.

Kouprina, N., Tsouladze, A., Koryabin, M., Hieter, P., Spencer, F., and Larionov, V. (1993). Identification and genetic mapping of CHL genes controlling mitotic chromosome transmission in yeast. Yeast *9*, 11-19.

Kozubek, S., Lukasova, E., Jirsova, P., Koutna, I., Kozubek, M., Ganova, A., Bartova, E., Falk, M., and Pasekova, R. (2002). 3D Structure of the human genome: order in randomness. Chromosoma *111*, 321-331.

Laroche, T., Martin, S.G., Gotta, M., Gorham, H.C., Pryde, F.E., Louis, E.J., and Gasser, S.M. (1998). Mutation of yeast Ku genes disrupts the subnuclear organization of telomeres. Curr Biol *8*, 653-656.

Laroche, T., Martin, S.G., Tsai-Pflugfelder, M., and Gasser, S.M. (2000). The dynamics of yeast telomeres and silencing proteins through the cell cycle. J Struct Biol *129*, 159-174.

Lechner, J., and Carbon, J. (1991). A 240 kd multisubunit protein complex, CBF3, is a major component of the budding yeast centromere. Cell *64*, 717-725.

Lendvay, T.S., Morris, D.K., Sah, J., Balasubramanian, B., and Lundblad, V. (1996). Senescence mutants of Saccharomyces cerevisiae with a defect in telomere replication identify three additional EST genes. Genetics *144*, 1399-1412.

Lengauer, C., Kinzler, K.W., and Vogelstein, B. (1998). Genetic instabilities in human cancers. Nature *396*, 643-649.

Lewis, A., Felberbaum, R., and Hochstrasser, M. (2007). A nuclear envelope protein linking nuclear pore basket assembly, SUMO protease regulation, and mRNA surveillance. J Cell Biol *178*, 813-827.

Li, Y., Bachant, J., Alcasabas, A.A., Wang, Y., Qin, J., and Elledge, S.J. (2002). The mitotic spindle is required for loading of the DASH complex onto the kinetochore. Genes Dev *16*, 183-197.

Lieberman-Aiden, E., van Berkum, N.L., Williams, L., Imakaev, M., Ragoczy, T., Telling, A., Amit, I., Lajoie, B.R., Sabo, P.J., Dorschner, M.O., *et al.* (2009). Comprehensive mapping of long-range interactions reveals folding principles of the human genome. Science *326*, 289-293.

Lim, H.H., Goh, P.Y., and Surana, U. (1996). Spindle pole body separation in Saccharomyces cerevisiae requires dephosphorylation of the tyrosine 19 residue of Cdc28. Mol Cell Biol *16*, 6385-6397.

Loayza, D., and de Lange, T. (2004). Telomerase regulation at the telomere: a binary switch. Cell *117*, 279-280.

Loeb, L.A. (1991). Mutator phenotype may be required for multistage carcinogenesis. Cancer Res *51*, 3075-3079.

Loeb, L.A., Loeb, K.R., and Anderson, J.P. (2003). Multiple mutations and cancer. Proc Natl Acad Sci U S A *100*, 776-781.

Longtine, M.S., McKenzie, A., 3rd, Demarini, D.J., Shah, N.G., Wach, A., Brachat, A., Philippsen, P., and Pringle, J.R. (1998). Additional modules for versatile and economical PCR-based gene deletion and modification in Saccharomyces cerevisiae. Yeast *14*, 953-961.

Longtine, M.S., Wilson, N.M., Petracek, M.E., and Berman, J. (1989). A yeast telomere binding activity binds to two related telomere sequence motifs and is indistinguishable from RAP1. Curr Genet *16*, 225-239.

Lukasova, E., Kozubek, S., Kozubek, M., Falk, M., and Amrichova, J. (2002). The 3D structure of human chromosomes in cell nuclei. Chromosome Res *10*, 535-548.

Lundblad, V., and Szostak, J.W. (1989). A mutant with a defect in telomere elongation leads to senescence in yeast. Cell *57*, 633-643.

Lustig, A.J. (1998). Mechanisms of silencing in Saccharomyces cerevisiae. Curr Opin Genet Dev *8*, 233-239.

Maiato, H., DeLuca, J., Salmon, E.D., and Earnshaw, W.C. (2004). The dynamic kinetochore-microtubule interface. J Cell Sci *117*, 5461-5477.

Maillet, L., Boscheron, C., Gotta, M., Marcand, S., Gilson, E., and Gasser, S.M. (1996). Evidence for silencing compartments within the yeast nucleus: a role for telomere proximity and Sir protein concentration in silencer-mediated repression. Genes Dev *10*, 1796-1811.

Maizels, N. (2005). Immunoglobulin gene diversification. Annu Rev Genet *39*, 23-46.

Marcand, S., Buck, S.W., Moretti, P., Gilson, E., and Shore, D. (1996). Silencing of genes at nontelomeric sites in yeast is controlled by sequestration of silencing factors at telomeres by Rap 1 protein. Genes Dev *10*, 1297-1309.

Marston, A.L., Tham, W.H., Shah, H., and Amon, A. (2004). A genome-wide screen identifies genes required for centromeric cohesion. Science *303*, 1367-1370.

Martou, G., and De Boni, U. (2000). Nuclear topology of murine, cerebellar Purkinje neurons: changes as a function of development. Exp Cell Res *256*, 131-139.

McCleland, M.L., Gardner, R.D., Kallio, M.J., Daum, J.R., Gorbsky, G.J., Burke, D.J., and Stukenberg, P.T. (2003). The highly conserved Ndc80 complex is required for kinetochore assembly, chromosome congression, and spindle checkpoint activity. Genes Dev *17*, 101-114.

McEwen, B.F., Dong, Y., and VandenBeldt, K.J. (2007). Using electron microscopy to understand functional mechanisms of chromosome alignment on the mitotic spindle. Methods in cell biology *79*, 259-293.

McMurray, M.A., and Gottschling, D.E. (2003). An age-induced switch to a hyper-recombinational state. Science *301*, 1908-1911.

Meaburn, K.J., and Misteli, T. (2007). Cell biology: chromosome territories. Nature *445*, 379-781.

Measday, V., Hailey, D.W., Pot, I., Givan, S.A., Hyland, K.M., Cagney, G., Fields, S., Davis, T.N., and Hieter, P. (2002). Ctf3p, the Mis6 budding yeast homolog, interacts with Mcm22p and Mcm16p at the yeast outer kinetochore. Genes Dev *16*, 101-113.

Mishra, K., and Shore, D. (1999). Yeast Ku protein plays a direct role in telomeric silencing and counteracts inhibition by rif proteins. Curr Biol *9*, 1123-1126.

Misteli, T. (2000). Cell biology of transcription and pre-mRNA splicing: nuclear architecture meets nuclear function. J Cell Sci *113 (Pt 11)*, 1841-1849.

Misteli, T. (2001). Protein dynamics: implications for nuclear architecture and gene expression. Science *291*, 843-847.

Misteli, T. (2005). Concepts in nuclear architecture. Bioessays *27*, 477-487.

Misteli, T. (2009). Self-organization in the genome. Proc Natl Acad Sci U S A *106*, 6885-6886.

Moazed, D., Rudner, A.D., Huang, J., Hoppe, G.J., and Tanny, J.C. (2004). A model for step-wise assembly of heterochromatin in yeast. Novartis Found Symp *259*, 48-56; discussion 56-62, 163-169.

Moretti, P., Freeman, K., Coodly, L., and Shore, D. (1994). Evidence that a complex of SIR proteins interacts with the silencer and telomere-binding protein RAP1. Genes Dev *8*, 2257-2269.

Moretti, P., and Shore, D. (2001). Multiple interactions in Sir protein recruitment by Rap1p at silencers and telomeres in yeast. Mol Cell Biol *21*, 8082-8094.

Murray, A.W., Schultes, N.P., and Szostak, J.W. (1986). Chromosome length controls mitotic chromosome segregation in yeast. Cell *45*, 529-536.

Mythreye, K., and Bloom, K.S. (2003). Differential kinetochore protein requirements for establishment versus propagation of centromere activity in Saccharomyces cerevisiae. J Cell Biol *160*, 833-843.

Nasmyth, K. (2005). How might cohesin hold sister chromatids together? Philosophical transactions of the Royal Society of London Series B, Biological sciences *360*, 483-496.

Nasmyth, K., and Haering, C.H. (2005). The structure and function of SMC and kleisin complexes. Annu Rev Biochem *74*, 595-648.

Oakes, M., Aris, J.P., Brockenbrough, J.S., Wai, H., Vu, L., and Nomura, M. (1998). Mutational analysis of the structure and localization of the nucleolus in the yeast Saccharomyces cerevisiae. J Cell Biol *143*, 23-34.

Oakes, M., Nogi, Y., Clark, M.W., and Nomura, M. (1993). Structural alterations of the nucleolus in mutants of Saccharomyces cerevisiae defective in RNA polymerase I. Mol Cell Biol *13*, 2441-2455.

Okada, M., Cheeseman, I.M., Hori, T., Okawa, K., McLeod, I.X., Yates, J.R., 3rd, Desai, A., and Fukagawa, T. (2006). The CENP-H-I complex is required for the efficient incorporation of newly synthesized CENP-A into centromeres. Nat Cell Biol *8*, 446-457.

Olson, M.O., Dundr, M., and Szebeni, A. (2000). The nucleolus: an old factory with unexpected capabilities. Trends Cell Biol *10*, 189-196.

Ortiz, J., Stemmann, O., Rank, S., and Lechner, J. (1999). A putative protein complex consisting of Ctf19, Mcm21, and Okp1 represents a missing link in the budding yeast kinetochore. Genes Dev *13*, 1140-1155.

Paques, F., and Haber, J.E. (1999). Multiple pathways of recombination induced by double-strand breaks in Saccharomyces cerevisiae. Microbiol Mol Biol Rev *63*, 349-404.

Parada, L., and Misteli, T. (2002). Chromosome positioning in the interphase nucleus. Trends Cell Biol *12*, 425-432.

Parada, L.A., Sotiriou, S., and Misteli, T. (2004). Spatial genome organization. Exp Cell Res *296*, 64-70.

Pereira, G., Tanaka, T.U., Nasmyth, K., and Schiebel, E. (2001). Modes of spindle pole body inheritance and segregation of the Bfa1p-Bub2p checkpoint protein complex. EMBO J *20*, 6359-6370.

Pot, I., Measday, V., Snydsman, B., Cagney, G., Fields, S., Davis, T.N., Muller, E.G., and Hieter, P. (2003). Chl4p and iml3p are two new members of the budding yeast outer kinetochore. Mol Biol Cell *14*, 460-476.

Raghuraman, M.K., Winzeler, E.A., Collingwood, D., Hunt, S., Wodicka, L., Conway, A., Lockhart, D.J., Davis, R.W., Brewer, B.J., and Fangman, W.L. (2001). Replication dynamics of the yeast genome. Science *294*, 115-121.

Rine, J., and Herskowitz, I. (1987). Four genes responsible for a position effect on expression from HML and HMR in Saccharomyces cerevisiae. Genetics *116*, 9-22.

Rodley, C.D., Bertels, F., Jones, B., and O'Sullivan, J.M. (2009). Global identification of yeast chromosome interactions using Genome conformation capture. Fungal Genet Biol *46*, 879-886.

Rusche, L.N., Kirchmaier, A.L., and Rine, J. (2002). Ordered nucleation and spreading of silenced chromatin in Saccharomyces cerevisiae. Mol Biol Cell *13*, 2207-2222.

Rusche, L.N., Kirchmaier, A.L., and Rine, J. (2003). The establishment, inheritance, and function of silenced chromatin in Saccharomyces cerevisiae. Annu Rev Biochem *72*, 481-516.

Santaguida, S., and Musacchio, A. (2009). The life and miracles of kinetochores. EMBO J *28*, 2511-2531.

Sazer, S. (2005). Nuclear envelope: nuclear pore complexity. Curr Biol *15*, R23-26.

Schober, H., Ferreira, H., Kalck, V., Gehlen, L.R., and Gasser, S.M. (2009). Yeast telomerase and the SUN domain protein Mps3 anchor telomeres and repress subtelomeric recombination. Genes Dev *23*, 928-938.

Schober, H., Kalck, V., Vega-Palas, M.A., Van Houwe, G., Sage, D., Unser, M., Gartenberg, M.R., and Gasser, S.M. (2008). Controlled exchange of chromosomal arms reveals principles driving telomere interactions in yeast. Genome Res *18*, 261-271.

Sharp, J.A., Krawitz, D.C., Gardner, K.A., Fox, C.A., and Kaufman, P.D. (2003). The budding yeast silencing protein Sir1 is a functional component of centromeric chromatin. Genes Dev *17*, 2356-2361.

Shrivastav, M., De Haro, L.P., and Nickoloff, J.A. (2008). Regulation of DNA double-strand break repair pathway choice. Cell Res *18*, 134-147.

Simonis, M., Klous, P., Splinter, E., Moshkin, Y., Willemsen, R., de Wit, E., van Steensel, B., and de Laat, W. (2006). Nuclear organization of active and inactive chromatin domains uncovered by chromosome conformation capture-on-chip (4C). Nat Genet *38*, 1348-1354.

Singer, M.S., and Gottschling, D.E. (1994). TLC1: template RNA component of Saccharomyces cerevisiae telomerase. Science *266*, 404-409.

Smith, J.S., and Boeke, J.D. (1997). An unusual form of transcriptional silencing in yeast ribosomal DNA. Genes Dev *11*, 241-254.

Spector, D.L. (1990). Higher order nuclear organization: three-dimensional distribution of small nuclear ribonucleoprotein particles. Proc Natl Acad Sci U S A *87*, 147-151.

Spector, D.L., Fu, X.D., and Maniatis, T. (1991). Associations between distinct pre-mRNA splicing components and the cell nucleus. EMBO J *10*, 3467-3481.

Straight, A.F., Belmont, A.S., Robinett, C.C., and Murray, A.W. (1996). GFP tagging of budding yeast chromosomes reveals that protein-protein interactions can mediate sister chromatid cohesion. Curr Biol *6*, 1599-1608.

Taddei, A., Hediger, F., Neumann, F.R., Bauer, C., and Gasser, S.M. (2004). Separation of silencing from perinuclear anchoring functions in yeast Ku80, Sir4 and Esc1 proteins. EMBO J *23*, 1301-1312.

Taggart, A.K., Teng, S.C., and Zakian, V.A. (2002). Est1p as a cell cycle-regulated activator of telomere-bound telomerase. Science *297*, 1023-1026.

Tanabe, H., Muller, S., Neusser, M., von Hase, J., Calcagno, E., Cremer, M., Solovei, I., Cremer, C., and Cremer, T. (2002). Evolutionary conservation of chromosome territory arrangements in cell nuclei from higher primates. Proc Natl Acad Sci U S A *99*, 4424-4429.

Tanaka, K., Mukae, N., Dewar, H., van Breugel, M., James, E.K., Prescott, A.R., Antony, C., and Tanaka, T.U. (2005). Molecular mechanisms of kinetochore capture by spindle microtubules. Nature *434*, 987-994.

Tanaka, T., Cosma, M.P., Wirth, K., and Nasmyth, K. (1999). Identification of cohesin association sites at centromeres and along chromosome arms. Cell *98*, 847-858.

Therizols, P., Duong, T., Dujon, B., Zimmer, C., and Fabre, E. (2010). Chromosome arm length and nuclear constraints determine the dynamic relationship of yeast subtelomeres. Proc Natl Acad Sci U S A *107*, 2025-2030.

Thompson, M., Haeusler, R.A., Good, P.D., and Engelke, D.R. (2003). Nucleolar clustering of dispersed tRNA genes. Science *302*, 1399-1401.

Tsukamoto, Y., Kato, J., and Ikeda, H. (1997). Silencing factors participate in DNA repair and recombination in Saccharomyces cerevisiae. Nature *388*, 900-903.

Tytell, J.D., and Sorger, P.K. (2006). Analysis of kinesin motor function at budding yeast kinetochores. J Cell Biol *172*, 861-874.

Walter, J., Schermelleh, L., Cremer, M., Tashiro, S., and Cremer, T. (2003). Chromosome order in HeLa cells changes during mitosis and early G1, but is stably maintained during subsequent interphase stages. J Cell Biol *160*, 685-697.

Weaver, B.A., and Cleveland, D.W. (2007). Aneuploidy: instigator and inhibitor of tumorigenesis. Cancer Res *67*, 10103-10105.

Weaver, B.A., Silk, A.D., Montagna, C., Verdier-Pinard, P., and Cleveland, D.W. (2007). Aneuploidy acts both oncogenically and as a tumor suppressor. Cancer Cell *11*, 25-36.

Westermann, S., Cheeseman, I.M., Anderson, S., Yates, J.R., 3rd, Drubin, D.G., and Barnes, G. (2003). Architecture of the budding yeast kinetochore reveals a conserved molecular core. J Cell Biol *163*, 215-222.

Wigge, P.A., and Kilmartin, J.V. (2001). The Ndc80p complex from Saccharomyces cerevisiae contains conserved centromere components and has a function in chromosome segregation. J Cell Biol *152*, 349-360.